AD_____

Award Number: DAMD17-02-1-0095

TITLE: Hyaluronic Acid and Hyaluronidase in Prostate Cancer: Evaluation of Their Therapeutic and Prognostic Potential

PRINCIPAL INVESTIGATOR: Vinata B. Lokeshwar, Ph.D.

CONTRACTING ORGANIZATION: University of Miami School of Medicine
Miami, Florida 33136

REPORT DATE: January 2005

TYPE OF REPORT: Annual

PREPARED FOR: U.S. Army Medical Research and Materiel Command
Fort Detrick, Maryland 21702-5012

REPORT DOCUMENTATION PAGE

Form Approved
OMB No. 074-0188

1. AGENCY USE ONLY (Leave blank)	2. REPORT DATE	3. REPORT TYPE AND DATES COVERED
	January 2005	Annual (1 Jan 2004 - 31 Dec 2004)

4. TITLE AND SUBTITLE
Hyaluronic Acid and Hyaluronidase in Prostate Cancer: Evaluation of Their Therapeutic and Prognostic Potential

5. FUNDING NUMBERS
DAMD17-02-1-0095

6. AUTHOR(S)
Vinata B. Lokeshwar, Ph.D.

7. PERFORMING ORGANIZATION NAME(S) AND ADDRESS(ES)
University of Miami School of Medicine
Miami, Florida 33136

E-Mail: vlokeshw@med.miami.edu

8. PERFORMING ORGANIZATION REPORT NUMBER

9. SPONSORING / MONITORING AGENCY NAME(S) AND ADDRESS(ES)
U.S. Army Medical Research and Materiel Command
Fort Detrick, Maryland 21702-5012

10. SPONSORING / MONITORING AGENCY REPORT NUMBER

11. SUPPLEMENTARY NOTES
Original contains color plates: All DTIC reproductions will be in black and white.

12a. DISTRIBUTION / AVAILABILITY STATEMENT
Approved for Public Release; Distribution Unlimited

12b. DISTRIBUTION CODE

13. ABSTRACT (Maximum 200 Words)

Identification of accurate prognostic indicators could aid in individualization of treatment and better prediction of outcome or prostate cancer patients. Treatment modalities that target these molecules could effectively control CaP progression. The results of this project identify HYAL1 type hyaluronidase (HAase) as one such molecule. HA is a glycosaminoglycan and HAase is an enzyme that degrades HA into angiogenic fragments. Immunohistochemical analysis using archival radical prostatectomy CaP specimens from patients on whom there is 72 - 131 month follow-up show that HYAL1 and combined HA-HYAL1 inferences staining are independent predictors for biochemical recurrence. Studies on HYAL1 transfectants show that blocking HYAL1 expression in CaP cells, decreases growth and invasive activity by 3-4-fold. Lack of HYAL1 expression blocks CaP cells in G2-M phase of the cell cycle. HYAL1-AS transfectants show a 4-7-fold decrease in tumor growth, and generate tumors that are non-infiltrating and less vascularized. HAase inhibitors such as inhibit CaP cell growth in a dose-dependent manner. Transfectants expressing **high HYAL1 levels** also grow 4-fold slower and undergo apoptosis. **High HYAL1 producing transfectants** show either decreased tumor growth (3-fold) or **do not form tumors**. Ongoing studies are examining the effect of HAase inhibition on gene expression by cDNA microarray analysis.

14. SUBJECT TERMS
No subject terms provided.

15. NUMBER OF PAGES
75

16. PRICE CODE

17. SECURITY CLASSIFICATION OF REPORT	18. SECURITY CLASSIFICATION OF THIS PAGE	19. SECURITY CLASSIFICATION OF ABSTRACT	20. LIMITATION OF ABSTRACT
Unclassified	Unclassified	Unclassified	Unlimited

Table of Contents

1. Ekici, S, Cerwinka, W H, Duncan, RC, Gomez, P, Civantos, F, Soloway, MS, Lokeshwar, VB., Comparison of the Prognostic Potential of Hyaluronic Acid, Hyaluronidase (HYAL-1), CD44V6 and Microvessel Density For Prostate Cancer. Int. J. Cancer 112:121-129, 2004

2 Lokeshwar, VB, Cerwinka WH, Lokeshwar B., Hyal 1 Hyaluronidase in Prostate Cancer: A tumor Promotor or Suppressor.
MS Submitted to Proc. Natl. Acad. Sci. USA January 2005

3. HYAL-1 Hyaluronidase: Amolecular Determinant of Bladder Tumor Growth and Invasion. Cancer Research (In Press)

Principal Investigator: Vinata B. Lokeshwar, Ph.D.

Project Title: Hyaluronic acid and hyaluronidase in prostate cancer: Evaluation of their therapeutic and prognostic potential.

1. A. INTRODUCTION AND OBJECTIVES: There are two overall objectives of this funded project. The first is to evaluate the independent prognostic potential of two tumor markers, identified in our laboratory, i.e., hyaluronic acid (HA) and HYAL1 type hyaluronidase (HAase). The second objective is to evaluate the effect of HYAL1 inhibition on prostate cancer (CaP) growth and metastasis using two complementary approaches, i.e., the antisense approach and the use of a HAase inhibitor, VERSA-TL 502. We also plan to examine the mechanism by which HYAL1 regulates CaP cell growth and metastasis.

The majority of the newly diagnosed prostate cancer (CaP) patients have clinically organ-confined disease. However, limited knowledge about which CaP is likely to progress, as well as, when it will recur severely impedes individualized selection of therapy and subsequent prediction of outcome (1-5). Advances in tumor biology have unraveled genes and their products that closely associate and function in CaP growth, metastasis and angiogenesis (1,6-8). Some of the molecules may serve as accurate prognostic indicators. Moreover, treatment modalities that target the functions of these molecules could effectively control CaP progression. In preliminary studies we identified that HA and HYAL1 type HAase may be such markers. HA is a glycosaminoglycan that is made up of repeating disaccharide units, D-glucuronic acid and N-acetyl-D-glucosamine. It is abundantly present in tissues and tissue fluids. In addition to its structural role, HA regulates several cellular processes (9-10). Concentrations of HA are elevated in several cancers including those of colon, breast and in bladder (11-19). In a published report that we had presented as the preliminary evidence at the time of submission of this funded project, we demonstrated that HA levels are 4-8-fold elevated in CaP tissues, when compared to the normal prostate and benign prostatic hyperplasia tissues (20). Immunohistochemical analysis demonstrated that HA present in CaP tissues mostly localizes to the tumor-associated stroma. Small fragments of HA are known to be anigogenic and we showed the presence of such angiogenic HA fragments in high-grade CaP tissues.

HAase is an endoglycosidase that cleaves internal β-N-acetyl-D-glucosaminic linkages in the HA polymer, yielding HA fragments (21). At present 6 HAase genes have been identified, which cluster into two tightly linked triplets on chromosomes 3p21.3 (HYAL1, HYAL2 and HYAL3) and 7q31.3 (HYAL4, PH20, HYALp1) (22). Using RT-PCR, cDNA cloning/sequencing, cell-culture, immunoblotting and pH activity profile studies, we confirmed that HYAL1 is the HAase that is expressed in CaP tissues and it is secreted by CaP cells (23). We also showed that HAase levels are elevated in CaP tissues when compared to the levels in NAP and BPH tissues. Furthermore, the increase in HAase levels correlates with CaP progression (metastatic > high-grade >> low-grade (Gleason 5/6) > NAP/BPH) (23). By immunohistochemical analysis, which was presented as the preliminary evidence during the submission of this funded project, we showed that the HYAL1 type HAase is exclusively expressed in CaP cells. Based on our immunoshistochemical studies we hypothesized that HA and HYAL1 may be potentially accurate prognostic indicators for CaP. To investigate the function of HYAL1 we had stablely transfected DU145 cells with full-length HYAL1 cDNA in the sense and antisense orientation and planned to study the behavior of DU145, as well as, PC3-ML transfectants both *in vitro* and *in vivo*. In addition, we had identified a HAase inhibitor, VERSA-TL502 (24). This inhibitor inhibits the HAase activity secreted by CaP cells (IC_{50} 2 µg/ml). We had hypothesized that VERSA-TL 502 may also inhibit CaP cell growth and invasive behavior, both *in vitro* and *in vivo*.

The following is a succinct report of the progress in achieving our objectives in the three years.

B. (BODY): Progress related to Aim 1: To correlate HA and HYAL1 staining intensity and its pattern in CaP tissues with clinical outcome.

Rationale and background: Two studies were conducted under this aim. The first study involved evaluation of the prognostic potential of HA and HYAL1 to predict biochemical recurrence within 64 months (i.e., within 5-years). Our results show that HYAL1 either alone or in combination with HA is an independent predictor of biochemical recurrence in CaP patients. This study was presented in detail in the first year's progress report and has been published (25; Appendix 1). Out of the 70 patients that were included in that study follow-up of ≥ 72 months (72 to 131 months) was available on 66 patients. In the study described below, we compared the prognostic ability of HA and HYAL1 with two other potential prognostic indicators of CaP (i.e., CD44v6 and microvessel density (MVD)) to predict biochemical recurrence up to 131 months.

We chose to compare CD44v6 and MVD with HA and HYAL1 since all of these molecules are biologically related. For example, CD44 denotes a family of cell surface transmembrane glycoproteins which serve as the cell surface receptor for HA (26,27). Alternative splicing of CD44 mRNA in 10 of the 20 exons generates several variant CD44 isoforms (27,28). The correlation between tumor progression and CD44s and/or its isoforms is controversial. We and others have shown that the androgen insensitive CaP line PC-3 and primary PCa cells express CD44s and CD44 variants (e.g., CD44v3 and CD44v6), however, the androgen sensitive poorly metastatic line LNCaP does not express CD44 (29-31). Contrary to these findings, it has been shown that the over-expression of CD44v6 in a rat CaP line decreases metastasis (32). Recently, Ekici et al showed that decreased expression of CD44v6 could be a predictor of poor prognosis in clinically localized CaP (33). Aaltomaa et al also reported similar results (34).

Angiogenesis is an essential process for tumor growth and metastasis (35-37). As discussed above, degradation of HA by HAase generates angiogenic HA fragments. Clinical significance of angiogenesis, measured as microvessel density (MVD), has been demonstrated for several tumor types, including, gastrointestinal, breast, bladder and renal cell carcinomas (38-41). Studies that compared various endothelial cell markers (i.e., CD31, CD34 and Factor VIII) have shown that CD34 is a sensitive endothelial cell marker for measuring MVD (42,43). At the present time, the clinical significance of MVD, as an independent predictor of pathological stage and recurrence in PCa remains controversial (42-45).

Since HYAL1 degrades HA and generates angiogenic fragments and CD44 acts as a cell-surface receptor for both HA and HA fragments, it is interesting to examine whether these biologically linked molecules are accurate prognostic indicators for PCa, and whether they influence each other's prognostic capabilities.

Experimental procedures:

Specimens and study individuals: We initially chose 150 archival specimens from CaP patients who underwent retropubic prostatectomy for clinically localized CaP between 1992 and 1996. Out of these 150 patients, on 66 patients, a minimum available follow-up of 72 months was available. Of the 66 patients, 25 patients had biochemical or clinical recurrence before 72 months (mean time to recurrence: 21.3 months; range: 3 to 61 months), and 41 patients were free of disease recurrence (mean follow-up: 103 months; range: 72 - 131 months). Biochemical recurrence was defined as a PSA level ≥ 0.4 ng/ml in 2 successive measurements after the operation, in which case the first date of elevated PSA level was considered as the

date of failure. The patient characteristics with respect to age, preoperative PSA, and tumor (i.e., Gleason sum, stage, margin, extraprostatic extension (EPE) and seminal vesicle invasion) are shown in Table 1.

Table 1: Distribution of pre- and post-operative parameters among study patients. Note that biochemical recurrence with post-operative PSA levels ≥ 0.4 ng/ml within 72 months was used a cut point for defining progression. Thus, any CaP patient who showed a biochemical recurrence within 72 months was included in the progressed category.

Preoperative parameters				Postoperative parameters			
Progression	Age (yrs)	PSA (ng/ml)	Clinical Stage	Gleason sum	EPE	Margin	Seminal vesicle invasion
Biochemical recurrence (n = 25)	Median: 64 Mean: 65.1	Median: 9.0 Mean: 14.04	T1c: 10 T2a: 5 T2b: 10	6 = 2 7 = 14 8 = 6 9 = 3	(+) = 21 (-) = 4	(+)=18 (-)=7	(+) = 14 (-) = 11
No biochemical or clinical recurrence (n = 41)	Median: 65 Mean: 62.98	Median: 6 Mean: 8.1	T1c: 22 T2a: 5 T2b: 14	5 = 7 6 = 9 7 = 20 8 = 5	(+) = 4 (-) = 37	(+)=9 (-)=32	(+) = 3 (-) = 38

HA and HYAL1 staining: IHC localization of HA and HYAL1 in CaP tissues was carried out as described previously (20). For all specimens, paraffin-embedded blocks containing CaP tissues representing the majority of the Gleason sum were selected by the study's pathologist (Dr. Francisco Civantos). The blocks were cut into 3-μm thick sections and placed on positively charged slides. The specimens were deparafinized, rehydrated and treated with an Antigen-retrieval solution (Dako Laboratories). For each specimen, two slides were prepared, one for HA and the other for HYAL1 staining. For HA staining, the slides were incubated with 2 μg/ml of a biotinylated bovine nasal cartilage protein at room temperature for 35 min (20). The specificity of HA staining was established as described previously (20). Following incubation with the HA-binding protein, the slides were washed in phosphate buffered saline (PBS) and sequentially incubated with streptavidin peroxidase at room temperature for 30 min and 3,3'-diaminobenzidine (DAB) chromogen substrate solution (Dako Laboratories). The slides were counterstained with hematoxylin, dehydrated and mounted.

For HYAL1 staining, the slides were incubated with 3.7 μg/ml of anti-HYAL1 IgG at 4^0 C for 16 hr. Rabbit polyclonal anti-HYAL1 IgG was generated against a peptide sequence present in HYAL1 protein (amino acids 321 to 338) and its specificity for IHC was confirmed as described previously (20, 25). Following incubation with anti-HYAL1 IgG, the slides were washed in PBS and incubated with a linking solution containing a biotinylated goat anti-rabbit IgG (Dako LSAB kit) at room temperature for 30 min. The slides were then treated with streptavidin peroxidase and DAB chromogen. The slides were counterstained with hematoxylin, dehydrated and mounted.

Slide grading for HA and HYAL1: Two readers independently evaluated all slides in a blinded fashion. Any discrepancy in assigning staining intensity was resolved by both readers reexamining those slides simultaneously. The staining for HA and HYAL-1 was graded as 0 (no staining), 1+, 2+, and 3+. For HA staining, both the tumor-associated stroma and tumor cells

were graded in each slide. The overall staining grade for each slide was assigned based on the staining intensity of the majority of the tumor tissue in the specimen. However, if ~ 50% of the tumor tissue stained as 1+ and the other 50% as 3+, the overall staining grade was 2+. If the staining distribution was ~ 50% of the tumor staining 2+ and the remaining staining as 3+, the overall staining inference was assigned as 3+. The staining scale was further subcategorized into low grade and high grade. For HA staining, low-grade staining included 0, 1+ and 2+ staining, and high-grade staining included 3+ intensity. In those cases (n = 2) where the stromal tissues were evaluated as low-grade staining but the tumor cells stained as 3+, the overall HA staining was considered as high grade. For HYAL1, high-grade staining represented 2+ and 3+ staining, whereas low-grade staining included 0 and 1+ staining intensities. For the combined HA-HYAL-1 staining, a positive result was indicated only when both HA (stromal, tumor cells, or both) and HYAL-1 staining intensities were of high grade. Any other combination was considered negative. All slides were reviewed out of order to prevent direct comparison of individual cases for HA and HYAL1.

CD34 staining: Following the antigen retrieval step (as described above), the slides were incubated with a mouse monoclonal anti-human hematopoietic progenitor cell CD34 antibody (dilution of 1:20; DAKO, Denmark) at 4°C for 15 hours. The slides were then incubated with a biotinylated anti-mouse antibody and an avidin-peroxidase conjugate solution (Vectastain ABC Kit, Vector Laboratories, Burlingame, CA). To visualize peroxidase binding sites, the slides were incubated with a 3,3'-diaminobenzidine (DAB) chromogen substrate solution (Dako Laboratories) for 10 minutes. The slides were counterstained with hematoxylin, dehydrated and mounted.

The method described by Weidner et al (42) was used for scoring of the microvessels stained with CD34. The area of the highest MVD in each tissue specimen was localized under 40X magnification and was designated as "hot spot". The microvessels in the hot spots were counted under 400X-magnification. Any vessel with lumen and endothelial cell or endothelial cell cluster stained positively for CD34 was considered to be a single countable microvessel. MVD count was defined as the mean value of the counts obtained in 3 separate, contiguous but not overlapping areas within the hot spot. A cutoff value was determined using the receiver operating characteristic (ROC) curve and according to this value two groups of low and high MVD were assigned. Microvessels were examined and counted by the three readers (S.E., V.B.L. and W.H.C.) independently and without the knowledge of the clinical and pathological status of the patients. The sections were reviewed out of order to prevent direct comparison of individual cases for CD34.

CD44v6 staining: Following antigen retrieval, the slides were incubated with a mouse monoclonal anti-human CD44v6 antibody (dilution of 1:50; Bender Med systems, Vienna, Austria) at 4°C for 15 hours. The sections were then incubated with a biotinylated secondary antibody and an avidin-peroxidase conjugate solution (Vectastain ABC Kit, Vector Laboratories, Burlingame, CA). To visualize peroxidase binding sites, the slides were incubated with a 3,3'-diaminobenzidine (DAB) chromogen substrate solution (Dako Laboratories) for 10 minutes. The slides were counterstained with hematoxylin, dehydrated and mounted.

The slides for CD44v6 were scored as described by Ekici et al (33). All sections included normal prostate tissue and/or benign prostatic hyperplasia glands as internal controls. Intensity of staining was graded as 0 for no staining, 1 for weak intensity, 2 for moderate intensity and 3 for strong intensity. A combined staining score based on an estimate of the percentage of tumor cells stained and the intensity of staining was developed. The areas of tumor cells stained with maximum intensity (primary area) and the other tumor cells stained with lesser intensity (secondary area) were determined in percentage values. The combined score is obtained by adding the scores of the primary and secondary areas. Staining intensities were examined and

scored by two readers (S.E. and V.B.L.), independently and in a blinded fashion. A cutoff value was determined from the ROC curve and according to this value two groups of low and high CD44v6 staining were assigned.

Statistical Analysis:

The inter-assay variability regarding staining intensity was determined by Pearson's correlation analysis. The Spearman's bivariate correlation coefficients were 0.85, 0.9, 0.98 and 0.95 for HA, HYAL1, CD34 and CD44v6 staining, respectively. For all the markers, a high-grade staining was considered as a true positive if the patient had biochemical recurrence. Consequently, low-grade staining was considered as a true negative, if the patient had no biochemical recurrence. The sensitivity, specificity, positive predictive value (PPV), and negative predictive value (NPV) for HA, HYAL1, HA-HYAL1, CD34 and CD44v6 staining inferences were calculated using the 2 x 2 contingency table (high-grade/low-grade staining and progressed/non-progressed CaP patients) at 72, 84, 100 and 112 month cut-off limits. For CD44v6 and MVD, Receiver Operating Characteristic curves were developed for determining the optimal cut-off limits that yielded the best possible sensitivity and specificity values. The cut-off limits for CD44v6 and MVD were 180 and 41, respectively. The sensitivity is defined as: true positive (i.e., No. of recurred patients predicted by a marker) ÷ total no. of recurred patients. Specificity: true negatives (i.e., No. of non-recurred patients predicted by a marker) ÷ total no. of non-recurred patients. Accuracy: No. of True positive + No. of true negatives ÷ total no. of CaP patients in the study. PPV: No. of true positive ÷ No. of true positive + No. of false positive. NPV: No. of true negative ÷ No. of true negative + No. of false negative. The data on various, biochemical, surgical, and pathologic parameters, as well as HA, HYAL1, HA-HYAL1, CD34 and CD44v6 staining inferences, were analyzed by Cox Proportional Hazard model, using single variable analysis (univariate analysis) or step-wise selection analysis. Stratified Kaplan-Meier analyses were performed on the variables that were found to be significant in the multivariate Cox Proportional Hazard model. Statistical analysis was carried out under the direction of project's statistician, Dr. Robert Duncan, using the SAS Software Program (version 8.02; SAS Institute, Cary, NC).

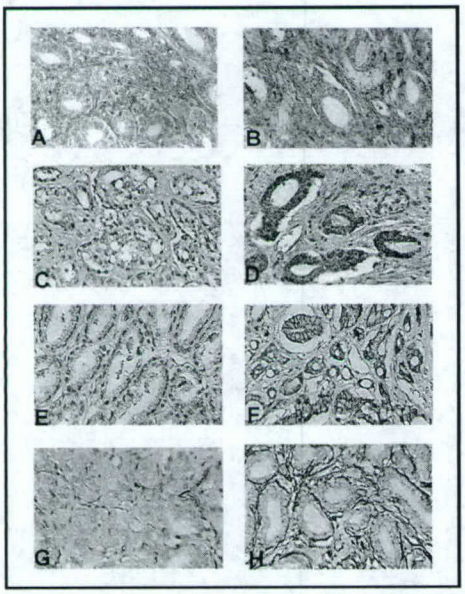

Fig 1. Localization of HA, HYAL1, CD44v6 and MVD in CaP tissues: A non-recurred patient (panels A, C, E, G) and a recurred patient (panels B, D, F, H). Panels A and B: HA; Panels C and D: HYAL1; Panels E and F: CD44v6; Panels G and H: MVD

Results:

Immunohistochemistry of the tissue markers:

Fig. 1 shows immunohistochemical localization of HA, HYAL1, CD44v6 and MVD in 2 Gleason 7 PCa specimens, one each from a non-recurred (panels A, C, E, G) and a recurred (panels B, D, F, H) patient, respectively. As shown in Fig. 1 panel A, very little HA staining is seen in PCa tissue from a patient who did not progress within 72 months. Among the 41 PCa specimens from non-recurred patients, 25 showed low-grade staining. Panel B shows high-grade HA staining in PCa specimen from a patient who had biochemical recurrence in < 72 months (median time to recurrence: 19 months; mean time to recurrence: 21.3 months). The HA staining is seen mainly in tumor-associated stroma.

However, high-grade HA staining was also seen in tumor cells in 8 out of 25 patients who had biochemical recurrence. Out of the 25 patients who had recurred, 24 showed high-grade HA staining.

As shown in Fig. 1 panel C, little HYAL1 staining is seen in the PCa tissue from a non-recurred patient. Out of the 41 non-recurred patients, PCa specimens from 33 had low-grade staining. In the PCa specimen from a patient who later recurred, high-grade HYAL1 staining is seen (Fig. 1, panel D). The HYAL1 expression is seen exclusively in tumor cells. Out of the 25 patients who recurred within 72 months, 21 had high-grade HYAL1 staining. Contrary to some earlier reports (33,34), low-grade CD44v6 staining is observed in the PCa specimen from a non-recurred patient (Fig. 1, panel E) and high-grade CD44v6 staining is observed in the PCa tissue from a recurred patient (Fig. 1, panel F). CD44v6 staining is mostly associated with the plasma membrane of tumor cells. We also observed CD44v6 in non-neoplastic epithelial cells in normal prostate and benign prostatic hyperplasia glands. However, the staining intensity of CD44v6 in non-neoplastic cells was less than that in tumor cells. Using a cut-off limit of 180 on the scoring scale, 23 out of 41 PCa specimens from non-recurred patients showed low-grade staining, whereas, out of the 25 patients who recurred, 17 showed high-grade staining.

As shown in Fig. 1 panel G, MVD is low in the PCa tissue from a non-recurred patient. As determined from the Receiver Operating Characteristic curve, a cut-off limit of 41 was set to score low or high MVD. Out of the 41 non-recurred patients, PCa tissues from 25 patients had low MVD. However, the MVD was high in 19 out of 25 PCa tissues obtained form patients who had a recurrence. Fig. 1 panel H shows high MVD in the PCa specimen from a patient who later recurred.

Determination of sensitivity, specificity, accuracy: We determined sensitivity, specificity, accuracy HA, HYAL1, combined HA-HYAL1, CD44v6, and MVD at 72-, 84-, 100- and 112-months of follow-up. Data on 72 and 112 months is shown here (For details please see Appendix 2; ref. 46). As shown in Table 2, the sensitivity of HA, HYAL1, combined HA-HYAL1, CD44v6, and MVD for predicting CaP recurrence is 96%, 84%, 84%, 76% and 68%, respectively within 72 months. The specificity, of HA (61%), CD44v6 (56.1%), and MVD (61%) was lower than that of HYAL1 (80.5%) and combined HA-HYAL1 (87.8%). The accuracy of the

Parameter	**HA (%)** 72 months	112 months	**HYAL1 (%)** 72 months	112 months	**HA-** 72 months	**HYAL1 (%)** 112 months
Sensitivity	96	92.6	84	85.2	84	81.5
Specificity	61 (25/41)	80.6	80.5	94.4	87.8	94.4
Accuracy	74.2	91.1	81.8	88.9	86.4	86.7
Parameters	**CD44v6 (%)** 72 months	112 months	**MVD (%)** 72 months	112 months		
Sensitivity	72 months	112 months	72 months	112 months		
Specificity	76	77.8	68	62.9		
Accuracy	61	77.8	56.1	61.1		

Table 2: 72 and 112 months were used a cut point for determining biochemical recurrence.

HA-HYAL1 (86.4%) was the highest, followed by HYAL1 (81.8%), HA (74.2%), MVD (66.7%), and CD44v6 (57.6%). Follow-up information of ≥112 month was available on 45 patients (mean follow-up 121 months; median 120.2; range 112 – 131 months). At 112 month, the sensitivity of HA, HYAL1, HA-HYAL1, MVD and CD44v6 was 92.6%, 85.2%, 81.5%, 77.8% and 62.9% respectively. At final analysis, both HYAL1 and combined HA-HYAL1 had the best specificity (94.4%, 94.4%) and accuracy (88.9%, 86.7%), followed by HA, MVD and CD44v6 (Table 2).

Evaluation of the prognostic capabilities of pre-operative and post-operative parameters and histological markers:

Univariate analysis:

Since the study patients in this cohort had variable follow-up between 72 and 131 months, we used Cox Proportional Hazard model and single parameter analysis to determine the prognostic significance of each of the pre-operative (i.e., age, PSA and clinical stage) and post-operative parameters (i.e., Gleason sum, margin +/-, EPE +/-, seminal vesicle invasion +/-), as well as, staining inferences of HA, HYAL1, combined HA-HYAL1, CD44v6 and MVD. In the univariate analysis, age (p = 0.5104; hazard ratio = 1.019), clinical stage (p = 0.2683, hazard ratio = 1.2620) and CD44v6 staining (p = 0.131 hazard ratio = 1.826) were not significant in predicting biochemical recurrence. However, pre-operative PSA (p = 0.0006, hazard ratio/unit PSA change = 1.048), Gleason sum overall (p = 0.0002; hazard ratio = 2.5), margin status (p = 0.0003; hazard ratio = 4.5), EPE (p<0.0001; hazard ratio = 12.781), seminal vesicle invasion (p<0.0001; hazard ratio = 6.56), HA staining (p=0.0008; hazard ratio = 12.091), HYAL1 staining (p<0.0001; hazard ratio = 13.192), HA-HYAL1 staining (p<0.0001; hazard ratio = 10.749) and MVD (p = 0.0015; hazard ratio = 4.36) significantly predicted biochemical recurrence. (Please see Appendix 2 for details, ref. 46).

Parameter	P Value	Hazard Ratio
PSA	< 0.0001*	1.068
EPE	0.0016*	6.222
HYAL1	0.0009*	8.196
HA-HYAL1	0.0021*	5.191

Table 3: HA and HYAL1 or HA-HYAL1were included in the multivariate analysis; *: Statistically significant

Multivariate analysis:

To determine the smallest number of variables that could jointly predict biochemical recurrence in this cohort of study patients, we used Cox Proportional Hazard model and step-wise selection analysis. When age, pre-operative PSA, clinical stage, Gleason sum (overall or ≥ 7), EPE, seminal vesicle invasion and staining inferences of HA, HYAL1, CD44v6, and MVD were included in the model, only pre-operative PSA (p < 0.0001, hazard ratio/unit PSA change = 1.086), EPE (p = 0.0016, hazard ratio = 6.222) and HYAL1 (p = 0.0009, hazard ratio = 8.1896) reached statistical significance in predicting biochemical recurrence (Table 3).

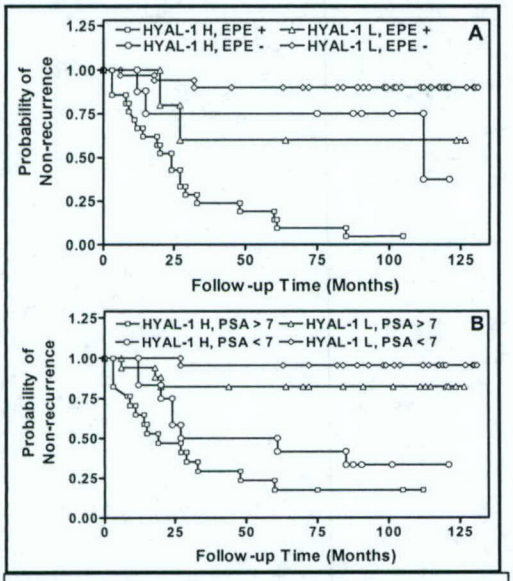

Fig. 2: Kaplan-Meier analysis: Data on parameters significant in multivariate analysis (Table 3) were stratified to perform Kaplan-Meier analysis.

The inclusion of the combined HA-HYAL1 staining inference instead of HA and HYAL1 staining inferences, in the multiple regression model again showed that pre-operative PSA (p = 0.0002, hazard ratio/unit PSA change 1.077), EPE (p = 0.0009, hazard ratio = 6.906) and HA-HYAL1 (p = 0.0021, hazard ratio = 5.191) were significant in predicting biochemical recurrence (Table 3 B). None of the other pre-operative (PSA, clinical stage) and post-operative parameters (Gleason sum and seminal veicle) or CD44v6 and MVD staining inferences reached statistical significance in the multivariate model (P > 0.05, in each case).

Kaplan-Meier analysis: The joint effect of HYAL1 and EPE or HYAL1 and PSA on biochemical analysis was evaluated using stratified Kaplan-Meier analysis. As shown in **Fig. 2 A,** the probability of biochemical recurrence was highest when HYAL1 and was high and EPE was positive and a patient had the lowest probability of

recurrence when HYAL1 was low and EPE was negative. Since PSA was a continuous estimate, with values ranging between 0.5 and 62 ng/ml for the entire study cohort (n = 66), the cohort was divided into those with PSA < 7 and > 7 ng/ml. PSA > 7 ng/ml was used as a cut-off limit, since that was the median value for the entire cohort. As shown in **Fig 2 B**, individuals with high HYAL1 and PSA 7 ng/ml had the highest probability of recurrence, followed HYAL1 high, PSA < 7 ng/ml individuals. CaP patients with low HYAL1 staining and PSA < 7 ng/ml had the lowest probability of recurrence. Identical results were obtained with HA-HYAL1 staining inferences were included in the Kaplan-Meier analysis instead of HYAL1 inferences. These data confirm the multivariate analysis results (as discussed above), which selected HYAL1 (or HA-HYAL1), pre-operative PSA and EPE as independent prognostic indicators.

Summary: The results, which we have obtained, demonstrate that HYAL1 and HA-HYAL1 are independent prognostic indicators for predicting biochemical recurrence of CaP. An additional point that deserves attention is that in this study we had long follow-up on each patient (minimum follow-up 72 months), which was sufficient to detect any biochemical recurrence. This long follow-up makes a strong case that HYAL1 and HA-HYAL1 are potentially useful prognostic indicators for CaP.

C. (BODY): Progress related to Aim 2: To evaluate the effect of HYAL1 inhibition on CaP growth and metastasis.

Rationale and background: When we submitted the above referenced grant we had generated DU145 transfectants that either over produced (HYAL1 sense) or under produced (HYAL1-antisense) HYAL1-type HAase. Contrary to our hypothesis that HYAL1 enhances CaP growth, when we injected these transfectants in athymic nude mice to study the effect of HYAL1 on tumor growth, we found that both the HYAL1-sense and HYAL1-antisense transfectants did not generate palpable tumors in 30 days, whereas, the vector only transfectants (i.e., wild type) generated palpable tumors in 7 days. As a result, we generated DU145 transfectants again and12 this time we selected two different types of HYAL1-sense transfectant clones: 1. Moderately HYAL1 over-producing 2. Highly HAase over-producing. Since PC3-ML cells express little HYAL1, we generated only HYAL1-sense transfectants and again selected moderately HAase-overproducing and highly HAase-overproducing clones. Both the *in vitro* and *in vivo* analysis of these clones demonstrates that both, the over and under production of HYAL1 decreases CaP growth and its invasive potential.

Experimental procedures:

Generation of DU145 and PC3-ML transfectants: The entire HYAL1 cDNA coding region (nucleotides 618 – 1925 GenBank # HSU03056) was amplified by RT-PCR analysis as described previously (47). The amplified cDNA was directly cloned into pcDNA 3.1/v5/His-TOPO eukaryotic expression vector, using a TOPO-TA cloning kit (Invitrogen). This vector allows bi-directional cloning of PCR products, i.e., the cDNA has a 50:50 chance of insertion into the vector either in the sense or antisense orientation with respect to the CMV promoter. HYAL1-sense (HYAL1-S) and HYAL1-antisense (HYAL1-AS) constructs were used for transfection studies. Since DU145 cells produce high levels of HAase, we generated both HYAL1-S and HYAL1-AS transfectants. However, for PC3-ML cells, we generated only HYAL1-S transfectants since these produce very little HAase (1-3 mU/10^6 cells). CaP cells (2 x 10^5) were transfected with 5-µg DNA of HYAL1-S, HYAL1-AS or pcDNA3.1/v5-His vector constructs using Effectene™ transfection reagent and a protocol supplied by the manufacturer (Qiagen).

The transfectants were selected in geneticin (400-µg/ml for DU145 and 300-µg/ml for PC3-ML). 25 to 30 transfectant clones for each construct were analyzed and data on 2 representative clones are presented.

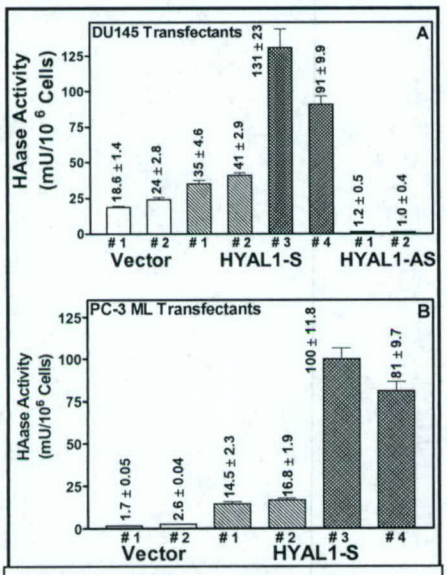

Figure 3: Analysis of HAase activity. Data: mean ± SD (Triplicates in 3 experiments).

Analysis of HYAL1 expression in transfectants: HAase test: To measure HAase activity secreted by different transfectant clones, actively growing cultures of transfectants (~ 10^5 cells/24-well plates) were incubated for 48 hr in RPMI 1640 containing insulin, selenium and transferrin (RPMI+ITS) and the conditioned media (CM) were assayed for HAase activity using the HAase test. Briefly, microtiter plates coated with 200 µg/ml HA were incubated with transfectant CM in a HAase assay buffer (48) at 37^0 C for 12-15 h. Following incubation, the degraded HA was washed off and HA remaining on the wells was detected using the biotinylated HA binding protein and an avidin-biotin detection system. HAase activity (mU/ml) was normalized to cell number. As shown in **Fig. 3 A**, DU145 HYAL1-S clones # 1 and # 2 secrete 1.5-2.3-fold more HAase activity and HYAL1-S # 3 and # 4 clones secrete 3.8-7.3-fold more HAase activity, when compared to vector # 1 and # 2 clones. There is > 90% reduction in HAase secretion in HYAL1-AS clones. PC-3 ML HYAL1-S clones # 1 and # 2 secrete HAase activity similar to that secreted by DU145 vector clones, and it is about 10-fold more than that secreted by PC-3 ML vector clones (**Fig. 3 B**). HYAL1-S # 3 and # 4 clones secrete HAase activity similar to that secreted by DU145 # 3 and # 4 clones.

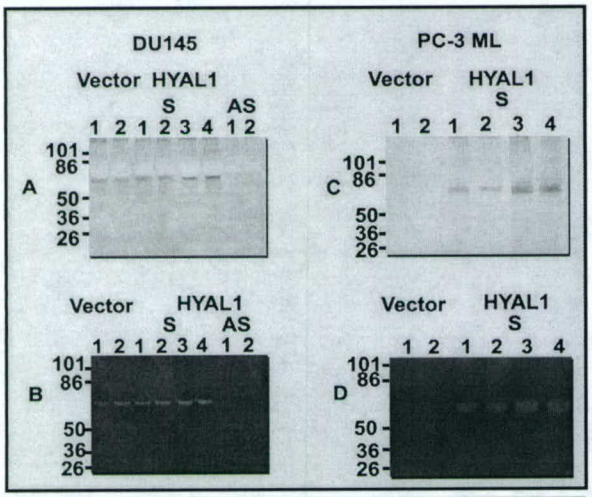

Figure 4: Detection of HYAL1 expression in DU145 and PC-3 ML transfectants. A & C. HYAL1 immunoblot analysis: **B & D:** Substrate (HA)-gel assay.

Anti-HYAL1 immunoblotting: To detect HYAL1 expression, CM (10-µg protein) were immunoblotted using the anti-HYAL1 IgG. A ~ 60-kDa HYAL1 protein is secreted in the CM of DU145 vector and HYAL1-S clones but not in HYAL1-AS clones. (**Fig 4 A, photo-image Appendix A**). In PC-3 ML clones, HYAL1 protein is detected in the CM of HYAL1-S transfectants but not in vector clones. The amount of HYAL1 protein detected in HYAL1-S clones # 3 and # 4 is higher than that detected in HYAL1-S # 1 and # 2 clones (**Fig 4 B**).

Substrate (HA)-gel analysis: To confirm the expression of active HAase, we separated the CM of DU145 and PC-3 ML transfectants on a SDS-polyacrylamide gel containing HA and the gel was incubated in the HAase assay buffer. Following incubation, the gel was stained and destained to visualize active HAase (Appendix 1). As shown in **Fig 4 C and D**, a ~ 60-kDa active HAase species is detected in the CM of DU145 vector and HYAL1-S clones and in PC-3 ML HYAL1-S clones. As expected from HAase activity and HYAL1 immunoblotting results, the ~

60-kDa active HAase species is absent in CM of DU145 HYAL1-AS and PC-3 ML vector clones (Fig 4 C, D).

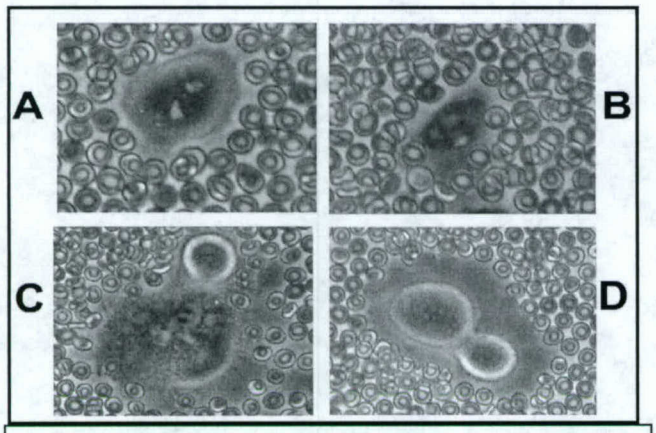

Fig 5: Examination of pericellular matrix. A: Vector # 1; **B:** HYAL1-S # 1; **C:** HYAL1-S # 4; **D:** HYAL1-AS # 2.

Effect of HYAL1 expression on pericellular matrix formation: We next determined whether HYAL1 expression regulates pericellular matrix that surrounds CaP cells and whether HA is an important component of it. 24-h cultures of DU145 transfectant clones ($1x10^4$ cells/6-cm dish) were overlaid with formaldehyde fixed human erythrocytes and observed under a phase contrast microscope. Cells showing a bright region around the entire periphery with width ≥the diameter of an erythrocyte (i.e., pericellular matrix) were counted in 10 fields (49, 50). Results were expressed as % cells with pericellular matrix ± S.D. As shown in **Figure 5**, vector #1 and HYAL1-S clones (# 1 and # 3) do not exhibit pericellular matrices as the erythrocytes closely abut the surface of each cell. However, HYAL1-AS cells (clone # 1) exhibit a clear pericellular matrix. There was a 3- and 4.6-fold increase in the percentage of cells with pericellular matrix for HYAL1-AS transfectants when compared to vector, moderate HYAL1 over-producing and high HYAL1 over-producing transfectants, respectively ($P < 0.001$). Thus, HA is an important component of the pericellular matrix of prostate cancer cells and it is degraded by HYAL1.

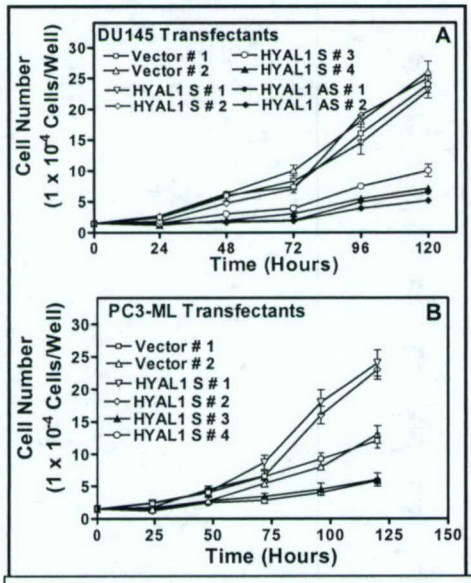

Figure 6: Determination of proliferation rate of transfectants. Data: mean ± SD from duplicate measurements in 3 experiments.

Effect of HYAL1 expression on cell proliferation, cell cycle and apoptosis:

Cell proliferation: Vector, HYAL1-S and HYAL1-AS clones of CaP cells (2×10^4/well) were plated on 24-well culture plates in growth medium. Cells were counted in duplicate wells every 24-h for a total period of 120-h, in 2 independent experiments. As shown in **Fig 6 A**, the growth rate o f DU145 vector and HYAL1-S # 1 and # 2 transfectant is comparable (doubling time ~ 26-28 hr). However, both HYAL1-AS clones and also HYAL1-S # 3 and # 4 clones (which secrete ≥ 100 $mU/10^6$ HAase activity) grow 4-5-fold slower than vector clones (doubling time ~ 90-96 hr). PC-3 ML HYAL1-S # 1 and HYAL1-S # 2 clones grow 1.5-2-fold faster than the vector clones, however, the high HYAL1 producer clones, HYAL1-S # 3 and # 4 grow 2-2.5-fold slower than the vector clones (**Fig. 6 B**).

Cell-cycle analysis: Cultures of transfectants (10^6 cells/ml) were lysed in a hypotonic solution containing 0.1% NP40 and 50 µg/ml propidium iodide and analyzed using an EPICS XL flow cytometer equipped with a long pass red filter, FL3 (630 nm). FL3 histograms were analyzed by Modfit Easy (Lite) Program (Veritas Software, ME). As shown in **Table 4**, decreased growth rate of HYAL1-AS transfectants is due to cell-cycle arrest in the G2-M phase. There is a 200% - 300% increase in the number of HYAL1-AS #1 cells in G2-M phase when compared to vector

and all HYAL1-S transfectant clones. Correspondingly, the % of HYAL1-AS cells in S-phase is decreased when compared to vector and HYAL1-S cells. The increase in the G2-M phase of cell cycle in HYAL1-AS transfectants is statistically significant ($P < 0.001$; Tukey's test). Interestingly, for HYAL1-S # 3 and # 4, we observed an extra peak to the left of the G0-G1 peak, possibly representing apoptotic cells. In PC3-ML transfectants, HYAL1 expression also increased the number of cells in the S-phase with a corresponding decrease in the number of cells in G2-M phase (data not shown).

Name	G0-G1	S	G2-M
Vector # 1	52.6%	35.9%	11.5%
Vector # 2	50.4%	37.2%	12.4%
HYAL1-S # 1	52.3%	36.4%	11.3%
HYAL1-S # 2	49.4%	38.5%	12.1%
HYAL1-S # 3	50.9%	37.6%	11.5%
HYAL1-S # 4	53.4%	36.9%	9.7%
HYAl1-AS # 1	48.9%	28.8%	**22.3%**
HYAL1-AS # 2	43.9%	24.8%	**31.3%**

Table 4: Cell cycle Analysis of DU145 transfectants. Shaded area: G2-M block

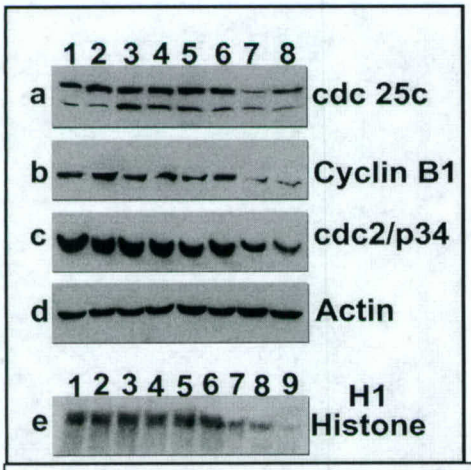

Figure 7: Analysis of G2-M cell cycle regulators. Lanes 1 & 2: vector clones # 1 & 2; lanes 3-6: HYAL1-S clones 1 - 4; lanes 7 & 8: HYAL1-AS clones # 1 & 2. **e**: Lanes 1 - 8 are the same as above; lane 9: negative control.

Analysis of G2-M regulators: We analyzed the expression of G2-M regulators, i.e., cdc25c, cyclin B1, and cdc2/p34 proteins in various clones by immunoblot analysis, using commercially available antibodies (49,50). As shown in **Fig. 7**, both cdc25c bands, plausibly representing active (phosphorylated) and native forms, are detected in all DU145 transfectants. There is ~ 3-fold decrease in the expression of active cdc25c in HYAL1-AS transfectants when compared to the vector and HYAL1-S transfectant clones. There is also ~ 3-fold and 2-fold decrease in the expressions of cyclin B1 and cdc2/p34 in HYAL1-AS transfectants when compared to vector and HYAL1-S clones (**Fig 7**). We also examined cdc2/p34 kinase activity, which is elevated upon binding of cyclin B1 to cdc2/p34 during G2-M transition. The kinase activity assay was performed by immunoprecipitating the cell lysates of DU145 transfectant clones with cdc2/p34 using a mouse anti-cdc2/p34 IgG and protein-A agarose. The immunoprecipitates were incubated in a kinase assay buffer containing H1 histone (2.5-µg), 5-µM ATP, 5-µCi γ-^{32}P-ATP. Histone H1 was analyzed by SDS-PAGE and autoradiography (Appendix 4). As shown in **Fig 7**, a ~ 2.5- and 3-fold decrease in cdc2/p34-associated H1 histone kinase activity is observed in HYAL1-AS transfectant clones when compared to vector and all HYAL1-S transfectants. These results show that the slow proliferation rate of HYAL1-AS transfectants is due to G2-M arrest.

Analysis of apoptosis: We determined whether the reduced cell growth observed in high HYAL1 producing clones of CaP transfectants (i.e., HYAL1-S # and # 4 clones) was due to increased apoptosis, using free nucleosome release assay. Briefly, 96-h cultures of transfectants (10^5 cells/24-well plate) were lysed and the cell lysates were tested for free nucleosome release using the Cell Death ELISA kit (Roche Diagnostics). As shown in **Fig. 8 A**, there is a 3-fold increase in the intracellular levels of free nucleosomes in HYAL1-S # 3 and HYAL1-S # 4 cells when compared to vector, HYAL1-S #1 and #2, as well as, HYAL1-AS clones. Apoptotic activity was also high in PC-3 ML HYAL1-S # 3 and # 4 transfectant clones. We also found that partially purified HYAL1 at concentrations > 80 mU/ml induced apoptosis in DU145 vector, HYAL1- S # 1 and # 2 and HYAL1-AS clones (Data not shown). These results show that CaP cells which either do not express or moderately over-express HYAL1 can be induced to undergo apoptosis by exposing them to > 80 mU/ml HYAL1 concentration.

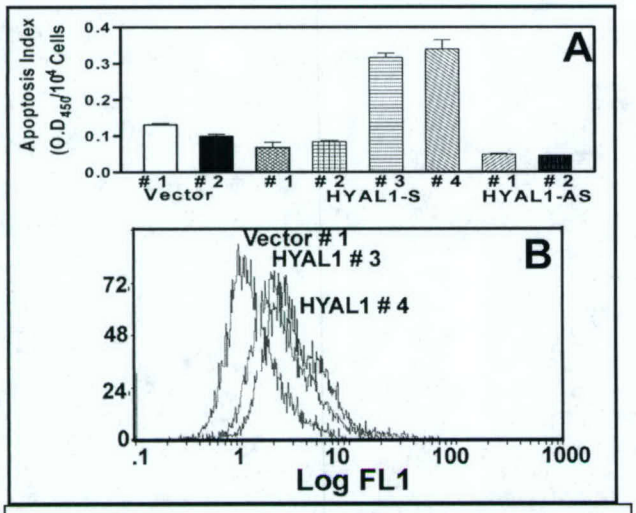

Figure 8: Examination of apoptosis. A: Apoptotic activity. Data: Mean ± S.D. (3 measurements each in 2 experiments). **B:** EGFP-Annexin V binding. Expt. was repeated twice.

To confirm the induction of apoptosis, we measured the outward translocation of plasma membrane phosphyatidyl serine by Annexin-V binding assay. Annexin-V binding was examined in 96-h cultures of HYAL1 vector and HYAL1-S # 3 and # 4 clones using the ApoAlert™ Annexin V-EGFP kit (BD-Clontech Laboratories, Inc.) and flow-cytometry. The median fluorescence intensity (Annexin V binding to PS) was compared among transfectants in the green fluorescence channel (log FL1). As shown in **Fig 8 B**, there is a distinct increase in EGFP-Annexin V binding to HYAL1-S # 3 and # 4 cell surface when compared to vector control (Median peak LogFL1: vector: 1.21; HYAL1-S # 3, 2.37; HYAL1-S # 4, 2.83). Therefore, the decreased cell growth observed in high HYAL1 producers is due to induction of apoptosis.

Fig 9: WOX1 expression. Lanes 1: Vector # 1; lanes 2 - 5: HYAL1-S # 1-4; lanes 6 & 7: HYAL1-AS 1 & 2

Analysis of WOX-1 expression in DU145 transfectants. To determine whether HYAL1-mediated apoptosis might involve WOX-1, we analyzed the expression of all WOX-1 isoforms by immunobloting using a WOX1 monoclonal antibody (EMD Biosciences). This antibody detects all of the 8 WOX1 isoforms, that are generated by mRNA splicing. As shown in **Fig 9**, DU145 cells express 2 WOX-1 isoforms (v1: 46 kDa and v8: 60 kDa). Expression of both of these isoforms is elevated ~ 3-fold in HYAL1-S # 3 and # 4 clones when compared to vector, moderate HYAL1 overproducers (HYAL1-S # 1) and HYAL1-AS transfectants. Both WOX1 v1 and v8 isoforms contain all of the function domains required for inducing apoptosis, as demonstrated in the L929 fibroblast system. (51).

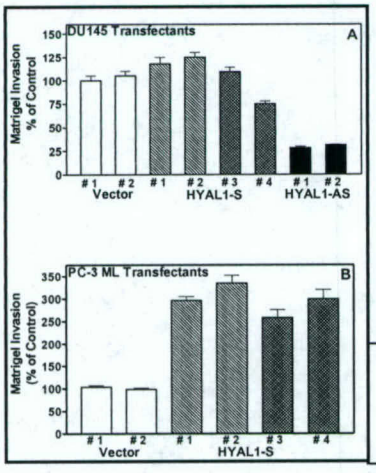

Fig 10: Invasion assay: Data: mean ± SD; n=2 measurements in 3 experiments.

C.c.5. Effect of HYAL1 expression on *in vitro* invasion: Matrigel invasion assay was performed to study the effect of HYAL1 expression on the invasive activity of HYAL1 transfectants. Briefly, membranes in 12-well Transwell plates were coated with Matrigel (100 µg/cm^2). Transfectants (3x10^5 cells/well) were plated on the upper chamber in a serum-free medium and the bottom chamber contained growth medium. Following 48-h incubation, invasion of cells through Matrigel into the bottom chamber was quantified using the MTT assay (49,50). To

normalize the differences in the rate of cell proliferation among various transfectants, invasion results were calculated as cells in the bottom chamber ÷ cells in upper + bottom chambers) x 100. The invasive activity of vector clones was considered as 100%. As shown in **Fig. 10 A**, the invasive activity of DU145 HYAL1-S clones (both moderate and high producers) is similar to that of vector clones. However, the invasive activity of HYAL1-AS clones is 3-fold less when compared to vector clones ($P < 0.001$; Tukey's test). As shown in **Fig. 10 B**, HYAL1 expression in PC3-ML cells increases their invasive activity by 3-3.5-fold ($P < 0.001$). These results show that HYAL1 expression increases the invasive activity of CaP cells.

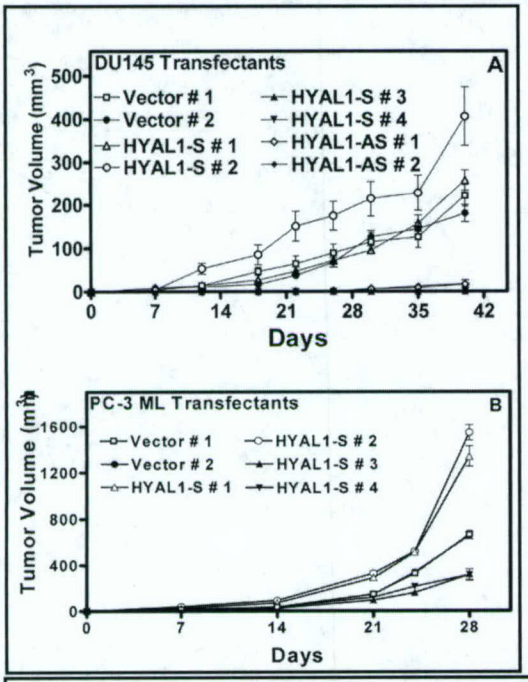

Fig 11: DU145 and PC-3 ML transfectant tumor growth. Data: mean ± SD.

C.c.6. Effect of HYAL1 expression on tumor xenografts: Transfectants (2 x 10^6 cells) were subcutaneously implanted on the dorsal flank of 5-week old male athymic mice (10 mice/clone). After tumors became palpable, tumor size was measured 2x weekly. Tumor volume was calculated assuming an ellipsoid shape (38). Following euthanasia (DU145: 42 day; PC-3 ML: 28 day), tumors were weighed.

As shown in **Fig. 11 A**, there is a 4-5-fold delay in the generation of palpable tumors in animals injected with DU145 HYAL1-AS transfectants (33 ± 4 days) when compared to vector and moderate HYAL1overproducing transfectants (6 – 8 days) ($P < 0.001$; Tukey's multiple comparison's test). Interestingly, **high HYAL1 producers did not form palpable tumors even on day 40 when necropsy was performed**. The weight (g) of vector (# 1: 0.17 ± 0.05; # 2: 0.14 ± 0.04) and moderate HYAL1 overproducers (HYAL1-S # 1: 0.21 ± 0.06; # 2: 0.27 ± 0.14) tumors was 4- and 7-fold more than HYAL1-AS tumors (#1: 0.03 ± 0.01; 0.04 ± 0.01) ($P < 0.001$). While **no animals injected with HYAL1-S # 3 or # 4 transfectants had visible evidence of tumor**, in some animals Matrigel™ plug-like material was visible. High HYAL1 producing transfectants generated in a 2nd transfection experiment also did not form tumors (data not shown).

Moderate HYAL1 producing PC-3 ML tumors (HYAL1-S # 1 and # 2) grow about 2-fold faster, whereas, high HYAL1 producing tumors grow 2-2.5-fold slower than vector tumors (**Fig. 11 B**). At day 28, the weights (g) of moderate HYAL1 producing tumors (#1: 0.57 ± 0.12; # 2: 0.6 ± 0.14) were 2-fold higher than vector tumors (# 1: 0.28 ± 0.06; # 2: 0.29 ± 0.04) and 3.5-fold higher than high HYAL1 producing tumors (# 3: 0.16 ± 0.03; # 4: 0.14 ± 0.05) ($P < 0.001$).

C.c.7. Tumor histology, HA, HYAL1 localization and MVD determination: Histology of tumor xenografts was performed at Charles River Laboratories. As shown in **Fig. 12,** histology reports and photomicrographs show that while DU145 vector and moderate HYAL1 producing tumors show high mitotic figures, invade skeletal muscle and lymph nodes and infiltrate lymphatic and blood vessels HYAL1-AS tumors are non-invasive (tumor does not invade muscle panel E). The Matrigel™ plug-like material removed from HYAL1-S # 3 and # 4 animals is ≥ 99% free of tumor cells and no mitotic figures are observed (Fig 12 A panel, F).

To confirm that transfectants retained their phenotype regarding HYAL1 expression, HYAL1 (and also HA) was localized in tumor xenografts using the methods described in section C.a. As shown in **Fig. 13 A**, tumor cells in vector, and HYAL1-S # 1 and # 2 xenografts express significant levels of HYAL1 but HYAL1-AS cells do not secrete HYAL1 (Fig 16). Interestingly, HA production increased in the tumor-associated stroma of vector and HYAL1-S # 1 tumor specimens when compared to HYAL1-AS # 1 tumor specimens (Fig 16). Since HYAL1-S # 3 and # 4 specimens contained only Matrigel, they were not evaluated for HA, HYAL1 or MVD determinations.

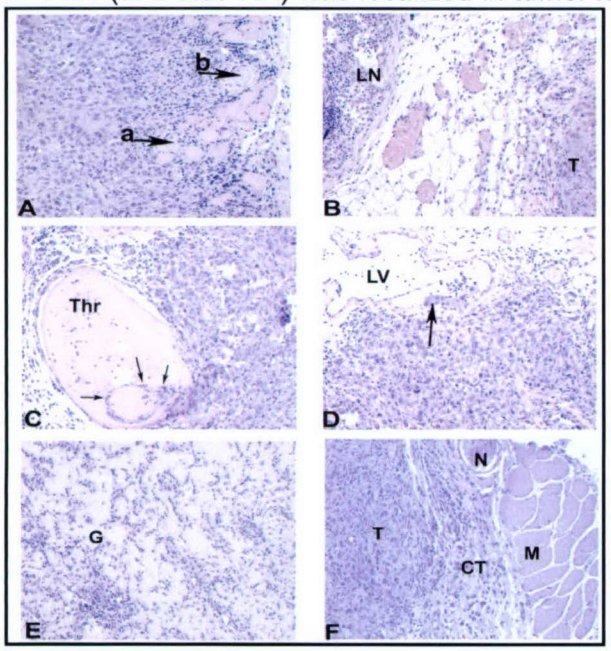

Fig 12: Tumor histology: A & B: Vector # 1, # 2; C & D: HYAL1-S # 1, # 2; E: HYAL1-S # 3; F: HYAL1-AS # 4

MVD was determined as described in section C.a using rat anti-mouse CD34 monoclonal antibody. MVD in vector was only 1.4-fold higher than HYAL1-AS tumors ($P > 0.05$). However, the length of capillaries in vector (817.4 ± 141.5 μm) and HYAL1-S (# 1: 1031 ± 262.5; # 2: 817.9 ± 305.3) tumors was 4-5-fold higher than of capillaries in HYAL1-AS tumors (# 1: 218.1 ± 103.4; # 2: 247.1 ± 96.1) (**Fig. 13 B**).

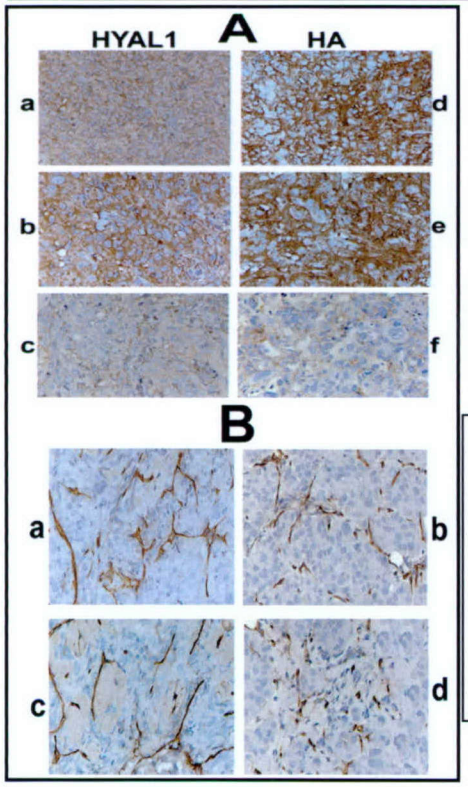

Figure 13: A: HYAL1 and HA localization: Panels a,b,c: HYAL1; Panels d,e,f: HA. Panels a & d: vector # 1; panels b & e: HYAL1-S # 1; panels c & f: HYAL1-AS # 1. **B: Localization of microvessels.** Panel a: vector # 1; panel b: HYAL1-S # 1; panel c: HYAL1-S # 2; panel d: HYAL1-AS # 1.

Screening of HAase inhibitors: To identify the most effective inhibitors of HYAL1 that are also somewhat selective, we screened 21 HAase inhibitors against HYAL1 and 3 other HAases, including bovine testicular HAase. The inhibitors included polymers of poly (styrene-4-sulfonate) (mol. wt. 1400 to 9.9×10^5 Dalton i.e., PSS1400 to PSS990,000; Fluka Biochem.) and O-sulfated HA derivative containing 2, 3, or 4 sulfonate groups (sHA 2.0; sHA 3.0; sHA 4.0), heparin and gossypol. sHA derivatives were synthesized using a method described by Barbucci et al. Briefly, tributylamine salt of human umbilical cord HA- sodium salt was suspended in anhydrous dimethyl formamide and mixed with various amounts of anhydrous SO_3^- pyridine under a stream of nitrogen. The amount of SO_3^- pyridine determines the number of O-sulfated groups on the HA (52). Sulfated HA was then precipitated, dialyzed against water and lyophilized. sHA compounds were analyzed in the NMR facility of University of Miami.

IC_{50} values of HAase inhibitors that inhibited HYAL1activity are shown in Table 6. Among HAase inhibitors, both PSS and sHA derivatives are the most effective inhibitors of HYAL1.

Inhibitors	HYAL1 IC_{50} (μM)	Bee venom HAase IC_{50} (μM)	Bovine PH20 IC_{50} (μM)	Strep. HAase IC_{50} (μM)
PSS 990,000	0.0096	0.0091	0.042*	0.39*
PSS 17,000	0.89	1.0	0.89	NI
PSS 1400	8.2	6.6	67.6*	NI
PSS 210	NI	NI	NI	NI
sHA 2.0	0.03	0.029	0.12*	NI
sHA 3.0	0.028	0.03	0.08	NI
sHA 4.0	0.014	0.02	0.064*	NI
Heparin	0.39	0.41	1694*	NI
Gossypol	NI	NI	NI	NI
1-Tetradecane sulfonic acid	63*	NI	NI	NI
Glycerrhizic acid	39.4*	NI	NI	NI

Table 6: IC_{50} values of HAase inhibitors for HYAL-1, bee, testicular and Streptomyces HAases. The IC_{50} value for each inhibitor was calculated by generating an inhibition curve. NI: No inhibition; *: Significant differences. Note: PSS 990,000 is same as VERSA-TL 502

C.2 Effect of HAase inhibitors on the growth of DU145, LNCaP and PC3-ML cells. In addition to testing the effect of VERSA-TL 502 on the growth of CaP cells, which was proposed in the application, we also tested the effect of lower mol. wt. PSS compounds (PSS17,000, 6,800 and 1400) on the growth of DU145, PC-3 ML and LNCaP. Briefly, CaP cells (1.5 x 10^4 cells/well) were plated on 24-well plates in growth medium in the presence of various concentrations (0-20 μg/ml) of VERSA-TL 502, PSS 17,000, 6,800 and PSS1400. Every 24-hr for 96-hr, cells were stained with trypan blue and counted. As shown in Fig. 14 and 15, HAase inhibitors inhibit the growth of DU145 and LNCaP cells, both of which secrete HAase and express HYAL1. However, the HAase inhibitors do not inhibit the growth of PC-3 ML cells which do not secrete HAase. These results show that PSS compounds inhibit the growth of CaP cells by inhibiting tumor-derived HAase.

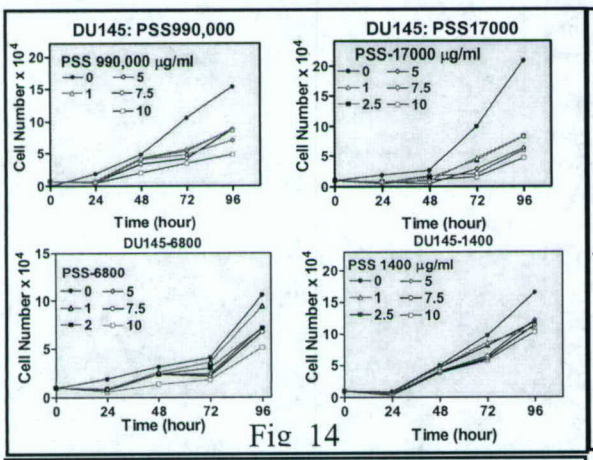

Fig 14

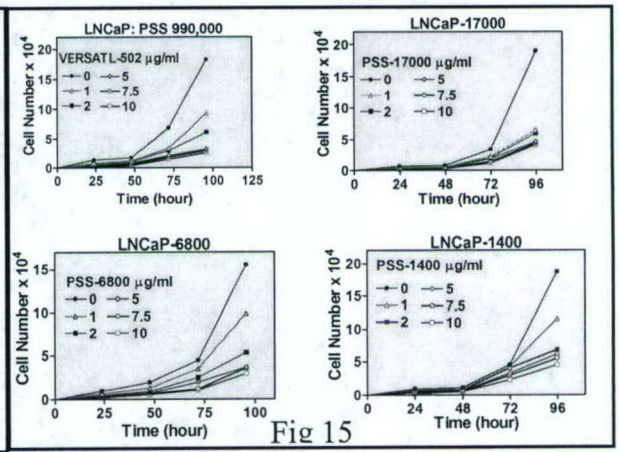

Fig 15

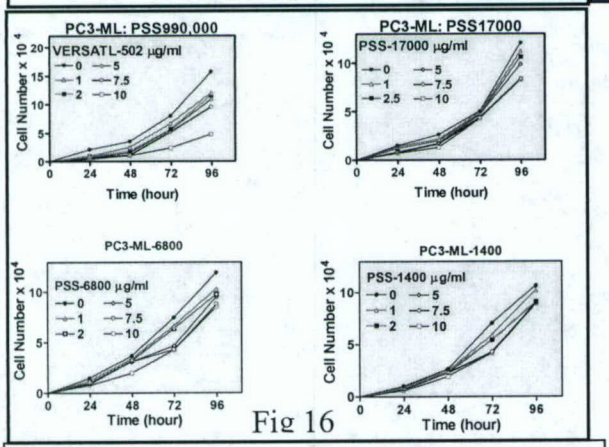

Fig 16

Figure 14, 15, 16: Effect of PSS compounds on the proliferation of DU145 (Fig 14), LNCaP (Fig 15) and PC3-ML (Fig 16)

D. (BODY) Experiments in progress : Progress related to Aim 3:

Rationale and background: Data presented in the above section show that HYAL1 is a molecular determinant of CaP growth and progression. This is the **first report** that demonstrates that depending upon the concentration, HYAL1 can act both as a tumor promoter and a suppressor. Since this is a novel finding the mechanisms by which HYAL1 can act as a tumor promoter and as a suppressor are unknown. To understand the mechanisms by which HYAL1 regulates both of these processes we performed cDNA microarray analysis on DU145 transfectants.

Experimental procedures:

Gene expression analysis: To examine the mechanisms by which HYAL1 (i.e., either its over-expression and inhibiton) may inhibit CaP growth, invasion and angiogenesis, microarray and bioinformatics analyses were performed in the DNA microarray facility of University of Miami. Briefly, total RNA was isolated from DU145 vector, HYAL1-S #3, HYAL1-S #4 and HYAL1-AS #1, #2 transfectants. The RNA was reverse transcribed and the cDNAs were labeled with either Cy-5 or Cy-3. Labeled cDNAs from 2 independent experiments were hybridized as pairs (vector: HYAL-S # 3 or vector : HYAL1-S # 4), to the 20K human oligo microarrays (Agilent Tech) as per the manufacturer's instructions. For each biological replicate we performed two technical sub-replicates for dye-swap. The microarrays were scanned using GenePix 4000A (Axon Instruments, Inc.). The microarrays were scanned at 10-□m resolution using a GenePix 4000A scanner (Axon Instruments; Molec. Devices). Resulting images were analyzed with the software package GenePix Pro 5.1 (Axon Instruments). Data extracted from the images were transferred to the software package Acuity 4.0 (Axon Instruments) for normalization and statistical analysis. Data from each array were normalized using both color normalization across the whole array and Lowess normalization. Only those genes, which showed differential expression in both clones, were selected for further analysis. To identify significantly expressed genes we used one class SAM (Significant Analysis of Microarray, http://www-

Gene name	HYAL1-S # 3 & # 4	HYAL1-AS # 1 & # 2
Cell growth		
Cyclin B1		2.6 ± 0 .87, 2.0 ± 0.53 ↓
DUSP1		2.0 ± 0.55, 1.9 ± 0.4↑
CKS2		2.8 ± 0.73, 2.0 ± 0.21↓
Apoptosis		
BAG1	2.0 ± 0.46, 3.1± 1.3 ↓	
IL 24	3.1 ± 0.75, 4.8 ± 0.82↑	
Clusterin	1.7 ± 0.32, 2.6 ± 0.35 ↑	
BAG5	2.4± 0.26, 2.7± 0.52 ↑	
JNK pathway		
CRKL	1.8 ± 0.25, 2.9 ± 0.61↑	
MAP4K5 (KHS1)	2.4 ± 0.37, 1.8 ± 0.28 ↑	
Angiogenesis		
CXCL1		2.0 ± 0.19, 3.4 ± 0.59 ↓
CXCL2		1.6 ± 0.14, 1.8 ± 0.37 ↓
b-FGF 2		2.4, 2.1 ↓
Invasion/metastasis		
Collagen type IV	2.4 ± 0.43, 3.3± 0.94 ↑	
MMP-1		46.0± 9.5, 28±8.6 ↓
CD44		3.8±0.78, 4.7±1.1 ↓
uPA		4.1±0.52, 2.8±0.63 ↓
Autocrine motility factor		1.7±0.33, 1.6±0.41 ↓

Table 5: Gene expression analysis. ↑: up-regulation; ↓: down-regulation

Microarray, http://www-stat.stanford.edu/~tibs/SAM) analysis and NIA Array Analysis ANOVA tool (http://lgsun.grc.nia.nih.gov/ANOVA). The selected genes were classified according to Gene Ontology category "biological process" using Onto-Express (http://vortex.cs.wayne.edu/Projects.html) (58, 59). Among the differentially expressed genes, we focused on genes related to cell cycle, apoptosis, invasion and angiogenesis.

As shown in **Table 5**, HYAL1 expression regulates the expression of several genes involved in cell cycle, apoptosis, angiogenesis and invasion/metastasis pathways. We used the software ( ) to perform pathway analysis. **Fig. 17** shows our working model regarding HYAL1 functions. In the cell cycle pathway, HYAL1 may influence the G2-M progression by modulating cyclin B1 and CKS2 expression and/or by activating the JNK pathway through regulation of CRKL and KHS1 gene expression. At the present time, there is no experimental evidence whether HYAL1 also influences the MEK-7-JNK-c-jun and induces ERK1/2 (similar to bovine testicular HAase) pathway for promoting G2-M transition. Over-expression of HYAL1 may induce apoptosis through a mitochondria-mediated pathway that involves WOX1, IL24, BAG1, BAG5 and/or JNK (please see section B.a). It is noteworthy that although we observed increased expression of WOX1 v1 and v8 proteins in HYAL1-S # 3 and #4 transfectants (section C.c.4), no over-expression of WOX1 was observed in the microarray analysis. However, the human oligo microarrays from Agilent include only WOX1 v2, v4 and v7 oligo arrays, thus, no information on WOX1 v1 and v8 differential expression could be obtained using by these microarrays. Induction of ERK1 and JNK pathways by HYAL1 may be responsible for the observed increase in the expression of MMP-1 and uPA genes, and thereby increasing the invasive activity of CaP cells.

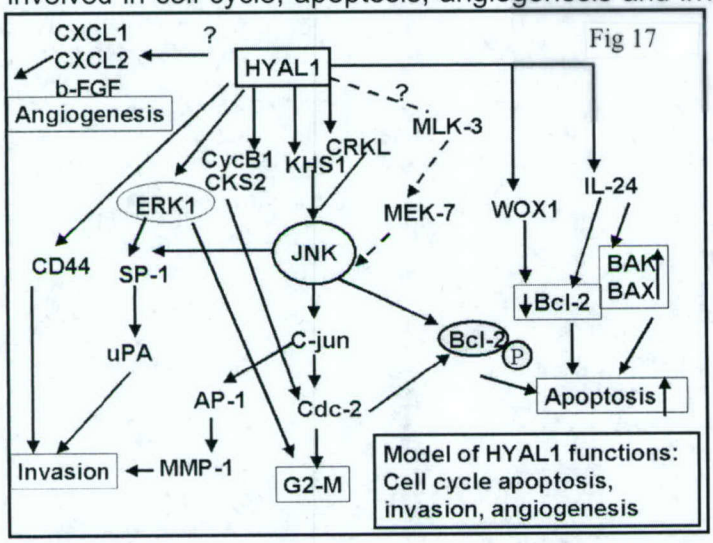

Fig 17

It is also noteworthy that HYAL1 increases the expression of the **gene for CD44**, which is a HA receptor. CD44 is a family of glycoproteins made up of several isoforms, some of which are associated with metastasis (e.g., CD44-v6). For example, DU145 and PC-3 ML cells express both CD44 standard form (~ 85-90 kDa) and CD44-v6 isoform. We have shown that CD44 v6 is over-expressed in CaP tissues (section B). If HYAL1 indeed regulates the expression of CD44 and its isoforms, it may explain why CD44 v6 was not found to be a prognostic indicator of biochemical recurrence when HYAL1 staining was included in the analysis (section C.b.2, Appendix 3).

At the present time it is unknown how HYAL1 induces the expression of genes that encode CD44, autcrine motility factor and angiogenesis promoting genes (i.e., CXCL1, CXCL2 and b-FGF), however, autocrine motility factor induces JNK1 and JNK2 expression ( ). We plan to test the validity the working model of HYAL1 function by examining the expression of the protein products of genes that are differentially expressed under high-HYAL1 and no-HYAL1 conditions.

Experiments in progress:

Examination of the effect of VERSA-TL 502 on CaP growth: We are in the planning process to study the effect of VERSA-TL 502 on the growth of DU145 cells in xenografts. These experiments will begin in March.

Effect of VERSA-TL 502 on CaP gene expression: In the next year, we will examine how HAase inhibitor VERSA-TL 502 affects gene expression in DU145 cells using cDNA microarray analysis. We will compare genes that are differentially expressed in VERSA-TL treated DU145 cells and those differentially expressed in DU145 HYAL1-AS transfectants. Since these are 2 different approaches to inhibit HYAL1 activity, the comparison will help us to identify cell cycle, invasion and apoptosis-related genes that are under HYAL1 regulation.

2 Key Research accomplishments:

A. Establishment of HYAL1 and combined HA-HYAL1 staining inferences as potentially accurate predictors of biochemical recurrence. The studies presented here are **the first**, which demonstrate the prognostic potential of HYAL1 in any type of cancer.

B. This is the **first demonstration** HYAL1 (or any other HAase) acts as both a tumor promoter and a suppressor depending upon the concentration to which tumor cells are exposed.

HYAL1 induces G2-M transition in CaP cells, stimulates CaP cell growth, invasion and angiogenesis.

At concentration > 100 mU/ml, HYAL1 acts as a **novel apoptotic protein** and high HYAL1 expression inhibits tumor generation.

C. Our findings that HYAL1 in general) can act both as a tumor promoter and a suppressor **resolve the controversy** regarding the role of HAases in cancer. These findings form the basis for testing potential of anti-HAase and high-HYAL1 treatment modalities to control CaP growth and progression

D. Synthetic HAase inhibitors inhibit HAase activity secreted by CaP cells and also inhibit the growth of CaP cells. The growth inhibitory activity of HAase inhibitors correlates with their ability to inhibit HAase activity.

3. Reportable outcomes:

A. Database of CaP patients with long-term follow-up (72 – 131 months).

B. Generation of HYAL1-sense (both moderately producing and overproducing) and HYAL1-antisense (under producing) stable cell lines of DU145 and PC3-ML cells.

C. Identification of intracellular pathways and signaling molecules involved in HYAL1-induced CaP growth and progression.

D. Identification of HAase inhibitors that may be used for controlling CaP growth.

E. I am applying for a NIH RO1 application entitled, Extracellular matrix glycosidases in prostate cancer. This application is possible only because of the funding that I received from the CDMRP/PCRP.

F. Publications:

1. Lokeshwar, V.B. Schroeder, G.L., Carey, R.I. Soloway, M.S., Iida, N. Regulation of hyaluronidase activity by alternative mRNA splicing. J. Biol. Chem. 277: 33654-33663, 2002.

2. Posey, J.T., Soloway, M.S., Ekici, S., Sofer, M., Civantos, F., Duncan, R.C., Lokeshwar, V.B. Evaluation of the prognostic potential of hyaluronic acid and hyaluronidase (HYAL1) for prostate cancer. Cancer Res. 63: 2638-2644, 2003.

3. Franzmann, E., Schroeder, G.L., Goodwin, G.J., Weed, D., and **Lokeshwar, V.B.** Expression of tumor markers, hyaluronic acid and hyaluronidase, in head and neck tumors. Int. J. Cancer 106: 438-445, 2003.

4. Ekici S., Cerwinka, W.H., Duncan, R. C. Gomez, P., Civantos, F., Soloway, M.S., Lokeshwar, V.B. Comparison of the prognostic potential of hyaluronic acid, hyaluronidase (HYALI-1), CD44v6 and Microvessel density for prostate cancer . Int J Cancer 112: 121-129, 2004

5. Lokeshwar, V.B. Cerwinka, W. H., Lokeshwar, B.L. HYAL1 hyaluronidase: A molecular determinant of bladder cancer growth and progression. Cancer Res. (In Press), 2005

6. Lokeshwar, V.B., Isoyama, T., Thwaites, F., Selzer, M.G., Carey, R.I. Schroeder, G.L. Differential selectivity of hyaluronidase inhibitors towards acidic and basic hyaluronidases (Submitted to Biochem. Biophys. Acta, 2005).

7. Lokeshwar, V.B. Cerwinka, W. H., Lokeshwar, B.L. HYAL1 hyaluronidase in prostate cancer: A tumor promoter and a suppressor. (To be submitted to Proc. Natl. Acad. Sci. USA).

E. Abstracts:

1. Lokeshwar, V.B.*, Posey, J.T., Schroeder, G.L. (2002) HA and HAase in prostate cancer: molecular markers with function. Fourth International Innovators in Urology Meeting, Miami, Florida. Prostate cancer and Prostatic Diseases 5: suppl. 1., S19.

2. Lokeshwar, V.B.*, Posey, J.T., Schroeder, G.L. (2002) HA and HAase in prostate cancer: molecular markers with function. Sylvester Comprehensive Cancer Center Poster Presentation (Annual Zubrad Lecture/Poster Meeting; First Prize in Faculty category).

3. Dandekar DS, **Lokeshwar, VB**, Cevallos E, Lokeshwar BL. (2003) Plant extract "BIRM" induces G0/G1 Arrest and caspase-mediated apoptosis in vitro and inhibits in vivo tumor growth and metastasis of prostate cancer. AACR Proceedings Vo 44, #648, p148.

5. Dandekar DS, Lokeshwar, VB, Cevallos E, Lokeshwar BL. (2003)Induction of caspase-mediated apoptosis and inhibition of prostate tumor grwoth and metastasis by a plant extract - BIRM.Miami Nature Biotechnology Short Reports. vol 14:106.

6. Ekici S., Cerwinka, W.H., Duncan, R. C. Gomez, P., Civantos, F., Soloway, M.S., Lokeshwar, V.B. Comparison of the prognostic potential of hyaluronic acid, hyaluronidase (HYALI-1), CD44v6 and Microvessel density for prostate cancer (AUA 2004; Accepted for Poster Discussion session).

7. Cerwinka, W.H., Lokeshwar, B.L., Lokeshwar, V.B. HYAL1 hyaluronidase in prostate cancer: A tumor promoter or a suppressor (AUA 2005, Discussed

Poster session).

F. Patents: No patents were filed or issued.

G. Clinical translational research: No clinical trials were undertaken.

H. Personnel and training provided: This award has allowed the P.I. to provide research training to two attending urologists. Dr. Sinan Ekici was a fellow of the Turkish Research Council and worked on Aim 1 of the project. Dr. Tadahiro Isoyama is currently working in the laboratory on work related to Aims 2 and 3. In addition, the award has allowed the P.I. to provide research training to a total of 5 urology residents in the Department of Urology at University of Miami. In addition to the trainees, a pathologist, a research associate a statistician and the P.I. worked on this project. One clinical fellow in the department of urology, together with the collaborating urologist, provided the clinical information.

4. Conclusions: Results derived from the experiments performed under Aim 1, demonstrate that HYAL1 and HA-HYAL1 are sensitive and specific markers for predicting biochemical recurrence for CaP patients who undergo radical prostatectomy. The multivariate analysis and long-term follow-up information establishes **for the first time**, the independent prognostic potential of HYAL1 type HAase for any type of cancer, in general, and for CaP in particular. The results derived from experiments performed under Aims 2 and demonstrate **for the first time** that tumor-derived HAase in general and HYAL1 in particular act as both a tumor promoter and a suppressor, depending upon the concentration to which tumor cells are exposed. These results demonstrate that **both anti-HAase and high-HYAL1 treatments may have merit** in controlling CaP growth and progression.

5. REFERENCES:

1. Pettaway, C.A. Prognostic markers in clinically localized prostate cancer. Tech. Urol., 4: 35-42, 1998.
2. Blute, M.L. Bergstralh, E.J., Iocca, A., Scherer, B., Zincke, H. Use of Gleason score, prostate specific antigenm seminal vesicle and margin status to predict biochemical failure after radical prostatectomy. J. Urol., 165: 119-125, 2001.
3. Muzzonigro, G., Galosi, A.B. Biological selection criteria for radical prostatectomy. Ann N Y Acad Sci. 963:204-212, 2002.
4. Small, E.J., Roach M 3rd. Prostate-specific antigen in prostate cancer: a case study in the development of a tumor marker to monitor recurrence and assess response. Semin Oncol. 29: 264-73, 2002.
5. Palisaan, R.J., Graefen, M., Karakiewicz, P.I., Hammerer, P.G., Huland, E., Haese, A., Fernandez, S., Erbersdobler, A., Henke, R.P., Huland, H. Assessment of clinical and pathologic characteristics predisposing to disease recurrence following radical prostatectomy in men with pathologically organ-confined prostate cancer. Eur Urol. 41:155-161, 2002.
6. Isaacs W, De Marzo A, Nelson W. Focus on prostate cancer. Cancer Cell. 2:113-116, 2002.
7. Muzzonigro, G., Galosi, A.B. Biological selection criteria for radical prostatectomy. Ann N Y Acad Sci. 963:204-212, 2002.
8. Partin, A.W., Murphy, G.P., Brawer, M.K. Report on Prostate Cancer Tumor Marker Workshop 1999. Cancer, 88: 955- 963, 2000.
9.Tool, BP. Hyaluronan is not just a gloo! J. Clin. Invest. 106: 335-336, 2000.
10. Delpech, B., Girard, N., Bertrand, P., Courel, N.M., Chauzy, C., Delpech, A. Hyaluronan: Fundamental principles and applications in cancer. J. Intern. Med. 242: 41-48, 1997.

11.Hautmann, S.H., Lokeshwar, V.B., Schroeder, G.L., Civantos, F., Duncan, R.C., Friedrich, M.G., Soloway, M.S. Elevated tissue expression of hyaluronic acid and hyaluronidase validate HA-HAase urine test for bladder cancer. J. Urol., 165: 2068-2074, 2000.
12. Setala, L.P., Tammi, M.I., Tammi, R.H., Eskelin, M.J., Lipponen, P.R., Argen, U.M., Parkkinen, J., Alhava, E.M., Kosma, V.M., Hyaluronan expression in gastric cancer cells is associated with local and nodal spread and reduced survival rate. Br. J. Cancer, 79: 1133-1138, 1999.
13. Auvinen, P., Tammi, R., Parkkinen, J., Tammi, M., Agren, U., Johansson, R., Hirvikoski, P., Eskelinen, M., Kosma, V.M., Hyaluronan in peritumoral stroma and malignant cells associates with breast cancer spreading and predicts survival. Am. J. Pathol., 156: 529-536, 2000.
14. Pirinen, R., Tammi, R., Tammi, M., Hirvikoski, P., Parkkinen, J.J., Johansson, R. Prognostic value of hyaluronan expression in non-small-lung cancer: increased stromal expression indicates unfavorable outcome in patients with adenocarcinoma. Int J Cancer 95: 12-27, 2001.
15. Knudson, W. Tumor associated hyaluronan: providing an extracellular matrix that facilitates invasion. Am. J. Pathol., 148: 1721-1726, 1996.
16. Ropponen, K., Tammi, M., Parkkinen, J., Eskelinen, M., Tammi, R., lipponen, P., Argen, V., Alhava, E., Kosma, V.M. Tumor-associated hyaluronan as an unfavorable prognostic factor in colorectal cancer. Cancer Res., 58:342-347, 1998.
17. Lipponen, P., Aaltomaa, S., Tammi, R., Tammi, M., Agren, U., Kosma, V.M. High stromal hyaluronan level is associated with poor differentiation and metastasis in prostate cancer. Eur. J. Cancer 37: 849-856, 2001.
18. Lokeshwar, V.B., Obek, C., Pham, H.T., Wei, D.C., Young, M.J., Duncan, R.C, Soloway, M.S., Block, N.L. Urinary hyaluronic acid and hyaluronidase: Markers for bladder cancer detection and evaluation of grade. J. Urol., 163: 348-356, 2000.
19. Lokeshwar, V.B., Obek, C., Soloway, M.S., Block, N.L. Tumor-associated hyaluronic acid: A new sensitive and specific urine marker for bladder cancer. Cancer Res., 57: 773-777, 1997.
20. Lokeshwar, V.B., Rubinowicz, D., Schroeder, G.L., Forgacs, E., Minna, J.D., Block, N.L. Nadji, M., Lokeshwar, B.L. Stromal and epithelial expression of tumor markers hyaluronic acid and hyaluronidase in prostate cancer. J. Biol. Chem. 276: 11922-11932, 2001.
21. Roden, L., Campbell, P., Fraser, J.R.E., Laurent, T.C., Petroff, H., Thompson, J.N. Enzymatic pathways of hyaluronan catabolism. In: The biology of hyaluronan. Whelan, E, (ed), Wiley, Chichister, Ciba Foundation Symp., 143, pp-60-86, 1989.
22. Csoka, A.B., Frost, G.I., Stern, R. The six hyaluronidase-like genes in the human and mouse genomes. Matrix Biol. 20: 499-508, 2001.
23.Lokeshwar, V.B., Lokeshwar, B.L., Pham, H.T., Block, N.L. Association of hyaluronidase, a matrix-degrading enzyme, with prostate cancer progression. Cancer Res., 56: 651-657, 1996.
24. Anderson, A.R., Feathergill, K., Diao, X., Cooper, M., Kirpatrick, R., Spear, P., Waller, D.P., Chany, C., Doncel, G.E., Herold, B., Zaneveld, L.J.D. Evaluation of poly(styrene-4-sulfonate) as a preventive agent for conception and sexually transmitted diseases. J. Androl., 21: 862-875, 2000.
25. Posey, J.T., Soloway, M.S., Ekici, S., Sofer, M., Civantos, F., Duncan, R.C., Lokeshwar, V.B. Evaluation of the prognostic potential of hyaluronic acid and hyaluronidase (HYAL1) for prostate cancer. Cancer Res. 63: 2638-2644, 2003.
26. Lesley, J, Hascall, VC, Tammi, M, Hyman, R. Hyaluronan binding by cell surface CD44. J Biol Chem. 2000 275: 26967-26975.
27. Cichy, J, Pure, E. The liberation of CD44. J Cell Biol. 2003, 161: 839-843.
28. Naor, D, Nedvetzki, S, Golan, I, Melnik, L, Faitelson, Y. CD44 in cancer. Crit Rev Clin Lab Sci. 2002, 39: 527-579.
29. Lokeshwar, BL, Lokeshwar, VB, Block, NL. Expression of CD44 in prostate cancer cells: association with cell proliferation and invasive potential. Anticancer Res. 1995, 15: 1191-

30. Welsh, CF, Zhu, D, Bourguignon, LY. Interaction of CD44 variant isoforms with hyaluronic acid and the cytoskeleton in human prostate cancer cells. J Cell Physiol. 1995, 64: 605-612.
31. Iczkowski, KA, Bai, S, Pantazis, CG. Prostate cancer overexpresses CD44 variants 7-9 at the messenger RNA and protein level. Anticancer Res. 2003 234: 3129-3140.
32. Gao, AC., Lou, W., Sleeman, JP, Isaacs, JT. Metastasis suppression by the standard CD44 isoform does not require the binding of prostate cancer cells to hyaluronate. Cancer Res. 1998, 58: 2350-2352.
33. Ekici, S, Ayhan, A, Kendi, S, Ozen, H. Determination of prognosis in patients with prostate cancer treated with radical prostatectomy: prognostic value of CD44v6 score. J Urol, 167: 2037-2041, 2002.
34. Aaltomaa, S, Lipponen, P, Ala-Opas, M. Kosma, VM. Expression and prognostic value of CD44 standard and variant v3 and v6 isoforms in prostate cancer. Eur Urol., 2001 39:138-144.
35.Folkman, J, Browder, T, Palmblad, J. Angiogenesis research: guidelines for translation to clinical application. Thromb Haemost. 2001, 86: 23-33.
36. Sauer, G, Deissler, H. Angiogenesis: prognostic and therapeutic implications in gynecologic and breast malignancies. Curr Opin Obstet Gynecol. 2003, 15: 45-49.
37. Goddard, JC, Sutton, CD, Furness, PN, O'Byrne, KJ, Kockelbergh, R.C. Microvessel density at presentation predicts subsequent muscle invasion in superficial bladder cancer. Clin Cancer Res. 2003, 9: 2583-2586.
38. Poon, RT, Fan, ST, Wong, J. Clinical significance of angiogenesis in gastrointestinal cancers: a target for novel prognostic and therapeutic approaches. Ann Surg. 2003, 238: 9-28.
39. Zhang, X, Yamashita, M, Uetsuki, H, Kakehi, Y. Angiogenesis in renal cell carcinoma: Evaluation of microvessel density, vascular endothelial growth factor and matrix metalloproteinases. Int J Urol. 2002, 9: 509-514.
40. De La Taille, A, Katz, AE, Bagiella, E, Buttyan, R, Sharir, S, Olsson, CA, Burchardt, T, Ennis, RD, Rubin, MA. Microvessel density as a predictor of PSA recurrence after radical prostatectomy : A comparison of CD34 and CD31. Am J Clin Pathol 2000, 113: 555-562.
41. Bono, AV, Celato, N., Cova, V., Salvadore, M., Chinetti, S., Novario, R. Microvessel density in prostate carcinoma. Prostate Cancer Prostatic Dis. 2002, 5: 123-127.
42. Weidner, N., Carroll, P.R., Flax, J., Blumenfeld, W., Folkman, J. Tumor angiogenesis correlates with metastasis in invasive prostate carcinoma. Am J Pathol 1993, 143: 401-409.
43. Silberman, M.A., Partin, A.W., Veltri, R.W., Epstein, J.I. Tumor angiogenesis correlates with progression after radical prostatectomy but not with pathologic stage in Gleason sum 5 to 7 adenocarcinoma of the prostate. Cancer 1997, 79: 772-779.
44. Gettman, M.T., Bergstralh, E.J., Blute, M., Zincke, H., Bostwick, D.G. Prediction of patient outcome in pathologic stage T2 adenocarcinoma of the prostate: Lack of significance for microvessel density analysis. Urology 1998, 51:79-85.
45. Rubin, M.A., Buyyounouski, M., Bagiella, E., Sharir, S., Neugut, A., Benson, M., De La Taille, A., Katz, A.E., Olsson, C.A., Ennis, R.D. Microvessel density in prostate cancer : Lack of correlation with tumor grade, pathologic stage, and clinical outcome. Urology 1999, 53: 542-547.
46. Ekici S., Cerwinka, W.H., Duncan, R. C. Gomez, P., Civantos, F., Soloway, M.S., Lokeshwar, V.B. Comparison of the prognostic potential of hyaluronic acid, hyaluronidase (HYALI-1), CD44v6 and Microvessel density for prostate cancer Int J Cancer 2004, 112: 121-129.
47. Lokeshwar, V.B., Schroeder, G.L., Carey, R.I., Soloway, M.S., Iida, N. Regulation of hyaluronidase activity by alternative mRNA splicing. J Biol Chem. 277: 33654-33663, 2002.
48. Lokeshwar, V.B., Young M.J., Goudarzi, G., Iida, N., Yudin, A.I., Cherr, G.N., Selzer, M.G. Identification of bladder tumor-derived hyaluronidase: Its similarity to HYAL1. Cancer Res., 59: 4464-4470, 1999.

49. Lokeshwar, V.B., Cerwinka, W.H., Lokeshwar, B.L. HYAL1 hyaluronidase in bladder cancer: A molecular determinant of bladder cancer growth and progression. Cancer Res., 2005, In Press.
50. Lokeshwar, V.B., Cerwinka, W.H., Lokeshwar, B.L. HYAL1 hyaluronidase in prostate cancer: A tumor promoter and a suppressor (To be submitted to Proc. Natl. Acad. Sci, USA).
51. Chang, N.S., Doherty, J., Ensign, A. JNK1 physically interacts with WW domain-containing oxidoreductase (WOX1) and inhibits WOX1-mediated apoptosis. J Biol Chem. 2003; 278: 9195-202.
52. Barbucci, R., Lamponi, S., Magnani, A., Poletti, L.F., Rhodes, N.P., Sobel, M., Williams, D.F. Influence of Sulfation on Platelet Aggregation and Activation with Differentially Sulfated Hyaluronic Acids. J Thromb Thrombolysis. 1998, 6: 109-115.
53. Khatri, P., Draghici, S., Ostermeier, G.C., and Krawetz, S.A. Profiling gene expression using onto-express. Genomics, 2002, 79: 266–70.
54. Draghici, S., Khatri, P., Martins, R.P., Ostermeier, G.C., and Krawetz, S.A. Global functional profiling of gene expression. Genomics, 2003, 81: 98–104.

Int. J. Cancer: **112,** 121–129 (2004)

Publication of the International Union Against Cancer

COMPARISON OF THE PROGNOSTIC POTENTIAL OF HYALURONIC ACID, HYALURONIDASE (HYAL-1), CD44V6 AND MICROVESSEL DENSITY FOR PROSTATE CANCER

Sinan EKICI[1], Wolfgang H. CERWINKA[1], Robert DUNCAN[2], Pablo GOMEZ[1], Francisco CIVANTOS[1], Mark S. SOLOWAY[1] and Vinata B. LOKESHWAR[1,3,4]*

[1]*Department of Urology, University of Miami School of Medicine, Miami, FL, USA*
[2]*Department of Epidemiology, University of Miami School of Medicine, Miami, FL, USA*
[3]*Sylvester Comprehensive Cancer Center, University of Miami School of Medicine, Miami, FL, USA*
[4]*Department of Cell Biology and Anatomy, University of Miami School of Medicine, Miami, FL, USA*

Despite the development of nomograms designed to evaluate a prostate cancer (PCa) patient's prognosis, the information has been limited to PSA, clinical stage, Gleason score and tumor volume estimates. We compared the prognostic potential of 4 histologic markers, hyaluronic acid (HA), HYAL-1-type hyaluronidase (HAase), CD44v6 and microvessel density (MVD) using immunohistochemistry. HA is a glycosaminoglycan that promotes tumor metastasis. CD44 glycoproteins serve as cell surface receptors for HA, and the CD44v6 isoform is associated with tumor metastasis. HYAL-1-type HAase is expressed in tumor cells and, like other HAases, degrades HA into angiogenic fragments. Archival PCa specimens (n = 66) were obtained from patients who underwent radical prostatectomy for clinically localized PCa and had a minimum follow-up of 72 months (range 72–131 months, mean 103 months). For HA, HYAL-1 and CD44v6 staining and MVD determination, a biotinylated HA-binding protein, an anti-HYAL-1 IgG, an anti-CD44v6 IgG and an anti-CD34 IgG were used, respectively. HA and HYAL-1 staining was classified as either low- or high-grade. CD44v6 staining and MVD were evaluated quantitatively and then grouped as either low- or high-grade. Using 72 months as the cut-off limit for evaluating biochemical recurrence, HA, HYAL-1, combined HA–HYAL-1, CD44v6 and MVD staining predicted progression with 96%, 84%, 84%, 68% and 76% sensitivity, respectively. Specificity was, 61% (HA), 80.5% (HYAL-1), 87.8% (HA–HYAL-1), 56.1% (CD44v6) and 61% (MVD). Sensitivity and specificity values for each marker did not change significantly in a subset of 45 patients for whom follow-up of longer than 112 months was available. In univariate analysis using the Cox proportional hazards model, preoperative PSA, Gleason sum, margin status, seminal vesicle, extraprostatic extension (EPE), HA, HYAL-1, HA–HYAL-1 and MVD, but not CD44v6, age and clinical stage, were significant in predicting biochemical recurrence ($p < 0.05$). In multivariate analysis using stepwise selection, only preoperative PSA (hazard ratio/unit PSA change = 1.086, $p < 0.0001$), EPE (hazard ratio = 6.22, $p = 0.0016$) and HYAL-1 (hazard ratio = 8.196, $p = 0.0009$)/HA–HYAL-1 (hazard ratio = 5.191, $p = 0.0021$) were independent predictors of biochemical recurrence. HA was an independent predictor of prognosis if HYAL-1 staining inference was not included in the multivariate model. In our retrospective study with 72- to 131-month follow-up, EPE, preoperative PSA and HYAL-1 either alone or together with HA (*i.e.*, combined HA–HYAL-1) were independent prognostic indicators for PCa.

Key words: *prostate cancer; prognostic indicator; hyaluronic acid; hyaluronidase; HYAL-1; CD44v6; microvessel density*

Over the last decade, the number of curable PCa cases has significantly increased due to the widespread use of PSA.[1,2] However, despite careful selection of patients, the disease recurs in a substantial percentage of localized PCa cases undergoing curative treatment modalities (*i.e.*, radical prostatectomy and radiotherapy).[3–6] Accurate prediction of the risk of progression would be useful in choosing the type and timing of the most appropriate treatment. Although existing parameters, such as Gleason sum or preoperative PSA, provide some prognostic information, it is difficult to estimate prognosis in PCa patients since two-thirds of them have Gleason sum of 5–7 and serum PSA levels of 4–10 ng/ml.[6–11] Furthermore, all patients with the same pathologic stage and/or grade do not have the same prognosis. Thus, there is a need for accurate prognostic markers to identify the biologic behavior of the tumor. Previously, we showed that HYAL-1-type HAase, either alone or in combination with HA, appears to be an independent predictor of biochemical recurrence among radical prostatectomy patients.[12]

HA is a nonsulfated glycosaminoglycan made up of repeated disaccharide units, D-glucuronic acid and *N*-acetyl-D-glucosamine.[13] HA maintains the osmotic balance of tissues and regulates cellular processes such as adhesion, migration and proliferation.[13] The biologic functions of HA are mediated by different HA receptors, including CD44.[14] The concentration of HA is elevated in several tumor types, and in some tumors (*e.g.*, breast, colon), high-level HA expression in tumor-associated stroma and/or tumor cells predicts poor survival.[15–19] Increased urinary HA levels serve as an accurate diagnostic marker for bladder cancer, regardless of tumor grade and stage.[20] However, in PCa, HA is not an independent predictor for prognosis.[12,19]

HYAL-1-type HAase is present in serum and produced by bladder, prostate and head-and-neck cancer cells.[21–24] The HAase class of enzymes degrades HA into small fragments, some of which (3–25 disaccharide units) induce angiogenesis.[25,26] Angiogenic HA fragments stimulate endothelial cell proliferation, adhesion and migration by activating focal adhesion kinase and mitogen-activated protein kinase pathways.[26] We have previously shown the presence of angiogenic HA fragments in PCa tissues and in the urine and saliva of bladder and head-and-neck cancer patients, respectively.[22,24,27] Given the observations that HYAL-1

Abbreviations: DAB, 3,3′-diaminobenzidine; EPE, extraprostatic extension; HA, hyaluronic acid; HAase, hyaluronidase; IHC, immunohistochemistry; MAb, monoclonal antibody; MVD, microvessel density; NPV, negative predictive value; PCa, prostate cancer; PPV, positive predictive value; PSA, prostate-specific antigen ; ROC, receiver operating characteristic.

Grant sponsor: U.S. Department of Defense; Grant number: DAMD 170210005; Grant sponsor: National Cancer Institute; Grant number: RO1 CA 072821-06A2; Grant sponsor: American Cancer Society Florida Division.

*Correspondence to: Department of Urology (M-800), University of Miami School of Medicine, P.O. Box 016960, Miami, FL 33101, USA. Fax: +305-243-6893. E-mail: vlokeshw@med.miami .edu

Received 13 January 2004; Accepted after revision 31 March 2004

DOI 10.1002/ijc.20368
Published online 2 June 2004 in Wiley InterScience (www.interscience.wiley.com).

is the major tumor-derived HAase expressed and secreted by tumor cells and that it is active at pH $\leq$ 4.5, it is possible that in the tumor microenvironment, where the pH is acidic, secreted HYAL-1 degrades the HA present in the extracellular matrix into angiogenic HA fragments.[22,24,27,28] In a retrospective study with a minimum of 5-year follow-up, we showed that HYAL-1 staining predicts progression with 84% sensitivity and 80% specificity.[12] Furthermore, high HYAL-1 staining was an independent predictor for prognosis.

CD44 belongs to a family of cell surface transmembrane glycoproteins involved in cell-to-cell and cell-to-extracellular matrix interactions.[29,30] Alternative splicing of CD44 mRNA in 10 of the 20 exons generates several variant CD44 isoforms.[30,31] The standard form of CD44 (*i.e.,* CD44s) is an HA receptor expressed in a variety of normal and tumor cell types.[29,32] We have previously shown that an isoform of CD44 (ex14/v10) is involved in HA-mediated endothelial cell proliferation.[33] The correlation between tumor progression and CD44s and/or its isoforms is unclear. We and others have shown that the androgen-insensitive PCa line PC-3 and primary PCa cells express CD44s and CD44 variants (*e.g.,* CD44v3 and CD44v6); however, the androgen-sensitive, poorly metastatic line LNCaP does not express CD44.[34–36] Contrary to these findings, it has been shown that overexpression of CD44v6 in a rat PCa line decreases metastasis.[37] Ekici *et al.*[38] showed that decreased expression of CD44v6 could be a predictor of poor prognosis in clinically localized PCa. Aaltomaa *et al.*[39] reported similar results.

Angiogenesis is an essential process for tumor growth and metastasis.[40–42] The clinical significance of angiogenesis, measured as MVD, has been demonstrated for several tumor types, including gastrointestinal, breast, bladder and renal cell carcinomas.[43–46] Studies that compared various endothelial cell markers (*i.e.,* CD31, CD34 and factor VIII) have shown that CD34 is a sensitive endothelial cell marker for measuring MVD.[47,48] At the present time, the clinical significance of MVD as an independent predictor of pathologic stage and recurrence in PCa remains unclear.[47–52]

We compared the prognostic potential of markers HA, CD44v6, HYAL-1 and MVD with regard to clinically localized PCa. Since HYAL-1 degrades HA and generates angiogenic fragments and CD44 acts as a cell surface receptor for both HA and HA fragments, we examined whether these biologically linked molecules are accurate prognostic indicators for PCa and whether they influence each other's prognostic capability.

MATERIAL AND METHODS

Specimens and study patients

Sixty-six randomly selected PCa specimens were obtained from patients who underwent radical retropubic prostatectomy for clinically localized PCa between 1992 and 1995 at the University of Miami. Patients neither received neoadjuvant hormonal therapy nor had metastasis to regional pelvic lymph nodes. The minimum available follow-up on all patients was 72 months. The study was conducted under a protocol approved by the University of Miami's Institutional Review Board. Of the 66 patients, 25 had biochemical or clinical recurrence before 72 months (mean time to recurrence 21.3 months, range 3–61) and 41 were free of disease recurrence (mean follow-up 103 months, range 72–131). Biochemical recurrence was defined as a PSA level $\geq$ 0.4 ng/ml in 2 successive measurements after the operation, in which case the first date an elevated PSA level was recorded was considered the date of failure. Patient characteristics including age, preoperative PSA and tumor (*i.e.,* Gleason sum, stage, margin, EPE and seminal vesicle invasion) are shown in Table I.

IHC and slide grading

For all specimens, paraffin-embedded blocks containing PCa tissues representing the major Gleason score were selected by a pathologist. From each block, 8 slides were prepared. Four slides were used for HA, HYAL-1, CD44v6 and anti-CD34 (for MVD determination) staining. The remaining slides were used either for determining nonspecific staining corresponding to each staining reagent or for repeating the staining to evaluate its consistency. For all staining procedures, specimen slides were deparaffinized, rehydrated and treated with an antigen retrieval solution (Dako, Copenhagen, Denmark).

HA and HYAL-1 staining. IHC for localizing HA and HYAL-1 in PCa tissues was carried out as described previously.[12,22] HA was localized in PCa tissues using a biotinylated HA-binding protein purified from bovine nasal cartilage, as described previously by Tengblad.[53] HYAL-1 was localized using a rabbit polyclonal anti-HYAL-1 IgG, which was generated against a peptide sequence present in the HYAL-1 protein (amino acids 321–338).[12,22]

Staining for HA and HYAL-1 was graded as 0 (no staining), 1+, 2+ and 3+. For HA staining, both the tumor-associated stroma and tumor cells were graded in each slide. The overall staining grade for each slide was assigned based on the staining intensity of the majority of the tumor tissue in the specimen. However, if 50% of the tumor tissue stained as 1+ and the other 50% as 3+, the overall staining grade was 2+. If 50% of the tumor stained as 2+ and the remaining as 3+, the overall staining inference was assigned as 3+. The staining scale was further subcategorized into low- and high-grade. For HA staining, low-grade staining included 0, 1+ and 2+ staining and high-grade staining included 3+ intensity. For HA staining, high-grade staining in tumor-associated stroma and/or tumor cells was considered as high-grade. HA staining was graded as low only when both the tumor-associated stroma and tumor cells showed low-grade staining. Therefore, in cases (n = 2) where stromal tissues showed low-grade staining but the tumor cells stained as 3+, the overall

TABLE I – PRE- AND POSTOPERATIVE PARAMETERS OF STUDY PATIENTS

Progression	Preoperative parameters			Postoperative parameters			
	Age (years)	PSA (ng/ml)	Clinical stage	Gleason sum	EPE	Margin	Seminal vesicle invasion
Biochemical recurrence (n = 25)	Median: 64	Median: 9.0	T1c: 10	6 = 2	(+) = 21	(+) = 18	(+) = 14
	Mean: 65.1	Mean: 14.04	T2a: 5 T2b: 10	7 = 14 8 = 6 9 = 3	(−) = 4	(−) = 7	(−) = 11
No biochemical or clinical recurrence (n = 41)	Median: 65	Median: 6	T1c: 22	5 = 7	(+) = 4	(+) = 9	(+) = 3
	Mean: 62.98	Mean: 8.1	T2a: 5 T2b: 14	6 = 9 7 = 20 8 = 5	(−) = 37	(−) = 32	(−) = 38

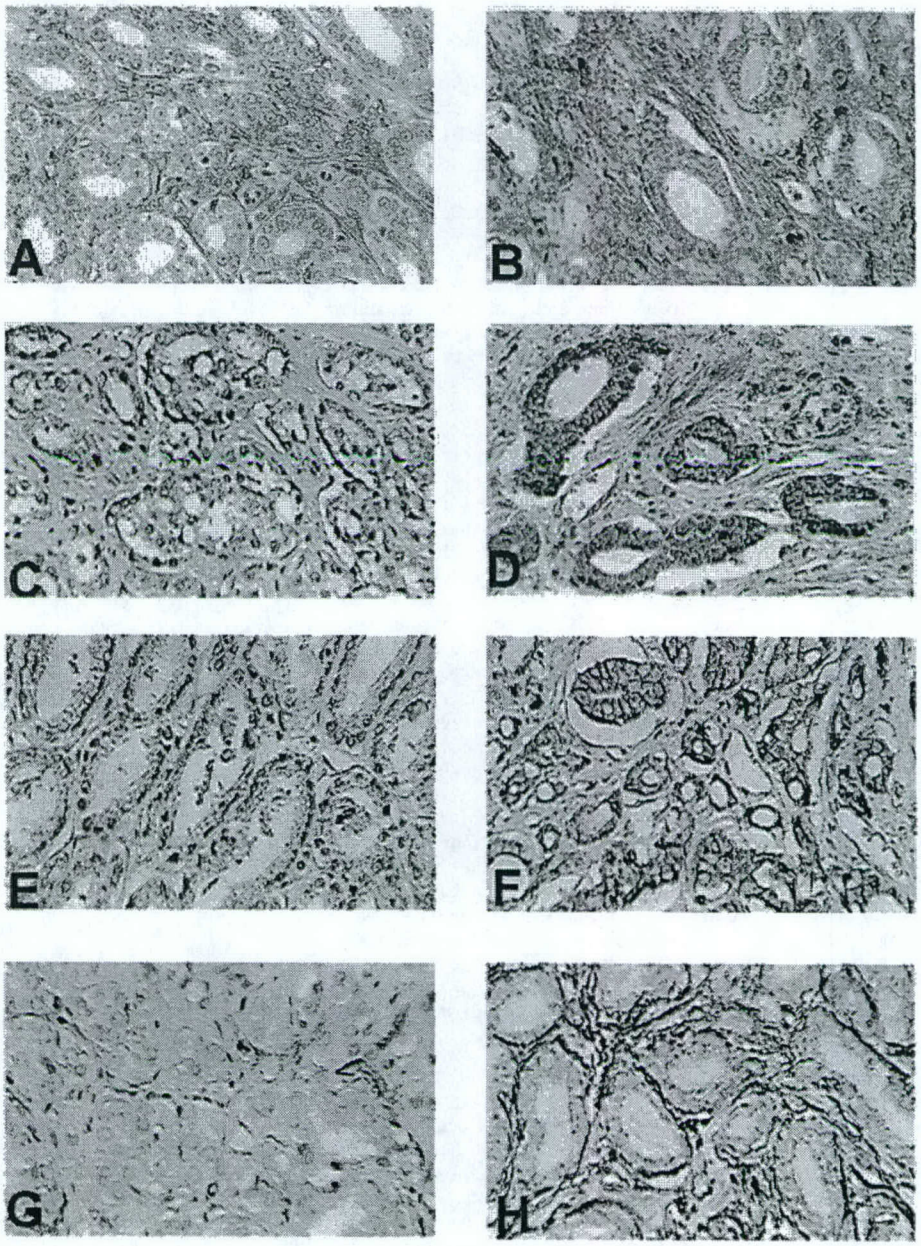

FIGURE 1 – Localization of HA, HYAL-1, CD44v6 and MVD in PCa tissues. Histologic markers were localized in PCa tissues from a nonprogressed patient *(a,c,e,g)* and a progressed patient *(b,d,f,h)*. *(a,b)* HA was localized in PCa tissues using a biotinylated HA-binding protein. *(c,d)* HYAL-1 was localized in PCa tissues using an anti-HYAL-1 antibody. *(e,f)* CD44v6 was localized in PCa tissues using an anti-CD44v6 MAb. *(g,h)* MVD was visualized using an anti-CD34 MAb. Magnification ×400.

HA staining was considered as high-grade. For HYAL-1, high-grade staining represented 2+ and 3+ staining, whereas low-grade staining included 0 and 1+ staining. For the combined HA–HYAL-1 staining, a positive result was indicated only when both HA (stromal, tumor cells or both) and HYAL-1 staining intensities were of high grade. Any other combination was considered negative. All slides were reviewed out of order, to prevent direct comparison of individual cases for HA and HYAL-1. Two readers independently evaluated all slides in a blinded fashion. Of the 132 total slides (*i.e.*, 66 each for HA and HYAL-1), there was discrepancy in 5 HA slides and 4 HYAL-1 slides. These discrepancies were resolved by both readers reexamining the slides simultaneously. In addition, to check for the repeatability of the evaluation system, a third reader randomly picked 35 slides each from the HA and HYLA1 sets and graded them for staining intensity. The discrepancy in slide evaluations by the third reader was <10%.

CD34 staining. Following the antigen retrieval step (as described above), slides were incubated with a mouse antihuman hematopoietic progenitor cell CD34 MAb (dilution 1:20; Dako) at 4°C for 15 hr. Slides were then incubated with a biotinylated antimouse antibody and an avidin-peroxidase conjugate solution (Vectastain ABC Kit; Vector, Burlingame, CA). To visualize peroxidase binding sites, slides were incubated with a DAB chromogen substrate solution (Dako) for 10 min. Slides were counterstained with hematoxylin, dehydrated and mounted.

The method described by Weidner *et al.*[49] was used for scoring the microvessels stained with CD34. The area of the highest MVD in each tissue specimen was localized under ×40 magnification and designated as a "hot spot". Microvessels in the hot spots were counted under ×400 magnification. Any vessel with lumen and endothelial cells or an endothelial cell cluster stained positively for CD34 was considered to be a single countable microvessel. MVD

TABLE II – SENSITIVITY, SPECIFICITY, ACCURACY, PPV AND NPV OF HA, HYAL-1, COMBINED HA–HYAL-1, CD34 AND CD44V6 STAINING INFERENCES

Parameter	HA, HYAL-1 and HA–HYAL-1								
	HA (%)				HYAL-1 (%)				HA-HYAL-1 (%)
	72 months	84 months	100 months	112 months	72 months	84 months	100 months	112 months	72 months
Sensitivity	96 (24/25)	96 (24/25)	92.3 (24/26)	92.6 (25/27)	84 (21/25)	84 (21/25)	84.6 (22/26)	85.2 (23/27)	84 (21/25)
Specificity	61 (25/41)	61.1 (22/36)	65.4 (17/26)	80.6 (16/18)	80.5 (33/41)	80.6 (29/36)	84.6 (22/26)	94.4 (17/18)	87.8 (36/41)
Accuracy	74.2 (49/66)	75.4 (46/61)	78.8 (41/52)	91.1 (41/45)	81.8 (54/66)	82 (50/61)	84.6 (44/52)	88.9 (40/45)	86.4 (57/66)
PPV	60 (24/40)	63.2 (24/38)	77.4 (24/31)	92.6 (25/27)	70 (21/30)	75 (21/28)	84.6 (22/26)	95.8 (23/24)	80.8 (21/26)
NPV	96.1 (25/26)	95.7 (22/23)	89.5 (17/19)	80.6 (16/18)	89.3 (34/37)	87.9 (29/33)	84.6 (22/26)	81 (17/21)	90 (36/40)

count was defined as the mean value of the counts obtained in 3 separate, contiguous but not overlapping areas within the hot spot. A cut-off value was determined using the ROC curve, and according to this value, 2 groups (low and high MVD) were assigned. Microvessels were examined and counted by the 3 readers (S.E., V.B.L. and W.H.C.) independently and without the knowledge of the clinical and pathologic status of the patients. Sections were reviewed out of order, to prevent direct comparison of individual cases for CD34.

CD44v6 staining. Following antigen retrieval, slides were incubated with a mouse antihuman CD44v6 MAb (dilution 1:50; Bender Med Systems, Vienna, Austria) at 4°C for 15 hr. Sections were then incubated with a biotinylated secondary antibody and an avidin-peroxidase conjugate solution (Vectastain ABC Kit). To visualize peroxidase binding sites, slides were incubated with DAB chromogen substrate solution for 10 min. Slides were counterstained with hematoxylin, dehydrated and mounted.

Slides for CD44v6 were scored as described by Ekici *et al.*[38] All sections included normal prostate tissue and/or benign prostatic hyperplasia glands as internal controls. Intensity of staining was graded as 0 for no staining, 1 for weak, 2 for moderate and 3 for strong. A combined staining score based on an estimate of the percentage of tumor cells stained and the intensity of staining was developed. Areas of tumor cells stained with maximum intensity (primary area) and with lesser intensity (secondary area) were determined in percentage values. The combined score was obtained by adding the scores of the primary and secondary areas. Staining intensities were examined and scored by 2 readers (S.E., V.B.L.) independently and in a blinded fashion. A cut-off value was determined from the ROC curve, and according to this value, 2 groups (low and high CD44v6 staining) were assigned.

Statistical analysis

Interassay variability regarding staining intensity was determined by Pearson's correlation analysis. Spearman's bivariate correlation coefficients were 0.85, 0.9, 0.98 and 0.95 for HA, HYAL-1, CD34 and CD44v6 staining, respectively. For all markers, high-grade staining was considered to be a true positive if the patient had biochemical recurrence. Consequently, low-grade staining was considered to be a true negative if the patient had no biochemical recurrence. The sensitivity, specificity, accuracy, PPV and NPV for HA, HYAL-1, HA–HYAL-1, CD34 and CD44v6 staining inferences were calculated using a 2×2 contingency table (high-grade/low-grade staining and progressed/nonprogressed PCa patients) at 72, 84, 100 and 112 month cut-off limits. For CD44v6 and MVD, ROC curves were developed for determining the optimal cut-off limits that yielded the best possible sensitivity and specificity values. The cut-off limits for CD44v6 and MVD were 180 and 41, respectively. Sensitivity was defined as true positive (*i.e.,* number of recurred patients predicted by a marker/total number of recurred patients). Specificity was defined as true negative (*i.e.,* number of nonrecurred patients predicted by a marker/total number of nonrecurred patients). Accuracy was determined as follows: (number of true positives + number of true negatives)/total number of PCa patients. PPV was determined as follows: number of true positives/(number of true positives + number of false positives). NPV was determined as follows: number of true negatives/(number of true negatives + number of false negatives). Data on various biochemical, surgical and pathologic parameters, as well as HA, HYAL-1, HA–HYAL-1, CD34 and CD44v6 staining inferences, were analyzed by the Cox proportional hazards model, using single-variable analysis (univariate analysis) or step-wise selection analysis. Stratified Kaplan-Meier analyses were performed on the variables found to be significant in the multivariate Cox proportional hazards model. For PSA subset analysis, Mantel-Haenszel χ^2 analysis or Student's *t*-test were used to determine statistical significance. Statistical analysis was carried out using the SAS software program (version 8.02; SAS Institute, Cary, NC).

RESULTS

IHC of tissue markers

The HA, HYAL-1, CD44v6 and CD34 antigens were localized in 66 archival PCa specimens obtained from patients who underwent radical retropubic prostatectomy for clinically localized disease. An increase in PSA levels $\geq$0.4 ng/ml was taken as an indicator of biochemical recurrence. Figure 1 shows IHC localization of HA, HYAL-1, CD44v6 and MVD in 2 Gleason 7 PCa specimens, one each from a nonrecurred (Fig. 1*a,c,e,g*) and a recurred (Fig. 1*b, d,f,h*) patient.

As shown in Figure 1*a,* very little HA staining was seen in PCa tissue from a patient who did not progress within 72 months. Among the 41 PCa specimens from nonrecurred patients, 25 showed low-grade staining. Figure 1*b* shows high-grade HA staining in a PCa specimen from a patient who had biochemical recurrence before 72 months (median time to recurrence 19 months, mean 21.3 months). HA staining was seen mainly in tumor-associated stroma. However, high-grade HA staining was also seen in tumor cells in 8 of 25 specimens from patients who had biochemical recurrence. Among these 8 specimens, 6 showed high-grade staining in tumor-associated stroma. Of the 25 patients who had recurred, 24 showed high-grade HA staining and only 1 showed low-grade staining in both tumor-associated stroma and tumor cells.

An anti-HYAL-1 peptide IgG was used to localize HYAL-1. As shown in Figure 1*c,* little HYAL-1 staining was seen in the PCa tissue from a nonrecurred patient. Of the 41 nonrecurred patients, PCa specimens from 33 had low-grade staining. In the PCa specimen from a patient who later recurred, high-grade HYAL-1 staining was seen (Fig. 1*d*). HYAL-1 expression was seen exclusively in tumor cells. Of the 25 patients who recurred within 72 months, 21 had high-grade HYAL-1 staining.

CD44v6 was localized using an anti-CD44v6 mouse MAb. Contrary to some earlier reports,[38,39] low-grade CD44v6 staining was observed in the PCa specimen from a nonrecurred patient (Fig. 1*e*) and high-grade CD44v6 staining, in the PCa tissue from a recurred patient (Fig. 1*f*). CD44v6 staining was mostly associated with the plasma membrane of tumor cells. We also observed CD44v6 in non-neoplastic epithelial cells in normal prostate and benign prostatic hyperplasia glands. However, the staining intensity of CD44v6 in non-neoplastic cells was less than that in tumor cells. There was a great degree of heterogeneity in CD44v6 staining. For these reasons, we used a semiquantitative method to grade CD44v6 staining.[38] Using a cut-off limit of 180 on the scoring scale, 23 of 41 PCa specimens from nonrecurred patients showed low-grade staining, whereas of the 25 patients who recurred, 17 showed high-grade staining.

H, HYAL-1 and HA–HYAL-1			CD34 and CD44v6							
HA-HYAL-1 (%)			MVD (%)				CD44v6 (%)			
84 months	100 months	112 months	72 months	84 months	100 months	112 months	72 months	84 months	100 months	112 months
84 (21/25)	80.8 (21/26)	81.5 (22/27)	76 (19/25)	76 (19/25)	76.9 (20/26)	77.8 (21/27)	68 (17/25)	68 (17/25)	65.4 (17/26)	62.9 (17/27)
88.9 (32/36)	88.5 (23/26)	94.4 (17/18)	61 (25/41)	61.1 (22/36)	65.4 (17/26)	77.8 (14/18)	56.1 (23/41)	52.8 (19/36)	50 (13/26)	61.1 (11/18)
86.9 (53/61)	84.6 (44/52)	86.7 (39/45)	66.7 (44/66)	67.2 (41/61)	71.1 (37/52)	77.8 (35/45)	57.6 (38/66)	59 (36/61)	57.7 (30/52)	62.2 (28/45)
84 (21/25)	87.5 (21/24)	95.7 (22/23)	54.3 (19/35)	57.6 (19/33)	69 (20/29)	84 (21/25)	48.6 (17/35)	50 (17/34)	56.7 (17/30)	70.8 (17/24)
88.9 (32/36)	85.2 (23/27)	77.3 (17/22)	80.6 (25/31)	78.6 (22/28)	73.4 (17/23)	70 (14/20)	74.2 (23/31)	70.4 (19/27)	59 (13/22)	52.4 (11/21)

It has been shown that visualization and scoring of microvessels using anti-CD34 staining are both sensitive and specific.[47,48,54] We therefore used an anti-CD34 MAb to visualize microvessels in PCa tissues. As shown in Figure 1*g*, MVD was low in the PCa tissue from a nonrecurred patient. As determined from the ROC curve, a cut-off limit of 41 was set to score low or high MVD. Of the 41 nonrecurred patients, PCa tissues from 25 patients had low MVD. However, MVD was high in 19 of 25 PCa tissues obtained form patients who had a recurrence. Figure 1*h* shows high MVD in the PCa specimen from a patient who later recurred.

Determination of sensitivity, specificity, accuracy, PPV and NPV

In all patients, a minimum 72-month follow-up was available (mean 103 months, median 104.2 months, range 72–131 months). Therefore, we determined the sensitivity, specificity, accuracy, PPV and NPV of HA, HYAL-1, combined HA–HYAL-1, CD44v6 and MVD at 72, 84, 100 and 112 months of follow-up. As shown in Table II, at 72 months the sensitivity of HA, HYAL-1, combined HA–HYAL-1, CD44v6 and MVD for predicting PCa recurrence was 96%, 84%, 84%, 76% and 68%, respectively. The specificity of HA (61%), CD44v6 (56.1%) and MVD (61%) was lower than that of HYAL-1 (80.5%) and combined HA–HYAL-1 (87.8%). Accuracy was highest for HA–HYAL-1 (86.4%), followed by HYAL-1 (81.8%), HA (74.2%), MVD (66.7%) and CD44v6 (57.6%). Due to higher specificity, the PPV of combined HA–HYAL-1 (80.8%) and HYAL-1 (70%) was high. However, the PPV of CD44v6 was the lowest (48.6%), followed by MVD (54.3%) and HA (60%). Due to high sensitivity, the NPV of HA staining (96.1%) was the highest, followed by HA–HYAL-1 (90%), HYAL-1 (89.3%), MVD (80.6%) and CD44v6 (74.2%) (Table II).

At 84-month follow-up, the cohort consisted of 61 patients (mean follow-up 107.9 months, median 112 months, range 85–131 months), of whom 36 were in the nonrecurred group. Thus, the sensitivity values of all markers remained unchanged at 84 months compared to 72 months (Table II). There was also no significant change in the specificity, accuracy, PPV and NPV values for HA (61.1%, 75.4%, 63.2%, 95.7%), HYAL-1 (80.6%, 82%, 75%, 87.9%), combined HA–HYAL-1 (88.9%, 86.9%, 84%, 88.9%), MVD (61.1%, 67.2%, 57.6%, 78.6%) and CD44v6 (52.8%, 59%, 50% and 70.4%), respectively. At 100 months, follow-up information was available on 52 patients (mean follow-up 117.1 months, median 117.8 months, range 101.6–131 months). Of these 52 patients, one who had been in the nonrecurred category up to the 84-month follow-up showed biochemical recurrence. Interestingly, this patient was scored as a false positive on HYAL-1 and CD34 at 72- and 84-month follow-up. Thus, the sensitivity of both HYAL-1 (84.6%) and CD34 (76.9%) increased slightly, whereas that of HA (92.3%), combined HA–HYAL-1 (80.8%) and CD44v6 (65.4%) decreased (Table II).

Follow-up information beyond 112 months was available for 45 patients (mean follow-up 121 months, median 120.2 months, range 112–131 months). At 112 months, one patient who was a false positive on HA, HYAL-1, combined HA–HYAL-1 and MVD markers up to 100 months showed biochemical recurrence. Thus, the sensitivity of HA, HYAL-1, combined HA–HYAL-1, MVD and CD44v6 was 92.6%, 85.2%, 81.5%, 77.8% and 62.9%, respectively. At final analysis, both HYAL-1 and combined HA–HYAL-1 had the best specificity (94.4%, 94.4%), accuracy (88.9%, 86.7%), PPV (95.8%, 95.7%) and NPV (81%, 77.3%), followed by HA (80.6%, 91.1%, 92.6%, 80.6%), MVD (77.8%, 77.8%, 84%, 70%) and CD44v6 (61.1%, 62.2%, 70.8%, 52.4%).

TABLE III – UNIVARIATE ANALYSIS OF PRE- AND POSTOPERATIVE PROGNOSTIC PARAMETERS AND IHC STAINING INFERENCES

Parameter	χ^2	p	Hazard ratio	95% CI[1]
Age	0.4332	0.5104	1.019	0.963–1.078
PSA	11.648	0.0006[1]	1.048	1.02–1.077
Gleason sum (overall)	14.19	0.0002[1]	2.5	1.552–4.024
Gleason ≥7	5.744	0.0165[1]	5.827	1.379–24.633
Clinical stage	1.226	0.2683	1.262	0.836–1.905
EPE	25.411	<0.0001	12.781	4.746–34.42
Surgical margin positivity	13.355	0.0003[1]	4.5	2.008–10.079
Seminal vesicle invasion	22.268	<0.0001	6.56	3.002–14.317
HA	11.319	0.0008[1]	12.091	2.831–51.648
HYAL-1	22.054	<0.0001[1]	13.192	4.5–38.716
HA–HYAL-1	25.364	<0.0001[1]	10.749	4.266–27.087
MVD	10.0314	0.0015[1]	4.36	1.753–10.845
CD44v6	2.277	0.131	1.826	0.835–3.994

[1]Statistically significant. CI, confidence interval. Cox proportional hazards model and single-parameter analysis were used to determine the prognostic significance of preoperative (age, preoperative PSA and clinical stage) and postoperative (Gleason sum overall and ≥ or ≤ 7, margin, EPE, seminal vesicle invasion) parameters and HA, HYAL-1, HA–HYAL-1, MVD and CD44v6 staining inferences.

Evaluation of the prognostic capability of pre- and postoperative parameters and histologic markers

Univariate analysis. Since the patients in this cohort had variable follow-up between 72 and 131 months, we used the Cox proportional hazards model and single-parameter analysis to determine the prognostic significance of each of the preoperative (*i.e.,* age, PSA and clinical stage) and postoperative (*i.e.,* Gleason sum, margin, EPE, seminal vesicle invasion) parameters, as well as staining inferences of HA, HYAL-1, combined HA–HYAL-1, CD44v6 and MVD. As shown in Table III, age ($p = 0.5104$, hazard ratio = 1.019), clinical stage ($p = 0.2683$, hazard ratio = 1.2620) and CD44v6 staining ($p = 0.131$, hazard ratio = 1.826) were not significant in predicting biochemical recurrence. However, preoperative PSA ($p = 0.0006$, hazard ratio/unit PSA change = 1.048), Gleason sum overall ($p = 0.0002$, hazard ratio = 2.5), margin status ($p = 0.0003$, hazard ratio = 4.5), EPE ($p < 0.0001$, hazard ratio = 12.781), seminal vesicle invasion ($p < 0.0001$, hazard ratio = 6.56), HA staining ($p = 0.0008$, hazard ratio = 12.091), HYAL-1 staining ($p < 0.0001$, hazard ratio = 13.192), HA–HYAL-1 staining ($p < 0.0001$, hazard ratio = 10.749) and MVD ($p = 0.0015$, hazard ratio = 4.36) significantly predicted biochemical recurrence (Table III). Patients with Gleason sum ≥7 have a greater risk of progression.[42] In single-parameter analysis, the hazard of developing biochemical recurrence in Gleason sum ≥7 patients ($p = 0.0165$, hazard ratio = 5.827) increased 2.3-fold when all Gleason sums were analyzed together (Table III).

Multivariate analysis. To determine the smallest number of variables that could jointly predict biochemical recurrence in this

TABLE IV – MULTIVARIATE ANALYSIS OF PRE- AND POSTOPERATIVE PROGNOSTIC PARAMETERS AND IHC STAINING INFERENCES

Parameters	HA and HYAL-1 separate				HA–HYAL-1 combined			
	χ^2	p	Hazard ratio	95% CI[1]	χ^2	p	Hazard ratio	95% CI
PSA	16.857	<0.0001[1]	1.086	1.044–1.130	14.127	0.0002[1]	1.077	1.036–1.12
EPE	9.939	0.0016[1]	6.222	1.997–19.384	10.998	0.0009[1]	6.906	2.204–21.640
HYAL-1	11.094	0.0009[1]	8.196	2.377–26.259	9.428	0.0021[1]	5.191	1.814–14.854

Cox proportional hazards model and stepwise selection were used to determine which of the preoperative (*i.e.,* age, PSA and clinical stage) and postoperative (*i.e.,* Gleason sum overall and ≥ or ≤ 7, EPE, margin and seminal vesicle invasion) parameters and HA, HYAL-1, HA–HYAL-1, MVD and CD44v6 staining inferences had independent prognostic significance. Significant parameters ($p > 0.05$) selected by the model are shown.

[1]Statistically significant. CI, confidence interval.

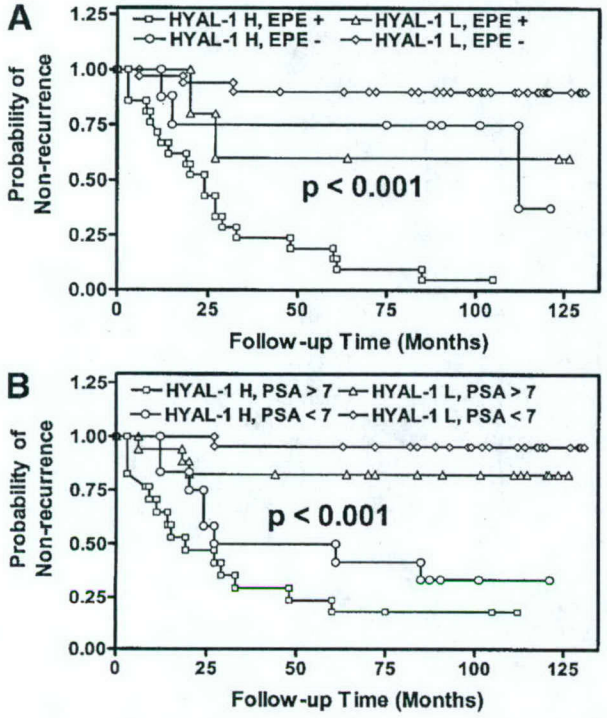

FIGURE 2 – Kaplan-Meier analysis was performed after stratifying the data as *(a)* HYAL-1 high (H)/low (L) and EPA^+/EPA^- and *(b)* HYAL-1 high (H)/low (L) and PSA < or > 7 ng/ml.

cohort of patients, we used the Cox proportional hazards model and step-wise selection analysis. When age, preoperative PSA, clinical stage, Gleason sum (overall or ≥7), EPE, seminal vesicle invasion and staining inferences of HA, HYAL-1, CD44v6 and MVD were included in the model, only preoperative PSA ($p < 0.0001$, hazard ratio/unit PSA change = 1.086), EPE ($p = 0.0016$, hazard ratio = 6.222) and HYAL-1 ($p = 0.0009$, hazard ratio = 8.1896) reached statistical significance in predicting biochemical recurrence (Table IV).

To demonstrate the joint effect of HYAL-1 and EPE or HYAL-1 and PSA on biochemical recurrence, we performed Kaplan-Meier analysis. As shown in Figure 2*a,* the probability of biochemical recurrence was highest when HYAL-1 was high and EPE was positive, and a patient had the lowest probability of recurrence when HYAL-1 was low and EPE was negative. Since PSA was a continuous estimate, with values ranging from 0.5 to 62 ng/ml, for the entire cohort ($n = 66$), we divided the cohort into those with PSA levels <7 and >7 ng/ml, 7 ng/ml PSA being used as the cut-off limit since that was the median value for the entire cohort. As shown in Figure 2*b,* individuals with HYAL-1 high and PSA > 7 ng/ml had the highest probability of recurrence, followed by those with HYAL-1 high and PSA < 7 ng/ml. Individuals with low HYAL-1 staining and PSA < 7 ng/ml had the lowest probability of recurrence. These data explain why multivariate analysis selected HYAL-1, EPE and PSA as independent prognostic indicators.

Inclusion of the combined HA–HYAL-1 staining inference instead of HA and HYAL-1 staining inferences in the multiple regression model again showed that preoperative PSA ($p = 0.0002$, hazard ratio/unit PSA change = 1.077), EPE ($p = 0.0009$, hazard ratio = 6.906) and HA–HYAL-1 ($p = 0.0021$, hazard ratio = 5.191) were significant in predicting biochemical recurrence (Table IV). None of the other preoperative (PSA, clinical stage) and postoperative (Gleason sum overall or Gleason stratification ≥ or ≤ 7 and seminal vesicle) parameters or CD44v6 and MVD staining inferences reached statistical significance in the multivariate model ($p > 0.05$ in each case). Kaplan-Meier analysis using HA–HYAL-1 and EPE or HA–HYAL-1 and PSA demonstrated that individuals with high HA–HYAL-1 and positive EPE or high HA–HYAL-1 and PSA > 7 ng/ml had the highest probability of biochemical recurrence (data not shown).

When HYAL-1 was omitted in the model during stepwise analysis, HA ($p = 0.0065$, hazard ratio = 8.658) together with preoperative PSA ($p = 0.0006$, hazard ratio/unit PSA change = 1.079) and EPE ($p < 0.0001$, hazard ratio = 9.073) were significant in predicting biochemical recurrence. Similarly, when PSA was omitted in the model, margin status reached independent prognostic significance together with EPE and HYAL-1 or HA–HYAL-1 (data not shown).

PSA subgroup analysis. It has been suggested that biochemical recurrence before 24 months indicates systemic disease, whereas biochemical recurrence beyond 24 months suggests local recurrence. To test whether any of the pre- and postoperative parameters as well as IHC markers under study distinguish between these groups, we performed Mantel-Haenszel χ^2 analysis (for testing Gleason sum, Gleason sum ≥ 7, EPE, margin status, seminal vesicle invasion, HA, HYAL-1, combined HA–HYAL-1 CD34 and CD44v6) or Student's *t*-test (for age and preoperative PSA). As shown in Table V, margin status could distinguish between PSA recurrence before and after 24 months ($p = 0.269$, $\chi^2 = 4.894$); however, none of the other parameters or markers reached statistical significance in this comparison.

DISCUSSION

We compared the prognostic potential of histologic markers HA, HYAL-1, CD44v6 and MVD for predicting biochemical recurrence in PCa patients since their biologic functions are interrelated. For example, HA, an extracellular matrix component, is a high-affinity ligand for CD44.[14,29] HA–CD44 interaction promotes cell adhesion, migration and proliferation.[14,29] HAase degrades HA into small fragments that promote angiogenesis, and MVD is an indicator of angiogenesis.[25,26,41] In addition to their biologic relatedness, each of these histologic markers has shown potential to predict prognosis for PCa patients.[12,19,38,39,47–52]

The prognostic capability of HA staining in tumors varies depending on the tissue where the cancer originates. HA staining in

TABLE V – PSA SUBGROUP ANALYSIS

Parameter	Variable	*p*
Age	0.66[1]	0.513
PSA	1.06[1]	0.298
Gleason sum (overall)	0.133[2]	0.453
Gleason ≥ 7	0.15[2]	0.699
Clinical stage	1.903[2]	0.168
EPE	0.736[2]	0.391
Surgical margin positivity	4.894[2]	0.0269*
Seminal vesicle invasion	0.122[2]	0.7265
HA	0.15[2]	0.699
HYAL-1	0.280[2]	0.596
HA–HYAL-1	0.0437[2]	0.834
MVD	1.322[2]	0.25
CD44v6	1.102[2]	0.294

[1]The ability of PSA and age to predict PSA recurrence within 24 months was determined using the *t*-test (since these were continuous variables).– [2]Mantel-Haenszel χ^2 analysis was used to evaluate the ability of clinical stage, post- operative parameters and IHC staining markers to predict PSA recurrence within 24 months.

tumor-associated stroma and/or tumor cells has prognostic capability in breast, colon and gastrointestinal cancers; however, it does not have independent prognostic capability in PCa.[13–19] We found that the HA staining had 92.3% sensitivity and 80.6% specificity to predict biochemical recurrence within 112 months. Interestingly, the specificity of HA staining to predict biochemical recurrence increased from 61% at 72-month follow-up to 80.6% at 112-month follow-up. We have previously shown that at 64-month follow-up, although HA staining had high sensitivity (96%), the specificity of this marker to predict biochemical recurrence was even lower (55.5%) compared to that at 72 months.[12] These results indicate that positive HA staining in PCa tissues means that the patient could have a recurrence within 112 months. In this and a previous study, we found that HA staining shows prognostic capability in univariate analysis; however, it is not an independent predictor of biochemical recurrence. Interestingly, however, if HYAL-1 staining inference is not included in the Cox proportional hazards model during stepwise analysis, HA together with preoperative PSA and EPE reaches independent prognostic significance. These results indicate that HYAL-1 provides all of the prognostic information supplied by HA staining, as well as some additional information. However, although there was <10% discrepancy between 3 readers who evaluated the HA and HYAL-1 staining, at present we do not know the repeatability of the staining evaluation system in another laboratory. Therefore, more studies need to be conducted to verify that HYAL-1 is a better prognostic indicator than HA in predicting biochemical recurrence for PCa patients. Nonetheless, the evaluation system, which involves grading of HA staining as high when tumor-associated stroma and/or tumor cells show high-grade staining and as low when tumor-associated stroma and/or tumor cells show low-grade staining, appears to be accurate. This is because the prognostic significance of HA staining, and consequently of HA–HYAL-1 staining, in both univariate and multivariate analyses remained unchanged when the 2 specimens in which HA staining was low-grade in tumor-associated stroma but high-grade in tumor cells were graded as low-grade instead of high-grade (unpublished results).

The prognostic significance of the CD44 standard form and its variant isoforms (*e.g.,* CD44v6) is unclear. Contrary to our finding that CD44v6 expression was elevated in patients who later had biochemical recurrence, 2 reports showed that a decrease in CD44v6 expression correlated with increased Gleason sum and disease progression.[38,39] For example, Ekici *et al.*[38] showed that CD44v6 expression inversely correlates with pathologic stage and disease progression and positively correlates with PSA-free survival. However, in that study, CD44v6 was not an independent predictor of prognosis. Contrary to the findings of Ekici *et al.*,[38] Aaltomaa *et al.*[39] found that CD44v6 is an independent predictor of survival. In the present study, increased CD44v6 expression had reasonable sensitivity to predict prognosis at 72-month (68%) or 112-month (62.9%) follow-up. However, among all of the markers, it had the lowest specificity (56.1% at 72 months and 61.1% at 112 months) to predict biochemical recurrence. This low specificity may explain why CD44v6 staining is not significant in predicting biochemical recurrence in both univariate and multivariate analyses. A likely explanation of why different studies report conflicting results regarding CD44v6 staining and prognosis for PCa is that PCa tissues have a high degree of heterogeneity with respect to CD44v6 staining. Aaltomaa *et al.*[39] reported variability in CD44v6 staining intensity and in the number of tumor cells that were positive for CD44v6. Similarly, Ekici *et al.*[38] reported the heterogeneous nature of CD44v6 expression and developed a semiquantitative method for scoring CD44v6 staining. We used this scoring method to evaluate CD44v6 staining. Nonetheless, it is likely that the heterogeneous nature of CD44v6 will limit its prognostic significance.

Determination of MVD in PCa tissues, using anti-CD34 antibodies, is sensitive and accurate in predicting prognosis.[47,48,54] Although problems exist in the methods of counting the vessels and in setting a universally accepted cut-off limit for MVD to predict recurrence, MVD has been correlated with Gleason sum, pathologic stage and outcome.[47–49] However, other studies have shown that MVD does not correlate with tumor grade, stage and clinical outcome.[50–52] In our study, MVD at a cut-off limit of 41 showed reasonably high sensitivity at both 72-month (76%) and 112-month (77.8%) follow-up. The specificity of MVD to predict biochemical recurrence increased from 61% at 72-month follow-up to 77.8% at 112-month follow-up, suggesting that in some false-positive patients high MVD may be indicative of biochemical recurrence before 112 months. Although in the univariate analysis MVD showed prognostic significance (Table III), in the multivariate analysis it had no additional prognostic significance. MVD did not reach independent prognostic significance even when HA alone, in the absence of HYAL-1, was included in the Cox model. It is possible that since HA, HYAL-1 and MVD are biologically related, all of the prognostic information provided by MVD inferences is contained in either HA or HYAL-1 staining inferences.

In our study, HYAL-1 staining alone had high sensitivity both at 72-month (84%) and at or beyond 112-month (85.2%) follow-up. Indeed, it had either the same or slightly higher sensitivity to predict biochemical recurrence as the combined HA–HYAL-1 staining inference (84% at 72 months and 81.5% at 112 months). The specificity of HYAL-1 staining inference (80.5%) at 72-month follow-up was slightly lower than that of HA–HYAL-1 (87.8%). However, HYAL-1 and HA–HYAL-1 staining inferences had the same specificity (94.4%) to predict biochemical recurrence at 112 months and beyond. Therefore, HYAL-1 either has the same or slightly better PPV and NPV to predict biochemical recurrence. Thus, contrary to our earlier report that combined HA–HYAL-1 has slightly better prognostic capability than HYAL-1 staining alone at 64 months,[12] our present study suggests that HYAL-1 alone is sufficiently accurate to predict biochemical recurrence at 72 months and beyond.

In the multivariate analysis, among all of the pre- and postoperative parameters and histologic markers, only preoperative PSA and EPE had additional prognostic significance if HYAL-1 (or HA–HYAL-1) was included in the analysis. In an earlier study, we found that EPE, margin status and HYAL-1 (or HA–HYAL-1) were independent predictors of prognosis. The difference between that study[12] and this is that in the earlier study we used 64-month follow-up as a cut-off limit and performed Wald's forward stepwise regression analysis, whereas in the present study we used the Cox proportional hazards model and stepwise selection to calculate the hazard of biochemical recurrence over the entire period of follow-up (*i.e.,* up to 131 months). Interestingly, when preoperative PSA was not included in the model, margin status reached independent prognostic significance together with EPE and

HYAL-1 (or HA–HYAL-1), suggesting that preoperative PSA provides all of the prognostic information related to margin status plus some additional information. Nonetheless, HYAL-1 appears to be an independent prognostic indicator for predicting biochemical recurrence.

As is the case for HA expression in tumor tissues, the prognostic significance of HYAL-1 expression may also vary based on the origin of cancer tissue. For example, in bladder cancer, HYAL-1 expression correlates with tumor grade.[21] Also, HAase levels are elevated in brain metastases of carcinomas compared to primary glioblastomas.[55] Furthermore, brain metastasis-derived cell lines have 1,000-fold more HAase than glioma-derived cell lines.[55] HYAL-1 levels are also elevated in the saliva of patients with squamous cell carcinoma of the head and neck.[24] However, HA accumulation without HAase activation has been associated with aggressiveness of ovarian cancer.[56] Similarly, HYAL-1 expression suppresses tumor growth in a rat colon carcinoma model.[57] However, HYAL-1 expression in PC-3 cells (a PCa cell line) increases their metastatic potential.[58] Thus, HYAL-1 expression is associated with PCa progression.

The major dilemma for clinicians in the management of PCa is the identification of the site of disease recurrence, which ultimately guides therapy decisions. It is generally accepted that PSA recurrence within 1–2 years relates to a higher risk of developing metastatic disease.[9,59] However, it is not understood whether existing pre- and postoperative parameters as well as histologic markers can distinguish between patients who will recur within 24 months and those who will not. In our study, PSA subset analysis showed that, except for margin status, none of the markers (*i.e.,* HA, HYAL-1, HA–HYAL-1, MVD and CD44v6) and preoperative (*i.e.,* age, clinical stage and preoperative PSA) and postoperative (*i.e.,* Gleason sum overall or ≥ 7, EPE, seminal vesicle invasion) was able to distinguish between patients who recurred within 24 months and those who did not. In this cohort, we had 25 patients who recurred within 72 months, of whom 17 (68%) recurred within 24 months and 3 more recurred at 27 months (mean time to recur for the entire cohort 21.3 months). Thus, the ability of various clinical and pathologic parameters as well as histologic markers to predict biochemical recurrence within 24 months may need to be studied in a larger group of biochemically recurred patients.

Nearly two-thirds of PCa patients have preoperative PSA levels of 4–10 ng/ml, stage T1C disease and a biopsy Gleason of 5–7.[2,10,11] For such patients, one or a combination of accurate prognostic indicators could improve the physicians' ability to identify PCas that are aggressive and will progress so that individualized treatments could be offered. In our study, although preoperative PSA was an independent predictor for prognosis, neither the overall Gleason sum nor Gleason sum $\leq$ or ≥ 7 was an independent predictor for prognosis. Among the 4 potential prognostic indicators for PCa that we compared, HYAL-1 appears to be an accurate and independent predictor.

ACKNOWLEDGEMENTS

S.E. was a fellow of The Scientific and Technical Council of Turkey (NATO Science Fellowship Program).

REFERENCES

1. Khan MA, Han M, Partin AW, Epstein JI, Walsh PC. Long-term cancer control of radical prostatectomy in men younger than 50 years of age: update 2003. Urology 2003;62:86–92.
2. Draisma G, Boer R, Otto SJ, van der Cruijsen IW, Damhuis RA, Schröder FH, de Koning HJ. Lead times and overdetection due to prostate-specific antigen screening: estimates from the European Randomized Study of Screening for Prostate Cancer. J Natl Cancer Inst 2003;95:868–78.
3. Palisaar RJ, Graefen M, Karakiewicz PI, Hammerer PG, Huland E, Haese A, Fernandez S, Erbersdobler A, Henke RP, Huland H. Assessment of clinical and pathologic characteristics predisposing to disease recurrence following radical prostatectomy in men with pathologically organ-confined prostate cancer. Eur Urol 2002;41:155–61.
4. Pound CR, Partin AW, Epstein JI, Walsh PC. Prostate-specific antigen after anatomic radical retropubic prostatectomy. Patterns of recurrence and cancer control. Urol Clin North Am 1997;24:395–406.
5. Neulander EZ, Soloway MS. Failure after radical prostatectomy. Urology 2003;61:30–6.
6. Symon Z, Griffith KA, McLaughlin PW, Sullivan M, Sandler HM. Dose escalation for localized prostate cancer: substantial benefit observed with 3D conformal therapy. Int J Radiat Oncol Biol Phys 2003;57:384–90.
7. Syed S, Petrylak DP, Thompson IM. Management of high-risk localized prostate cancer: the integration of local and systemic therapy approaches. Urol Oncol 2003;21:235–43.
8. Moul JW. Variables in predicting survival based on treating "PSA-only" relapse. Urol Oncol 2003;21:292–304.
9. Swindle PW, Kattan MW, Scardino PT. Markers and meaning of primary treatment failure. Urol Clin North Am 2003;30:377–401.
10. Blute ML, Bergstralh EJ, Iocca A, Scherer B, Zincke H. Use of Gleason score, prostate specific antigen, seminal vesicle and margin status to predict biochemical failure after radical prostatectomy. J Urol 2001;165:119–25.
11. Pettaway CA. Prognostic markers in clinically localized prostate cancer. Tech Urol 1998;4:35–42.
12. Posey JT, Soloway MS, Ekici S, Sofer M, Civantos F, Duncan RC, Lokeshwar VB. Evaluation of the prognostic potential of hyaluronic acid and hyaluronidase (HYAL-1) for prostate cancer. Cancer Res 2003;63:2638–44.
13. Tammi MI, Day AJ, Turley EA. Hyaluronan and homeostasis: a balancing act. J Biol Chem 2002;277:4581–4.
14. Turley EA, Noble PW, Bourguignon LY. Signaling properties of hyaluronan receptors. J Biol Chem 2002;277:4589–92.
15. Setälä LP, Tammi MI, Tammi RH, Eskelinen MJ, Lipponen PK, Ågren UM, Parkkinen J, Alhava EM, Kosma V-M. Hyaluronan expression in gastric cancer cells is associated with local and nodal spread and reduced survival rate. Br J Cancer 1999;79:1133–8.
16. Auvinen P, Tammi R, Parkkinen J, Tammi M, Ågren U, Johansson R, Hirvikoski P, Eskelinen M, Kosma V-M. Hyaluronan in peritumoral stroma and malignant cells associates with breast cancer spreading and predicts survival. Am J Pathol 2000;156:529–36.
17. Knudson W. Tumor-associated hyaluronan. Providing an extracellular matrix that facilitates invasion. Am J Pathol 1996;148:1721–6.
18. Ropponen K, Tammi M, Parkkinen J, Eskelinen M, Tammi R, Lipponen P, Ågren U, Alhava E, Kosma V-M. Tumor cell–associated hyaluronan as an unfavorable prognostic factor in colorectal cancer. Cancer Res 1998;58:342–7.
19. Lipponen P, Aaltomaa S, Tammi R, Tammi M, Ågren U, Kosma V-M. High stromal hyaluronan level is associated with poor differentiation and metastasis in prostate cancer. Eur J Cancer 2001;37:849–56.
20. Lokeshwar VB, Öbek C, Pham HT, Wei D, Young MJ, Duncan RC, Soloway MS, Block NL. Urinary hyaluronic acid and hyaluronidase: markers for bladder cancer detection and evaluation of grade. J Urol 2000;163:348–56.
21. Hautmann SH, Lokeshwar VB, Schroeder GL, Civantos F, Duncan RC, Gnann R, Friedrich MG, Soloway MS. Elevated tissue expression of hyaluronic acid and hyaluronidase validates the HA-HAase urine test for bladder cancer. J Urol 2001;165:2068–74.
22. Lokeshwar VB, Rubinowicz D, Schroeder GL, Forgacs E, Minna JD, Block NL, Nadji M, Lokeshwar BL. Stromal and epithelial expression of tumor markers hyaluronic acid and HYAL-1 hyaluronidase in prostate cancer. J Biol Chem 2001;276:11922–32.
23. Csoka AB, Frost GI, Stern R. The six hyaluronidase-like genes in the human and mouse genomes. Matrix Biol 2001;20:499–508.
24. Franzmann EJ, Schroeder GL, Goodwin WJ, Weed DT, Fisher P, Lokeshwar VB. Expression of tumor markers hyaluronic acid and hyaluronidase (HYAL-1) in head and neck tumors. Int J Cancer 2003;106:438–45.
25. West DC, Hampson IN, Arnold F, Kumar S. Angiogenesis induced by degradation products of hyaluronic acid. Science 1985;228:1324–6.
26. Lokeshwar VB, Selzer MG. Differences in hyaluronic acid–mediated functions and signaling in arterial, microvessel, and vein-derived human endothelial cells. J Biol Chem 2000;275:27641–9.
27. Pham HT, Block NL, Lokeshwar VB. Tumor-derived hyaluronidase: a diagnostic urine marker for high-grade bladder cancer. Cancer Res 1997;57:778–83.
28. Kumar S, West DC, Ponting JM, Gattamaneni HR. Sera of children with renal tumours contain low-molecular-mass hyaluronic acid. Int J Cancer 1989;44:445–8.

29. Lesley J, Hascall VC, Tammi M, Hyman R. Hyaluronan binding by cell surface CD44. J Biol Chem 2000;275:26967–75.
30. Cichy J, Pure E. The liberation of CD44. J Cell Biol 2003;161:839–43.
31. Naor D, Nedvetzki S, Golan I, Melnik L, Faitelson Y. CD44 in cancer. Crit Rev Clin Lab Sci 2002;39:527–79.
32. Lokeshwar VB, Fregien N, Bourguignon LY. Ankyrin-binding domain of CD44(GP85) is required for the expression of hyaluronic acid–mediated adhesion function. J Cell Biol 1994;126:1099–109.
33. Lokeshwar VB, Iida N, Bourguignon LY. The cell adhesion molecule, GP116, is a new CD44 variant (ex14/v10) involved in hyaluronic acid binding and endothelial cell proliferation. J Biol Chem 1996;271: 23853–64.
34. Lokeshwar BL, Lokeshwar VB, Block NL. Expression of CD44 in prostate cancer cells: association with cell proliferation and invasive potential. Anticancer Res 1995;15:1191–8.
35. Welsh CF, Zhu D, Bourguignon LY. Interaction of CD44 variant isoforms with hyaluronic acid and the cytoskeleton in human prostate cancer cells. J Cell Physiol 1995;164:605–12.
36. Iczkowski KA, Bai S, Pantazis CG. Prostate cancer overexpresses CD44 variants 7–9 at the messenger RNA and protein level. Anticancer Res 2003;23:3129–40.
37. Gao AC, Lou W, Sleeman JP, Isaacs JT. Metastasis suppression by the standard CD44 isoform does not require the binding of prostate cancer cells to hyaluronate. Cancer Res 1998;58:2350–2.
38. Ekici S, Ayhan A, Kendi S, Özen H. Determination of prognosis in patients with prostate cancer treated with radical prostatectomy: prognostic value of CD44v6 score. J Urol 2002;167:2037–41.
39. Aaltomaa S, Lipponen P, Ala-Opas M, Kosma V-M. Expression and prognostic value of CD44 standard and variant v3 and v6 isoforms in prostate cancer. Eur Urol 2001;39:138–44.
40. Sato Y. Molecular diagnosis of tumor angiogenesis and anti-angiogenic cancer therapy. Int J Clin Oncol 2003;8:200–6.
41. Sullivan DC, Bicknell R. New molecular pathways in angiogenesis. Br J Cancer 2003;89:228–31.
42. Folkman J, Browder T, Palmblad J. Angiogenesis research: guidelines for translation to clinical application. Thromb Haemost 2001;86:23–33.
43. Sauer G, Deissler H. Angiogenesis: prognostic and therapeutic implications in gynecologic and breast malignancies. Curr Opin Obstet Gynecol 2003;15:45–9.
44. Goddard JC, Sutton CD, Furness PN, O'Byrne KJ, Kockelbergh RC. Microvessel density at presentation predicts subsequent muscle invasion in superficial bladder cancer. Clin Cancer Res 2003;9:2583–6.
45. Poon RT, Fan ST, Wong J. Clinical significance of angiogenesis in gastrointestinal cancers: a target for novel prognostic and therapeutic approaches. Ann Surg 2003;238:9–28.
46. Zhang X, Yamashita M, Uetsuki H, Kakehi Y. Angiogenesis in renal cell carcinoma: evaluation of microvessel density, vascular endothelial growth factor and matrix metalloproteinases. Int J Urol 2002;9: 509–14.
47. de la Taille A, Katz AE, Bagiella E, Buttyan R, Sharir S, Olsson CA, Burchardt T, Ennis RD, Rubin MA. Microvessel density as a predictor of PSA recurrence after radical prostatectomy. A comparison of CD34 and CD31. Am J Clin Pathol 2000;113:555–62.
48. Bono AV, Celato N, Cova V, Salvadore M, Chinetti S, Novario R. Microvessel density in prostate carcinoma. Prostate Cancer Prostatic Dis 2002;5:123–7.
49. Weidner N, Carroll PR, Flax J, Blumenfeld W, Folkman J. Tumor angiogenesis correlates with metastasis in invasive prostate carcinoma. Am J Pathol 1993;143:401–9.
50. Silberman MA, Partin AW, Veltri RW, Epstein JI. Tumor angiogenesis correlates with progression after radical prostatectomy but not with pathologic stage in Gleason sum 5 to 7 adenocarcinoma of the prostate. Cancer 1997;79:772–9.
51. Gettman MT, Bergstralh EJ, Blute M, Zincke H, Bostwick DG. Prediction of patient outcome in pathologic stage T2 adenocarcinoma of the prostate: lack of significance for microvessel density analysis. Urology 1998;51:79–85.
52. Rubin MA, Buyyounouski M, Bagiella E, Sharir S, Neugut A, Benson M, de la Taille A, Katz AE, Olsson CA, Ennis RD. Microvessel density in prostate cancer: lack of correlation with tumor grade, pathologic stage, and clinical outcome. Urology 1999;53:542–7.
53. Tengblad A. Affinity chromatography on immobilized hyaluronate and its application to the isolation of hyaluronate binding properties from cartilage. Biochim Biophys Acta 1979;578:281–99.
54. Norrby K, Ridell B. Tumour-type-specific capillary endothelial cell stainability in malignant B-cell lymphomas using antibodies against CD31, CD34 and factor VIII. APMIS 2003;111:483–9.
55. Delpech B, Laquerriere A, Maingonnat C, Bertrand P, Freger P. Hyaluronidase is more elevated in human brain metastases than in primary brain tumours. Anticancer Res 2002;22:2423–7.
56. Hiltunen EL, Anttila M, Kultti A, Ropponen K, Penttinen J, Yliskoski M, Kuronen AT, Juhola M, Tammi R, Tammi M, Kosma VM. Elevated hyaluronan concentration without hyaluronidase activation in malignant epithelial ovarian tumors. Cancer Res 2002;62:6410–3.
57. Jacobson A, Rahmanian M, Rubin K, Heldin P. Expression of hyaluronan synthase 2 or hyaluronidase 1 differentially affect the growth rate of transplantable colon carcinoma cell tumors. Int J Cancer 2002;102:212–9.
58. Patel S, Turner PR, Stubberfield C, Barry E, Rohlff CR, Stamps A, McKenzie E, Young K, Tyson K, Terrett J, Box G, Eccles S, Page MJ. Hyaluronidase gene profiling and role of hyal-1 overexpression in an orthotopic model of prostate cancer. Int J Cancer 2002;97:416–24.
59. Canto EI, Shariat SF, Slawin KM. Biochemical staging of prostate cancer. Urol Clin North Am 2003;30:263–77.

Submitted to: Proc. Natl. Acad. Sci. USA

HYAL1 HYALURONIDASE IN PROSTATE CANCER: A TUMOR PROMOTER OR SUPPRESSOR

Vinata B. Lokeshwar[1,2,3]*, Wolfgang H Cerwinka[1], Bal Lokeshwar[1,2,4]
Departments of Urology (1), Sylvester Comprehensive Cancer Center (2), Cell Biology & Anatomy (3), and Radiation Oncology (4) University of Miami School of Medicine, Miami, Florida 33101

Running Title: HYAL1 functions in prostate cancer

*: Vinata B. Lokeshwar, Ph.D.
Department of Urology (M-800)
Miller School of Medicine
University of Miami
P.O. Box 016960
Miami, Florida, 33101

Phone: (305) 243-6321

Fax: (305) 243-6893

e-mail: vlokeshw@med.miami.edu

Key words: Prostate cancer; HYAL1 hyaluronidase; tumor growth; invasion; angiogenesis

Abbreviations: CM: conditioned medium; HA: hyaluronic acid; HAase: hyaluronidase; HYAL1-S: HYAL1 sense; HYAL1-AS: HYAL1 antisense; ITS: insulin, transferrin, selenium; MVD: microvessel density; PS: Phosphatidylserine

Grant support: DOD-DAMD 170210005 (VBL); NIH/NCI RO1 072821-06 (VBL); NIH/NCI 2RO1-CA061038 (BLL)

ABSTRACT

HYAL1 hyaluronidase (HAase) is an independent prognostic indicator of prostate cancer progression. HAases degrade hyaluronic acid, a glycosaminoglycan. HAase (e.g., HYAL1) function in tumor growth and progression is controversial, i.e., whether it is a tumor promoter or a suppressor. We stablely transfected androgen independent prostate cancer cell lines DU145 and PC-3 ML to generate HYAL1-sense (HYAL1-S), HYAL1-antisense (HYAL1-AS) and vector transfectants. Only vector and HYAL1-S transfectants were generated for PC3-ML since it expresses very little HYAL1. We selected HYAL1-S transfectants of DU145 and PC3-ML, which produced $\leq$ 42 mU HAase activity (moderate producers) or $\geq$ 80 mU HAase activity (high producers). HYAL1-AS transfectants of DU145 produced > 90% less HAase activity when compared to vector transfectants (18-24 mU).

While moderate producers and vector transfectants of DU145 had similar proliferation rate, both high producers and HYAL-AS transfectants grew 4-5-fold slower. In PC-3 ML, moderate HYAL1 expression increased proliferation rate by ~ 2-fold, but high production decreased growth by ~2.5-fold. HYAL1-AS transfectants were blocked in G2-M phase of the cell cycle, whereas, high HYAL1 production induced apoptosis. Blocking HYAL1 production decreased invasive activity of DU145, whereas, HYAL1 expression increased invasive activity, regardless of the expression level (i.e., moderate or high). Tumor xenograft studies showed that blocking HYAL1 (i.e., HYAL1-AS) inhibited tumor growth by 4-7-fold, whereas, high HYAL1 producers either did not form tumors (DU145 transfectants) or grew 3.5-fold slower (PC-3 ML transfectants). While vector and moderate HYAL1 producers generated muscle, lymph node and blood vessel infiltrating tumors, HYAL1-AS tumors were benign and contained smaller capillaries. The specimen of high HYAL1 producers was 99% free of tumor cells.

These results demonstrate that depending on the level of expression, HYAL1 could be a tumor promoter or a suppressor. This study may provide a basis for possible anti-HAase and high-HAase therapies.

INTRODUCTION

Hyaluronidase (HAase) is an endoglycosidase that degrades hyaluronic acid (HA). HA is a glycosaminoglycan made up of repeating disaccharide units D-glucuronic acid and N-acetyl-D-glucosamine (1, 2). In addition to maintaining hydration status and osmotic balance in tissues, HA also regulates cell adhesion, migration and proliferation (1). HA concentration is elevated in several tumors (4-8). We have shown that increased urinary HA levels serve as an accurate marker for detecting bladder cancer, regardless of the tumor grade (9,10). In prostate cancer tissues, HA is mainly produced by tumor-associated stroma, however, ~ 40% of tumor cells express HA (11,12). Tumor associated HA promotes invasive behavior including increased tumor cell migration, aiding in the loss of contact inhibition and offering protection against immune surveillance (13-15). Small fragments of HA (3 - 25 disaccharide units), generated by HAase, are angiogenic (16,17). We have detected such fragments in prostate cancer tissues, in bladder cancer patients' urine and in the saliva of head and neck cancer patients (7,9,18).

HAase is crucial for the spread of bacterial infections, and toxins/venoms (19,20). In the human genome, there are 6 HAase genes found on 2 chromosomes; 3p 21.3 (HYAL1, HYAL2, HYAL3) and 7q 21.3 (HYAL4, PH20 and HYALP1) (21). PH20 or testicular HAase induces acrosomal reaction during ovum fertilization (22). HYAL1 is present in human serum and urine and has a pH optimum of ~ 4.2. HYAL1 is 50% active at pH 5.0 (7,23,24). Lack of functional HYAL1 causes a mild disorder called type IX mucopolysaccharidosis (25). It is also the major HAase expressed in cancers of the prostate, bladder and head and neck, secreted by tumor cells (7,11,18,26,). In bladder cancer, increased HAase (i.e., HYAL1) serves as an accurate marker for detecting G2/G3 tumors (6,9,10). Using radical prostatectomy specimens from patients with 6 to 10 year follow-up, we found that HYAL1 is an independent predictor of biochemical recurrence (i.e., disease progression; 11,12). HAase levels increase in breast

cancer cells in the passage from primary to metastatic stage (27,28). We recently showed that blocking HYAL1 expression in an invasive bladder cancer line, decreases tumor growth by 9-17-fold, inhibits tumor infiltration and decreases microvessel density (MVD) by 4-9-fold (29). These results show that HYAL1 is involved in promoting tumor growth, invasion and angiogenesis. Expression of HYAL1 in PC-3 prostate cancer cells, that produce low levels of HAase, does not affect tumor growth but causes a slight increase in lung metastasis (30).

HYAL1 is also suggested to be a tumor suppressor because the 3p 21.3 locus is deleted in some lung cancer cell lines (31, 32). However, the tumor suppressor gene in the 3p 21.3 locus is none of the 3 HAase genes (33). Over-expression of HYAL1 in a rat carcinoma line suppresses tumor growth in xenografts and injection of 300 U of bovine testicular HAase also decreases growth of breast cancer xenografts (34,35).

Few studies have been conducted to explain the opposite effects of HYAL1 on tumor growth and invasion and whether in the same tumor system HYAL1 can act both as a tumor promoter and a suppressor. In this study we stablely transfected androgen independent prostate cancer cell lines DU145 and PC-3 ML to generate moderate HYAL1 producers, high HYAL1 producers and no/little HYAL1 producers to discern the tumor promoting and suppressing functions of HYAL1.

Materials and Methods:

Generation of HYAL1-S and HYAL1-AS stable transfectants: HYAL1 coding region was cloned into eukaryotic expression vector, pcDNA3.1/v5-His TOPO, in the sense and antisense orientation, with respect to CMV-promoter (29). DU145 and PC-3 ML cells (1×10^5/6-cm dish) were transfected with vector, HYAL1-S or HYAL1-AS cDNA constructs (1-µg DNA) using the Effectene™ transfection reagent (Qiagen). Transfectant clones were selected in a growth medium (RPMI 1640 + 10% fetal bovine serum + gentamicin) plus 400-µg/ml (DU145) or 300-µg/ml (PC-3 ML) geneticin (Invitrogen).

Analysis of HAase activity and HYAL1: HAase activity secreted in the serum-free conditioned media (CM) of transfectants was measured using a HAase ELISA-like assay and expressed as mU/10^6 cells as described previously (36). Active HAase species was detected in transfectant CM (secreted by $5x10^4$ cells, ~ 10-µg total protein) using a substrate (HA)-gel assay (26).

Immunoblot analysis and kinase assay: CM from the transfectant clones (secreted by $5x10^4$ cells, ~ 10-µg total protein) were immunoblotted using an anti-HYAL1 peptide IgG (i.e., anti-HYAL1 IgG) as described previously (29). Cell lysates ($4x10^4$ cells cells/transfectant) were immunoblotted using an anti-cyclin B1 IgG, anti-cdc2/p34 IgG or anti-cdc 25c IgG (29). Protein loading was verified by reprobing each blot with an anti-actin IgG (29). cdc2/p34 kinase was immunoprecipitated from cell lysates ($1x10^6$ cells/transfectant), using an anti-cdc/p34 antibody. Immunoprecipitates were used to perform the cdc2/p34-associated H1 histone kinase activity assay using H1 histone (29).

Cell proliferation assay: Transfectant clones were cultured on 24-well plates in growth medium + geneticin. Cells were counted in duplicate wells every 24-h for a total period of 120-h, in 2 independent experiments.

Cell-cycle analysis: Cell cycle phase distribution in actively growing cultures of transfectants was estimated by propidium iodide staining of DNA and flow cytometry using an EPICS XL flow cytometer, equipped with a FL3 filter (29). FL3 histograms were analyzed by Modfit Easy (Lite)

Program (Veritas Software, ME). Samples were assayed in duplicates in 2 independent experiments.

Apoptosis assay: 96-h cultures of transfectants (10^5 cells/24-well plate) were lysed and the cell lysates were tested for free nucleosome release using the Cell Death ELISA kit (Roche Diagnostics). All samples were assayed in triplicates in 2 independent experiments.

Annexin V binding: Annexin-V binding was examined in 96-h cultures of transfectants (~ $3x10^5$ cells/6-cm dish) using the ApoAlert™ Annexin V-EGFP kit (BD-Clontech Labs) and flow-cytometry. were used to determine the translocation of membrane phosphatidylserine (PS). Median fluorescence intensity (Annexin V binding to PS) was compared among transfectants in the green fluorescence channel (log FL1). Increase in green fluorescence intensity (log FL1) was taken as increase in Annexin V- PS binding.

Matrigel invasion assay: The membranes in 12-well Transwell plates were coated with Matrigel (100 µg/cm^2) plus or minus HA (50 µg/ml). Transfectants ($3x10^5$ cells/well) were plated on the upper chamber in a serum-free medium and the bottom chamber contained growth medium. Following 48-h incubation, invasion of cells through Matrigel into the bottom chamber was quantified using the MTT assay. Invasion of cells was calculated as (cells in the bottom chamber ÷ cells in upper + bottom chambers) x 100 (29).

Pericellular matrix assay: Formaldehyde fixed human erythrocytes were overlaid on overnight cultures of transfectants (10^4 cells/6-cm dish). Cells showing a bright region around the entire periphery with width ≥ the diameter of an erythrocyte (i.e., pericellular matrix) were counted in 10 fields. Results were expressed as % cells with pericellular matrix ± S.D. (29, 37).

Tumor xenografts and histology: Transfectants (2×10^6 cells) were subcutaneously implanted on the dorsal flank of 5-week old male athymic mice (10 mice/clone). After tumors became palpable, tumor size was measured 2x weekly. Tumor volume was calculated assuming an ellipsoid shape (38). Following euthanasia (DU145: 42 day; PC-3 ML: 28 day), tumors were weighed. Tukey's multiple comparison test was used to evaluate differences in tumor growth rate and tumor weight. Tumor histology was performed at Charles River Laboratories (Wilmington, MA).

HA, HYAL1 localization and microvessel density (MVD) determination: HA and HYAL1 were localized in tumor xenograft specimens by immunohistochemistry using a biotinylated HA-binding protein and the anti-HYAL1 IgG, respectively (29). MVD was evaluated using CD34 staining (rat anti-mouse CD34 IgG; Pharmingen) (29). MVD was determined by 2 readers independently counting microvessels in 10 fields and expressed as mean ± S.D. Length of microvessels was measured using a Nikon H550L microscope with a video screen camera equipped with measuring tools.

RESULTS:

Analysis of HYAL1 expression in DU145 and PC-3 ML transfectants: We have previously shown that DU145 cells secrete HAase activity in their CM however PC-3 ML cells secrete very little HAase (7). We generated HYAL1-S (HAase overproducing) transfectants of both DU145 and PC-3 ML cells, and only HYAL1-AS transfectants of DU145. We analyzed 25 – 30 clones of each transfectant type (vector, HYAL1-S and HYAL1-AS) for HAase production and HYAL1 expression. For HYAL-S transfectants we selected 2 types of clones, moderate HAase overproducing and high HAase overproducing. Data on 2 clones from each type are shown. As shown in Fig. 1 A, DU145 HYAL1-S clones # 1 and # 2 secrete 1.5-2.3-fold more HAase activity

and HYAL1-S # 3 and # 4 clones secrete 3.8-7.3-fold more HAase activity, when compared to vector # 1 and # 2 clones. There is > 90% reduction in HAase secretion in HYAL1-AS clones. PC-3 ML HYAL1-S clones # 1 and # 2 secrete HAase activity similar to that secreted by DU145 vector clones, and it is about 10-fold more than that secreted by PC-3 ML vector clones (Fig.1 B). HYAL1-S # 3 and # 4 clones secrete HAase activity similar to that secreted by DU145 # 3 and # 4 clones.

Anti-HYAL1 immunoblot analysis shows that a ~ 60-kDa HYAL1 protein is secreted in the CM of DU145 vector and HYAL1-S clones but not in HYAL1-AS clones. (Fig 2 A). In PC-3 ML clones, HYAL1 protein is detected in the CM of HYAL1-S transfectants but not in vector clones. The amount of HYAL1 protein detected in HYAL1-S clones # 3 and # 4 is higher than that detected in HYAL1-S # 1 and # 2 clones (Fig 2 B). The substrate (HA)-gel analysis confirms immunoblot results as it detects a ~ 60-kDa active HAase species in the CM of DU145 vector and HYAL1-S clones and in PC-3 ML HYAL1-S clones (Fig 2 C and D).

Effect of HYAL1 expression on cell proliferation, cell cycle and apoptosis: The growth rate of DU145 vector and HYAL1-S # 1 and # 2 transfectant is comparable (doubling time ~ 26-28 hr) (Fig. 3 A). However, both HYAL1-AS clones and also HYAL1-S # 3 and # 4 clones (which secrete $\geq$ 100 mU/10^6 HAase activity) grow 4-5-fold slower than vector clones (doubling time ~ 90-96 hr). PC-3 ML HYAL1-S # 1 and HYAL1-S # 2 clones grow 1.5-2-fold faster than the vector clones, however, the high HYAL1 producer clones, HYAL1-S # 3 and # 4 grow 2-2.5-fold slower than the vector clones (Fig. 3 B).

Cell cycle analysis revealed that decreased growth rate of HYAL1-AS transfectants was due to cell-cycle arrest in the G2-M phase. There was a 200% - 300% increase in the number of HYAL1-AS #1 (22.3%) and # 2 (31.2%) cells in G2-M phase when compared to vector (# 1: 11.5%; # 2: 12.4%) and all HYAL1-S transfectant clones (9.7% - 12.4%). Correspondingly, the % of HYAL1-AS cells in S-phase (#1: 24.8%; # 2: 28.8%) decreased when compared to vector and HYAL1-S cells (% cells in S-phase: 35.9% – 38.5%). The increase in the G2-M phase of cell cycle in HYAL1-AS transfectants was statistically significant ($P < 0.001$; Tukey's test). HYAL1 expression did not affect % of cells in G0-G1. Interestingly, for HYAL1-S # 3 and # 4, we observed an extra peak to the left of the G0-G1 peak, possibly representing apoptotic cells. In PC3-ML transfectants, HYAL1 expression also increased the number of cells in the S-phase with a corresponding decrease in the number of cells in G2-M phase (data not shown).

We next analyzed the expression of G2-M regulators, i.e., cdc25c, cyclin B1, and cdc2/p34 proteins in various clones. As shown in Fig. 4, both cdc25c bands, plausibly representing active (phosphorylated) and native forms, are detected in all DU145 transfectants. There is ~ 3-fold decrease in the expression of active cdc25c in HYAL1-AS transfectants when compared to the vector and HYAL1-S transfectant clones. There is also ~ 3-fold and 2-fold decrease in the expressions of cyclin B1 and cdc2/p34 in HYAL1-AS transfectants when compared to vector and HYAL1-S clones (Fig 4). A ~ 2.5- and 3-fold decrease in cdc2/p34-associated H1 histone kinase activity is observed in HYAL1-AS transfectant clones when compared to vector and all HYAL1-S transfectants (Fig 4). These results show that the slow proliferation rate of HYAL1-AS transfectants is due to G2-M arrest.

We next determined whether the slower growth of HYAL1-S # 3 and # 4 clones is due to high rate of apoptosis. As shown in Fig. 5 A, there is a 3-fold increase in the intracellular levels of free nucleosomes in HYAL1-S # 3 and HYAL1-S # 4 cells when compared to vector, HYAL1-S #1 and #2, as well as, HYAL1-AS clones. To confirm the induction of apoptosis, we measured the outward translocation of plasma membrane PS by Annexin-V binding. As shown in Fig 5 B,

there is a distinct increase in EGFP-Annexin V binding to HYAL1-S # 3 and # 4 cell surface when compared to vector control (Note the right shift in median green fluorescence channel; Median peak LogFL1: vector: 1.21; HYAL1-S # 3, 2.37; HYAL1-S # 4, 2.83). Therefore, the decreased cell growth observed in high HYAL1 producers is due to induction of apoptosis.

Effect of HYAL1 expression on *in vitro* invasion: In Matrigel™ invasion assay, invasive activity of DU145 vector # 1 clone (22.3 ± 4.3 %) was normalized as 100% and the invasive activity of other clones was expressed as % of vector. Invasive activity of all HYAL1-S clones (# 1 - # 4) varied between 109% and 118% and was not statistically different from that of vector clones. However, the invasive activity of HYAL1-AS clones (28.2 ± 1.7% and 31.5 ± 1.5%) was 3-fold less when compared to vector clones ($P < 0.001$; Tukey's test). HYAL1 expression in PC3-ML cells increased their invasive activity by 3-3.5-fold. When the invasive activity of the vector clones (# 1: 26.5 ± 3.4%; 28.3 ±3.1%) was considered as 100%, the invasive activity of HYAL1-S clones varied between 288% and 354% ($P < 0.001$). These results show that HYAL1 expression increases the invasive activity of prostate cancer cells.

Effect of HYAL1 expression on pericellular matrix formation: As shown in Figure 6, vector #1 and HYAL1-S clones (# 1 and # 3) do not exhibit pericellular matrices as the erythrocytes closely abut the surface of each cell. However, HYAL1-AS cells (clone # 1) exhibit a clear pericellular matrix. We counted cells with pericellular matrix in 10 fields at 100X magnification (# of cells counted/transfectant: 120 – 150). There was a 3- and 4.6-fold increase in the percentage of cells with pericellular matrix for HYAL1-AS transfectants (# 1: 94.2 ± 8.6%; # 2: 86.3 ± 9.0%) when compared to vector (#1: 27.8 ± 18%; # 2: 35.5 ± 11.1%), moderate HYAL1 over-producing (HYAL1-S #1: 25.5 ± 13.2%; # 2: 31.2 ± 18%) and high HYAL1 over-producing (HYAL1-S # 3: 22.3 ± 16.1%; 17.2 ± 13.2%) transfectants, respectively ($P < 0.001$). Thus, HA is an important component of the pericellular matrix of prostate cancer cells and it is degraded by HYAL1.

Effect of HYAL1 expression on tumor xenografts: In xenografts, there is a 4-5-fold delay in the generation of palpable tumors in animals injected with DU145 HYAL1-AS transfectants (33 ± 4 days) when compared to vector and moderate HYAL1overproducing transfectants (6 – 8 days) (Fig. 7 A, $P < 0.001$). Interestingly, high HYAL1 producers did not form palpable tumors even on day 40 when necropsy was performed. The weight (g) of vector (# 1: 0.17 ± 0.05; # 2: 0.14 ± 0.04) and moderate HYAL1 overproducers (HYAL1-S # 1: 0.21 ± 0.06; # 2: 0.27 ± 0.14) tumors was 4- and 7-fold more than HYAL1-AS tumors (#1: 0.03 ± 0.01; 0.04 ± 0.01), respectively ($P < 0.001$). HYAL1-S #1 and # 2 tumors also showed presence of large blood vessels. While no animals injected with HYAL1-S # 3 or # 4 transfectants had visible evidence of tumor, in some animals a Matrigel™ plug-like material was visible. Two additional high HYAL1 producing transfectants generated in a 2nd transfection experiment also did not form palpable tumors (data not shown).

Moderate HYAL1 producing PC-3 ML tumors (HYAL1-S # 1 and # 2) grow about 2-fold faster, whereas, high HYAL1 producing tumors grow 2-2.5-fold slower than vector tumors (Fig. 7 B). At day 28, the weights (g) of moderate HYAL1 producing tumors (#1: 0.57 ± 0.12; # 2: 0.6 ± 0.14) is 2-fold higher than vector tumors (# 1: 0.28 ± 0.06; # 2: 0.29 ± 0.04) and 3.5-fold higher than high HYAL1 producing tumors (# 3: 0.16 ± 0.03; # 4: 0.14 ± 0.05) ($P < 0.001$).

Histology reports and photomicrographs show that while DU145 vector and moderate HYAL1 producing tumors show high mitotic figures, invade skeletal muscle and lymph nodes and infiltrate lymphatic and blood vessels HYAL1-AS tumors are non-invasive (Fig 8 A).

The Matrigel™ plug-like material removed from HYAL1-S # 3 and # 4 animals is ≥ 99% free of tumor cells and no mitotic figures are observed (Fig 8 A). These results show that while blocking HYAL1 production significantly reduces tumor growth, overproduction of HYAL1 also decreases tumor growth and may even inhibit tumor generation.

HYAL1, HA expression and MVD in tumor xenografts: Tumor cells in vector, and HYAL1-S # 1 and # 2 xenografts express significant levels of HYAL1 but HYAL1-AS cells do not secrete HYAL1 (Fig 8 B). Interestingly as we had observed in bladder cancer xenografts (29), HA production increased in the tumor-associated stroma of vector and HYAL1-S # 1 tumor specimens when compared to HYAL1-AS # 1 tumor specimens (Fig 8 B). MVD in vector (39.09 ± 4.6; # 2: 36.5 ± 6.5), and moderate HYAL1 producing (HYAL1-S # 1: 47.64 ± 13; # 2: 51.3 ± 12.5) is slightly higher than HYAL1-AS (# 1: 34.3 ± 17.6; # 2: 27.3 ± 12.1) tumors ($P > 0.05$). However, the length of capillaries in vector (817.4 ± 141.5 μm) and HYAL1-S (# 1: 1031 ± 262.5; # 2: 817.9 ± 305.3) tumors is 4-5-fold higher than of capillaries in HYAL1-AS tumors (# 1: 218.1 ± 103.4; # 2: 247.1 ± 96.1) (Fig. 8 C).

DISCUSSION

The results of our study help to explain contradictory findings regarding the role of HYAL1 as a tumor promoter or suppressor. While in some cancers HAase (i.e., HYAL1 or PH20) serves as a diagnostic or prognostic indicator, in others, HAase levels slightly decrease in high-grade tumors (6,9-12,18,39-42). In bladder cancer HYAL1 is a molecular determinant of tumor growth, invasion and angiogenesis but in a rat colon cancer line, HYAL1 expression suppresses tumor growth and induces necrosis (29,34). Two possibilities can explain these contradictory results: 1. HAases (and HYAL1 in particular) function either as tumor promoters or suppressors depending on the tumor type 2. Tumor promoter and suppressor functions of HAase/HYAL1 are concentration dependent.

Our data on 2 prostate cancer lines show that in the same tumor cell system, HYAL1 can act both as a tumor suppressor and a promoter, depending on the level of expression. HYAL1-AS transfectants of prostate and bladder cancer cells grow 4-fold slower *in vitro*, are blocked in the G2-M phase of the cell cycle, are less invasive and generate small, less angiogenic non-invasive tumors (29). Expression of HYAL1 in PC3-ML cells, which express very little HAase, increases cell growth and invasive phenotype and enhances tumor growth. Furthermore, Patel et al have shown that HYAL1 expression in PC-3 increases their metastatic potential (30). Therefore, HYAL1 is necessary for tumor growth, invasion, and angiogenesis.

Mean HAase levels in the urine of G2/G3 bladder cancer patients (~ 25 mU/mg protein) and in high-grade prostate cancer tissues (~ 36 mU/mg protein) are comparable to the HAase activity secreted by DU145 vector and moderately HYAL1 over-expressing DU145 and PC-3 ML transfectants (14 – 40 mU/10^6 cells). This suggests that the HAase concentration found in tumor tissues is in the range that is stimulatory to tumor growth, invasion and angiogenesis.

HAase levels ≥ 80 – 100 mU/10^6 cells slow tumor cell growth *in vitro*, inhibit tumor generation by DU145 transfectants and decrease growth of PC-3 ML tumors. In the report that HYAL1 expression suppresses tumor growth in a rat colon carcinoma cell model, the transfectants expressed 220 – 360 mU HAase activity/10^6 cells (34). That study suggested that HA degradation due to increased HYAL1 may cause compression of structural organization in tumor tissues, resulting in diminished flow of nutrients or HYAL1 may induce apoptosis in tumor cells (34). Our results show that high HYAL1 producing prostate cancer cells undergo apoptosis. Furthermore, partially purified HYAL1 induces apoptosis in DU145 vector and

HYAL1- S # 1 and # 2 clones (Unpublished results). This finding may be important in cancer treatment, as tumor cells which either do not express or moderately over-express HYAL1 can be induced to undergo apoptosis by exposing them to > 100 mU/ml HYAL1 concentration.

The mechanism by which HYAL1 induces apoptosis in epithelial tumor cells (e.g., prostate cancer cells) is unknown. However, HAases including HYAL1 (transient transfection experiments) enhance tumor necrosis factor-mediated toxicity by inducing WOX1 (WW-domain binding oxidoreductase) expression in L929 murine fibroblast (43-44). WOX1 is localized in mitochondria and induces apoptosis in a p53 independent manner. It is also required for p53-mediated cell death (44). It is unknown whether tumor cells i.e., prostate cancer cells express WOX1, and whether HYAL1 regulates its expression. WOX1 coding gene, WWOX, maps to a fragile region in 16q locus that is deleted in prostate cancer at increased frequency and is a predictor of metastasis (45).

HAase treatment has been shown to overcome acquired drug resistance displayed by tumor cells growing in multicellular spheroids (46). In a few studies, extremely high doses of bovine testicular HAase (> 100,000 Units/kg) have been shown to improve efficacy of cytotoxic drugs (47). In those studies, HAase was believed to improve drug penetration. Based on our study, such high levels of HAase may also aid in controlling tumor growth by inducing apoptosis.

Taken together our study helps to resolve conflicting findings that are reported in the literature, regarding the role of HYAL1 both as a tumor promoter and suppressor. The study may also provide a basis for possible anti-HAase (HAase inhibition), as well as, "high-HAase" treatments for controlling cancer growth and progression.

Acknowledgments: We are grateful to Dr. Awtar Krishan Ganju, Department of Radiology and Microbiology and Immunology his advice on flow-cytometry. We thank Dr. Charles Clifford, Director of Pathology, Charles River Laboratories for his help in histology.

REFERENCES

1. Toole B.P. (2004) Nat Rev Cancer. **4**, 528-539.
2. Tammi, M.I., Day, A.J., & Turley, E.A. (2002) J. Biol. Chem. **277**, 4581-4584.
3. Turley, E.A., Noble, P.W., & Bourguignon, L.Y. (2002) J. Biol. Chem. **277**, 4589-92.
4. Setälä, L.P., Tammi, M.I., Tammi, R.H., Eskelinen, M.J., Lipponen, P.K., Ågren, U.M., Parkkinen, J., Alhava, E.M., & Kosma, V-M. (1999) Br. J. Cancer **79**, 1133-1138.
5. Auvinen, P., Tammi, R., Parkkinen J. Tammi, M., Ågren, U., Johansson, R., Hirvikoski, P., Eskelinen, M., & Kosma, V-M. (2000) Am. J. Pathol. **156**, 529-36.
6. Hautmann, S.H., Lokeshwar, V.B., Schroeder, G.L., Civantos, F., Duncan, R.C., Gnann, R., Friedrich, M.G., & Soloway, M.S. (2001) J. Urol. **165**, 2068-2074.
7. Lokeshwar, V.B., Rubinowicz, D., Schroeder, G.L., Forgacs, E., Minna, J.D., Block, N.L., Nadji, M., Lokeshwar, B.L. (2001) J. Biol. Chem. **276**, 11922-1932.
8. Lipponen, P., Aaltomaa, S., Tammi, R., Tammi, M., Ågren, U., & Kosma, V-M. (2001) Eur J Cancer **37**, 849-856.
9. Lokeshwar, V.B., Obek, C., Soloway, M.S., & Block, N.L. (1997) Cancer Res. **57,** 773-777. Erratum in: Cancer Res 1998; **58**, 3191.
10. Lokeshwar, V.B., Obek, C., Pham, H.T., Wei, D., Young, M.J., Duncan, R.C., Soloway, M.S., & Block, N.L. (2000) J Urol. **163**, 348-356.
11. Posey, J.T., Soloway, M.S., Ekici, S., Sofer, M., Civantos, F., Duncan, R.C., & Lokeshwar V.B. (2003) Cancer Res. **63**, 2638-2644.
12. Ekici, S., Cerwinka, W.H., Duncan, R., Gomez, P., Civantos, F., Soloway, M.S., & Lokeshwar, V.B. (2004) Int J Cancer. **112**,121-129.

13. Hayen, W., Goebeler, M., Kumar, S., Riessen, R., & Nehls, V. (1999) J Cell Sci. **112**, 2241- 2251.
14. Hobarth, K., Maier, U., Marberger M. (1992) Eur. Urol. **21**, 206-210.
15. Itano, N., Atsumi, F., Sawai, T., Yamada, Y., Miyaishi, O., Senga, T., Hamaguchi, M., Kimata K. (2002) Proc. Natl. Acad. Sci. **99**, 3609-3614.
16. Lees, V.C., Fan, T.P., West, D.C. (1995) Lab Invest. **73**, 259-266.
17. West, D.C., Hampson, I.N., Arnold, F., Kumar, S. (1985) Science **228**,1324-1326.
18. Franzmann, E.J., Schroeder, G.L., Goodwin, W.J., Weed, D.T., Fisher, P., & Lokeshwar, V.B. (2003) Int J Cancer **106**, 438-445.
19. Girish, K.S., Shashidharamurthy, R., Nagaraju, S., Gowda, T.V., & Kemparaju, K. (2004) Biochimie. **86**,193-202.
20. Kuhn-Nentwig, L., Schaller, J., & Nentwig, W. (2004) Toxicon. **43**, 543-553.
21. Csoka, A.B., Frost, G.I., & Stern, R. (2001) Matrix Biol. **20**, 499-508.
22. Cherr, G.N., Yudin, A.I., Overstreet, J.W. (2001) Matrix Biol. 20: 515-525.
23. Csoka, A.B., Frost, G.I., Wong, T., Stern, R. & Csoka TB. (1997) FEBS Lett. **417**, 307-310. Erratum in: FEBS Lett. **566**, 316.
24. Frost, G.I., Csoka, A.B., Wong, T., Stern, R., & Csoka, T.B. (1997) Biochem Biophys Res Commun. **236**, 10-155.
25. Triggs-Raine, B., Salo, T.J., Zhang, H., Wicklow, B.A. & Natowicz MR. (1999) Proc Natl Acad Sci USA **96**, 6296-300.
26. Lokeshwar, V.B., Young, M.J., Goudarzi, G., Iida, N., Yudin, A.I., Cherr, G.N. & Selzer M.G. (1999) Cancer Res. 59, 4464-4470.
27. Victor, R., Chauzy, C., Girard, N., Gioanni, J., d'Anjou, J., Stora De Novion H., & Delpech, B. (1999) Int J Cancer. **82**,77-83.
28. Madan, A.K., Yu, K., Dhurandhar, N., Cullinane, C., Pang, Y., & Beech, D.J.(1999) Oncol Rep. **6**, 607-609.
29. Lokeshwar, V.B., Cerwinka, W.H., & Lokeshwar, B.L. (2004) Cancer Res., (Revised manuscript submitted).
30. Patel, S., Turner, P.R., Stubberfield, C., Barry, E., Rohlff, C.R., Stamps, A., McKenzie, E., Young, K., Tyson, K., Terrett, J., et al (2002) Int J Cancer **97**, 416-24. Erratum in: Int J Cancer 2002, **98**, 957.
31. Junker, N., Latini, S., Petersen, L.N., & Kristjansen, P.E. (2003)Oncol Rep. 10, 609-616.
32. Csoka, A.B., Frost, G.I., Heng, H.H., Scherer, S.W., Mohapatra, G., Stern,R., & Csoka, T.B. (1998) Genomics. **48**, 63-70.
33. Ji, L., Nishizaki, M., Gao, B., Burbee, D., Kondo, M., Kamibayashi, C., Xu, K., Yen, N., Atkinson, E.N., Fang, B., et al (2002) Cancer Res. **62**, 2715-2720.
34. Jacobson, A., Rahmanian, M., Rubin, K., & Heldin, P. (2002) Int J Cancer. **102**, 212-219.
35. Shuster, S., Frost, G.I., Csoka, A.B., Formby, B., & Stern, R. (2002) Int J Cancer. **102**, 192-197.
36. Pham, H.T., Block, N.L., & Lokeshwar, V.B. (1997) Cancer Res. **57**, 778-783. Erratum in: Cancer Res 1997, 57, 1622.
37. Zoltan-Jones, A., Huang, L., Ghatak, S., & Toole, B.P. (2003) J. Biol Chem. **278**, 45801-45810.
38. Dandekar, D.S., & Lokeshwar, B.L. (2004) Clin Cancer Res. **10**, 8037-8047.
39. Beech, D.J., Madan, A.K., & Deng, N. (2002) J Surg Res. **103**, 203-207.
40. Bertrand, P., Courel, M.N., Maingonnat, C., Jardin, F., Tilly, H., & Bastard C. (2005) Int J Cancer. **113**,207-212.
41. Tuhkanen, H., Anttila, M., Kosma, V.M., Yla-Herttuala, S., Heinonen, S., Kuronen, A., Juhola, M., Tammi. R., Tammi, M., & Mannermaa, A. (2004) Int J Cancer. **109**,247-252.

42. Hiltunen, E.L., Anttila, M., Kultti, A., Ropponen, K., Penttinen, J., Yliskoski, M., Kuronen, A.T., Juhola, M., Tammi, R., Tammi, M., et al (2002) Cancer Res. **62**, 6410-6413.
43. Chang, N.S., Doherty, J., & Ensign, A. (2003) J Biol Chem. **278**, 9195-9202.
44. Chang, N.S. (2002) BMC Cell Biol. **3**, 8.

45. Watson, J.E., Doggett, N.A., Albertson, D.G., Andaya, A., Chinnaiyan, A., van Dekken, H., Ginzinger, D., Haqq, C., James, K., Kamkar, S., et al (2004) Oncogene. **23**, 3487-3494.
46. Croix, B.S., Rak, J.W., Kapitain, S., Sheehan, C., Graham, C.H., & Kerbel, R.S. (1996) J Natl Cancer Inst. **88**, 1285-1296.
47. Klocker, J., Sabitzer, H., Raunik, W., Wieser, S., & Schumer, J. (1995) Am J Clin Oncol. **18**, 425-428.

FIGURE LEGENDS:

Figure 1: Analysis of HAase activity in DU145 and PC-3 ML transfectants. HAase activity (mU/mg) was measured using an ELISA-like assay. Data are presented as mean ± SD from 3 separate experiments.

Figure 2: Detection of HYAL1 expression in DU145 and PC-3 ML transfectants. A & C. Immunoblot analysis: CM (10 μg protein; CM of 50,000 cells) were subjected to anti-HYAL1 IgG immunoblotting. **B & D: Substrate (HA)-gel assay.** CM (10 μg protein; CM of 50,000 cells) were analyzed by substrate (HA)-gel.

Figure 3: Determination of proliferation rate of transfectants. The cell counting data presented are mean ± SD from duplicate measurements in 3 independent measurements. A: DU145; B: PC-3 ML.

Figure 4: Analysis of G2-M cell cycle regulators. Cell lysates of DU145 transfectants were analyzed by immunoblotting using anti- cdc25c (**a**), anti-cyclin B1 (**b**) and anti-cdc2/p34 (**c**) and β-actin (**d**) antibodies. Lanes 1 & 2: vector clones # 1 & 2; lanes 3-6: HYAL1-S clones 1 - 4; lanes 7 & 8: HYAL1-AS clones # 1 & 2. (**e**): Measurement of H1 histone kinase-associated activity. Lanes 1 - 8 are the same as described above; lane 9: negative control.

Figure 5: Examination of apoptosis. A: Apoptotic activity in various transfectants was evaluated using the Cell Death ELISA Plus assay kit. Data shown are Mean ± S.D. obtained from 3 measurements in 2 independent experiments. **B:** Cell surface EGFP-Annexin V binding to translocated PS was analyzed in transfectants using flow cytometry. Experiment was repeated twice.

Figure 6: Examination of pericellular matrix in DU145 transfectants Pericellular matrices surrounding DU145 transfectants were visualized using the particle exclusion assay. **A:** Vector # 1; **B:** HYAL1-S # 1; **C:** HYAL1-S # 4; **D:** HYAL1-AS # 2.

Figure 7: Figure 6: Examination of the growth of DU145 and PC-3 ML transfectant tumors in xenografts. DU145 and PC-3 ML transfectants were injected subcutaneously in athymic mice (10 animals/group) and tumor volume was measured as described in "Materials and Methods". The data are presented as mean ± SD. **A:** DU145 **B:** PC-3 ML.

Figure 8: Examination of tumor histology: A: Photomicrographs of hematoxylin and Eosin stained tumor specimens are shown at 100X magnification. **1. Vector # 1:** Muscle fibers are surrounded by tumor cells (arrow a) and the tumor impinges on an adjacent nerve (arrow b). **2. Vector # 2:** Tumor (T) approaches a lymph node (LN). Between the tumor and the lymph node is adipose tissue containing several blood vessels. **3. HYAL1-S # 1:** A thrombus (Thr) fills a blood vessel at the periphery of the tumor (T). Tumor cells (arrows) have infiltrated the blood vessel. **4. HYAL1-S # 2:** Tumor cells (arrow) have infiltrated a lymphatic vessel (LV). **5. HYAL1-S # 4:** Clusters of cells, mostly leukocytes, are scattered in pale staining Matrigel (G). **6. HYAL1-AS # 1:** The tumor (T) does not invade skeletal muscle (M) or a nerve (N) as connective tissue (CT) separates them. **B: HYAL1 and HA localization:** Panels a,b,c: HYAL1 localization; Panels d,e,f: HA localization. Panels a & d: vector # 1; panels b & e: HYAL1-S # 1; panels c & f: HYAL1-AS # 1. **C: Localization of microvessels.** The areas of the highest MVD from each type of tumor specimen are presented here; magnification, 400X. Panel a: vector # 1; panel b: HYAL1-S # 1; panel c: HYAL1-S # 2; panel d: HYAL1-AS # 1. Note: HYAL1-S # 3 and # 4 were not stained for HA, HYAL1 or microvessels as the specimen was tumor cell free.

Lokeshwar et al Fig 1

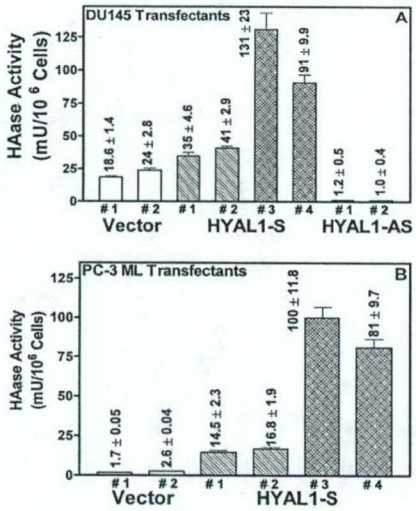

Lokeshwar et al Fig 2

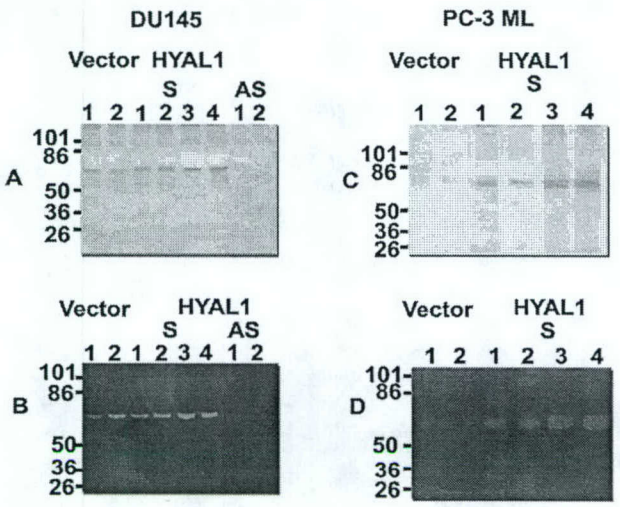

Lokeshwar et al Fig 3

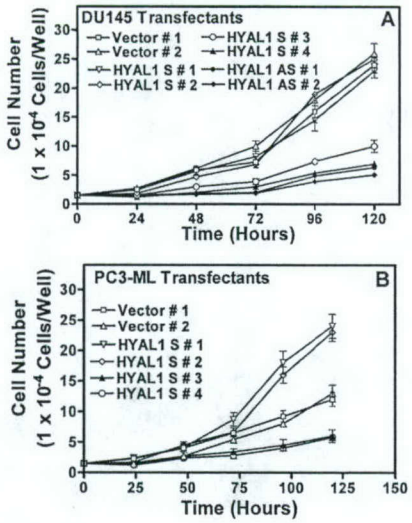

Lokeshwar Fig 4

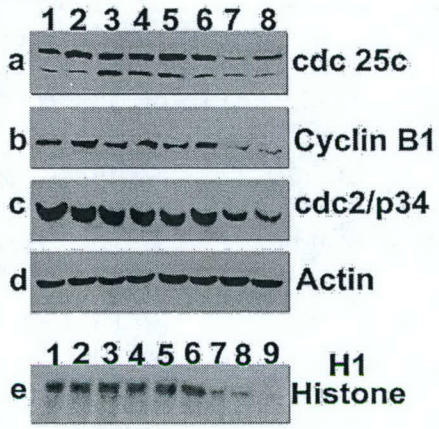

Lokeshwar Fig 5

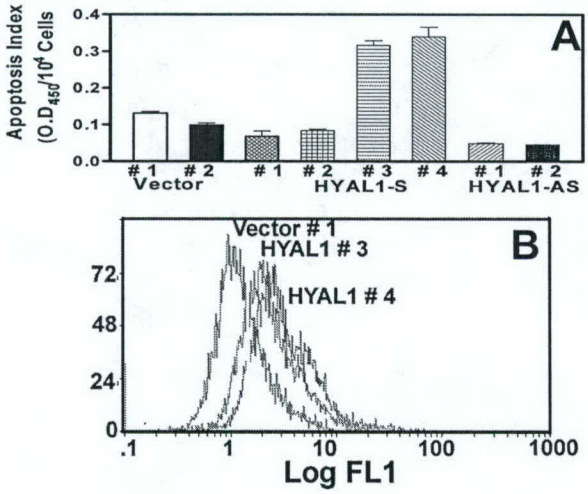

Lokeshwar Fig 6

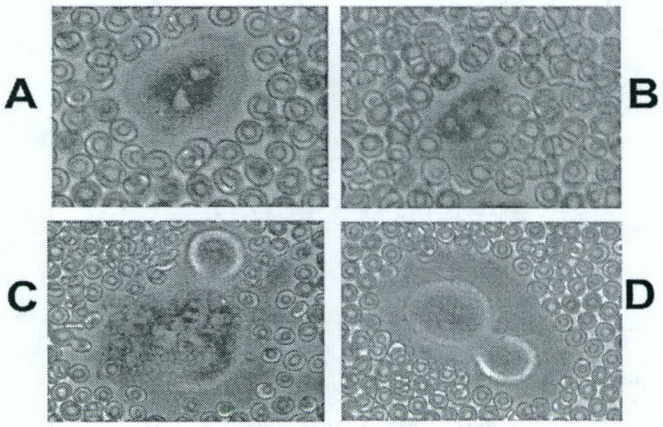

Lokeshwar Fig 7

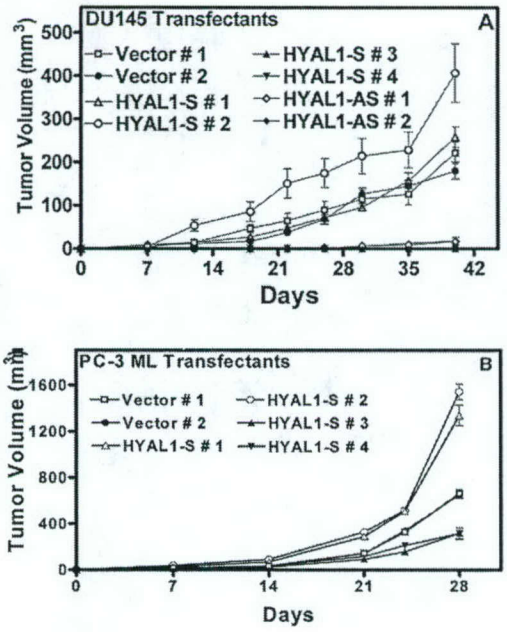

Lokeshwar Fig 8

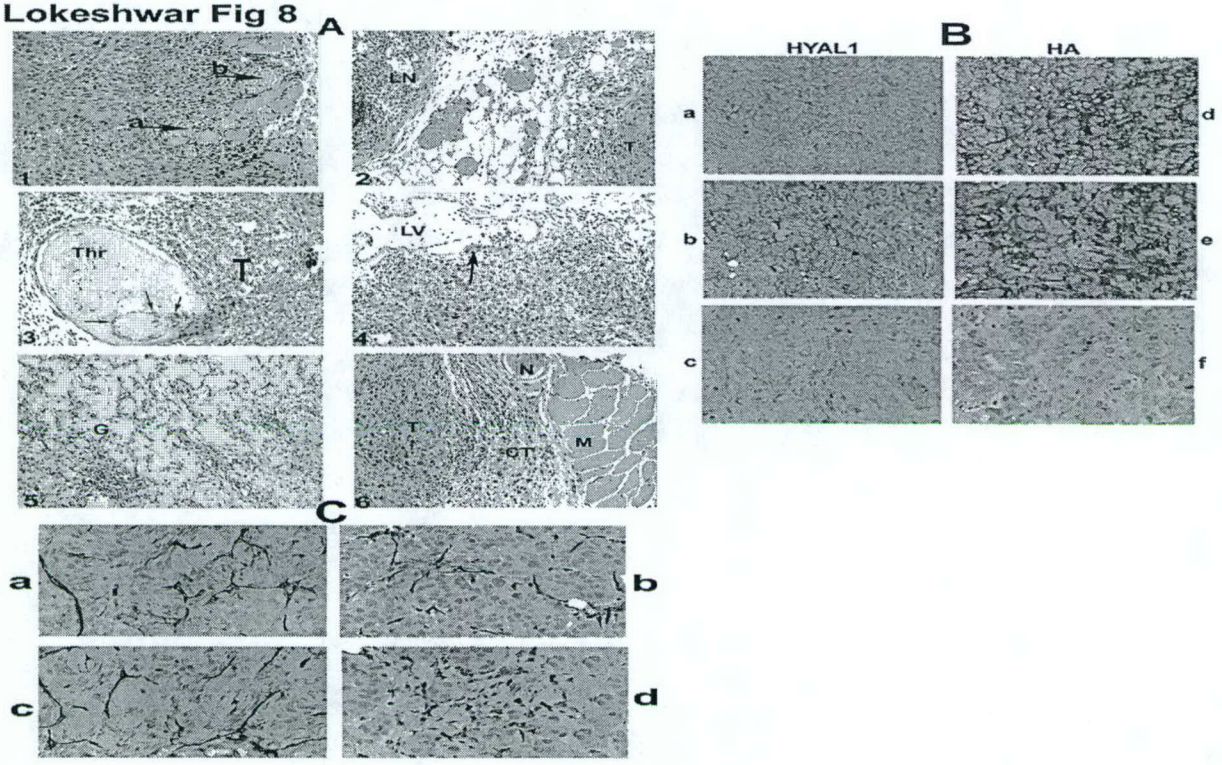

IN PRESS: Cancer Research 2005

HYAL1 HYALURONIDASE: A MOLECULAR DETERMINANT OF BLADDER TUMOR GROWTH AND INVASION

Vinata B. Lokeshwar[1,2,3*], Wolfgang H. Cerwinka[1], Bal L. Lokeshwar[1,2,4]

Departments of Urology (1), Sylvester Comprehensive Cancer Center (2), Cell Biology and Anatomy (3) and (4) Radiation Oncology University of Miami School of Medicine, Miami, Florida 33101

Running Title: Tumor promoting function of HYAL1 in bladder cancer

*: **Address for correspondence:**
Vinata B. Lokeshwar, Ph.D.
Department of Urology (M-800)
University of Miami School of Medicine
P.O. Box 016960
Miami, Florida, 33101

Phone: (305) 243-6321

Fax: (305) 243-6893

e-mail: vlokeshw@med.miami .edu

Key words: Bladder cancer; HyaluronidaseHYAL1; tumor growth, tumor invasion, angiogenesis

Abbreviations: HAase: hyaluronidase; MVD: microvessel density; HA: hyaluronic acid; HAS: hyaluronic acid synthase; HYAL1-S: HYAL1-sense; HYAL1-AS: HYAL1-antisense; ITS: insulin, transferrin, selenium; CM: conditioned medium/media; PBS: phosphate buffered saline

Grant Support: NCI grant RO1 CA 072821-06A2 (VBL); DOD-DAMD 170210005 (VBL); American Cancer Society Florida Division (VBL); 2RO1-CA061038 (BLL)

ABSTRACT

Hyaluronic acid (HA) and HYAL1 type hyaluronidase (HAase) show high accuracy in detecting bladder cancer and evaluating its grade, respectively. HA promotes tumor progression, however, the functions of HAase in cancer are largely unknown. In this study we stablely transfected HT1376 bladder cancer cells with HYAL1-sense (HYAL1-S), HYAL1-antisense (HYAL1-AS) or vector cDNA constructs. While HYAL1-S transfectants produced 3-fold more HYAL1 than vector transfectants, HYAL1-AS transfectants showed ~ 90% reduction in HYAL1 production.

HYAL1-AS transfectants grew 4-times slower than vector and HYAL1-S transfectants and were blocked in the G2-M phase of the cell cycle. The expression of cdc25c and cyclin B1, and cdc2/p34-associated H1 histone kinase activity also decreased in HYAL1-AS transfectants. HYAL1-S transfectants were 30% to 44% more invasive and the HYAL1-AS transfectants were ~ 50% less invasive than the vector transfectants, *in vitro*. In xenografts, there was a 4- to 5-fold delay in the generation of palpable HYAL1-AS tumors, and the weight of HYAL1-AS tumors was 9-17-fold less than vector and HYAL1-S tumors, respectively ($P < 0.001$). While, HYAL1-S and vector tumors infiltrated skeletal muscle and blood vessels, HYAL-AS tumors resembled benign neoplasia. HYAL1-S and vector tumors expressed significantly higher amounts of HYAL1 (in tumor cells) and HA (in tumor-associated stroma) than HYAL1-AS tumors. Microvessel density in HYAL1-S tumors was 3.8-fold and 9.5-fold higher than that in vector and HYAL1-AS tumors, respectively.

These results demonstrate that HYAL1 expression in bladder cancer cells regulates tumor growth and progression, and therefore, it serves as a marker for high-grade bladder cancer.

INTRODUCTION

Bladder tumors, in particular, transitional cell carcinomas show heterogeneity in their ability to invade and metastasize (1-4). For example, low-grade bladder tumors rarely progress, whereas, about 2/3rd of high-grade tumors are detected at stages $\geq$ T1 (i.e., invading lamina propria and beyond) (5). Muscle invasion by a bladder tumor indicates poor prognosis, as 50% of patients develop metastases within 2-years and 60% die within 5-years, regardless of treatment (6). Certain molecular markers, such as hyaluronidase (HAase) have been identified as highly sensitive and specific markers for detecting high-grade (i.e., grade (G)2 and G3) bladder cancer (7,8). However, the functions of HAase (if any) in bladder tumor growth and/or invasion are unknown.

Hyaluronic acid (HA) is the substrate of HAase. It is a glycosaminoglycan, made up of repeating disaccharide units, D-glucuronic acid and N-acetyl-D-glucosamine (9). HA is normally present in tissues and body fluids. HA keeps tissues hydrated in an osmotically balanced environment (10). It also regulates cell proliferation, migration and adhesion by interacting with cell surface HA receptors such as, CD44 (11). Concentrations of HA are elevated in cancers of the breast, colon, prostate, bladder and others (8, 12-18). In tumor tissues, elevated HA is mostly localized to tumor stroma, however, in some tumors including bladder cancer, it is also expressed in tumor cells (12-18). We have previously shown that HA levels are elevated in the urine of bladder cancer patients, regardless of the tumor grade (8, 19). Thus, the measurement of urinary HA levels (HA test) has 83% sensitivity and 90% specificity for detecting bladder cancer (8). In tumor tissues HA swells upon hydration and opens up spaces for tumor cell migration and tumor cells migrate on HA-rich matrix by interacting with HA receptors (10, 11). An HA coat around tumor cells causes a partial loss of contact-mediated growth and migration and offers protection against immune surveillance (20-23). Small fragments of HA (i.e., 3-25 disaccharide units) are angiogenic (24, 25). We have previously isolated such small fragments from the urine of G2/G3 bladder cancer patients, high-grade prostate cancer tissues and from the saliva of head and neck cancer patients (18, 19, 26).

Small fragments of HA are generated by limited digestion of the HA polymer with hyaluronidase (HAase). HAase levels have been shown to be elevated in cancers of the prostate, bladder and head and neck cancer, and in breast tumors and malignant glioma (7, 19, 26-32). For example, we have shown that urinary HAase levels measured using an ELISA-like assay (HAase test) is a highly sensitive (81% sensitivity) and specific (83.8% specificity) marker for detecting G2 and G3 bladder tumors (7, 8). Elevated HAase levels also appear to be a sensitive marker for detecting head and neck cancer (26). We partially purified and characterized the first tumor-derived HAase from the urine of high-grade bladder cancer patients and showed its identity to HYAL1 (33). Subsequently, we demonstrated HYAL1 expression in several invasive bladder, prostate and head and neck tumor cell lines (18, 26, 33). For example, we analyzed HYAL1 expression and HAase secretion in 11 bladder cancer cell lines (33). Among these HT1376 cells secrete the highest amount of HAase activity (32 $\pm$ 2.4 mU/mg protein) in their conditioned medium (CM) and HYAL1 is the major HAase expressed in these cells. We recently showed that HYAL1 expression in radical prostatectomy specimens is an independent predictor of biochemical recurrence in prostate cancer patients (27, 34). In tumor cells, the expression of enzymatically active HYAL1 appears to be regulated by alternative mRNA splicing (35-37).

Jacobson et al recently reported that over-expression of HYAL1 in a rat colon cancer line suppresses tumor growth in xenografts (38). Contrarily, Chauzy et al showed that passage of a human breast cancer line CAL 51 from the primary state to metastatic stage increases hyaluronidase production (39). Expression of HYAL1 in a prostate cancer line that produces

little HAase, did not affect tumor growth but caused a slight increase in lung metastasis (40). Thus, the functional significance of HYAL1 expression in human tumor cells, which normally express HYAL1, is still unknown.

At the present time, it is also unknown whether HYAL1 is only a marker for more aggressive bladder cancer or it also functions as one of the molecular determinants that control bladder tumor growth and invasion. In this study we examined the function of HYAL1 in bladder tumor growth, invasion and angiogenesis using HYAL1-antisense (HYAL1-AS) transfection to block HYAL1 expression and HYAL1-sense (HYAL1-S) cDNA transfection to over-express HYAL1.

MATERIALS AND METHODS

Construction of HYAL1-S and HYAL-AS cDNA constructs: HYAL1 cDNA containing the entire coding region was amplified by RT-PCR analysis and cloned into a eukaryotic expression vector, pcDNA3.1/v5-His TOPO, using a TOPO-TA cloning kit (Invitrogen; ref. 35). The TOPO-TA cloning allowed bidirectional cloning of the HYAL1 cDNA insert with respect to the cytomegalo virus promoter (i.e., HYAL1-S and HYAL1-AS cDNA constructs). HYAL1-S, HYAL1-AS and vector cDNA constructs were used for transfection studies.

Generation of HYAL1 transfectants: HT1376, a transitional cell carcinoma of the bladder cell line, was cultured in RPMI1640 medium containing 10% fetal bovine serum and gentamicin (growth medium). HT1376 cells (2×10^5 cells/6-cm dish) were transfected with 5-µg of vector, HYAL1-S or HYAL1-AS cDNA constructs using the Superfect™ transfection reagent (Qiagen). The transfectants were selected in growth medium containing 200-µg/ml geneticin (Invitrogen).

Analysis of HAase activity by HAase ELISA-like assay: HAase activity in serum-free conditioned media of transfectants ($1x10^6$ cells) was assayed using the HAase ELISA-like assay (7, 8, 33). HAase activity (mU/ml) was normalized to total protein concentration (mg/ml) and was expressed as mU/mg.

Substrate (HA)-gel assay: CM from HT1376 transfectants (secreted by $5x10^4$cells, ~ 10 µg total protein) were separated on a substrate (HA)-gel. Following incubation in a HAase assay buffer, the gel was stained and destained to visualize active HAase species (7,18).

Immunoblot analysis: CM from the transfectant clones ($5x10^4$ cells, ~ 10-µg total protein) were immunoblotted using an anti-HYAL1 peptide IgG (i.e., anti-HYAL1 IgG) as described previously (18, 33). Cell lysates ($4x10^4$ cells/transfectant) were subjected to immunoblot analysis using the following primary antibodies: 1 µg/ml of mouse anti-cyclin B1 IgG (Clone GNS1; Neomarkers, Inc), 1 µg/ml mouse anti-cdc2/p34 IgG (Clones A27.1.1 + POH-1) or 0.2 µg/ml of rabbit anti-cdc25c IgG (C-20, Santa Cruz Biotech. Inc). Protein loading was evaluated by reprobing the blots with mouse anti-actin IgG (Neomarkers, Inc).

Cell proliferation assay: HT1376 transfectants (2×10^4 cells/well) were plated on 24-well culture plates in growth medium + geneticin. Every 24-h for a total period of 5 days (0 – 120 h), cells were trypsinized and counted following trypan blue staining. Counts were obtained from triplicate wells in 2 independent experiments.

Cell-cycle analysis: HT1376 transfectant cultures (60% confluence) were lysed in a PI dye solution (0.1% sodium citrate, 0.4% NP40 and 25 µg/ml propidium iodide) and analyzed in an EPICS XL flow cytometer, equipped with a long pass red filter, FL3 (630 nm). The FL3

histograms were analyzed for estimating cell cycle phase distribution by Modift Easy (Lite) program (Veritas Software, ME) (41). All samples were assayed in duplicates in 2 independent experiments.

Immunoprecipitation and kinase assay: HT1376 transfectant cells ($1x10^6$) were solubilized in a lysis buffer and immunoprecipitated using 2 μg/ml of mouse anti-cdc2/p34 IgG and protein-A agarose (Sigma-Aldrich). In control samples, the primary antibody was excluded. The immunoprecipitates were incubated with histone H1 in a hot kinase solution (2.5 μg H1 histone, 5 μM ATP, 5 μCi γ-^{32}P-ATP in kinase buffer) at 37^0 C for 30 min. Histone H1 was analyzed by 12% SDS-PAGE and autoradiography (42).

Analysis of Apoptosis: 48-h cultures of transfectants (10^5 cells/24-well plate) were lysed and the cell lysates were tested for free nucleosome release using the Cell Death ELISA kit (Roche Diagnostics). All samples were assayed in triplicates in 2 independent experiments.

Matrigel invasion assay: The membranes in 12- well Transwell plates (Corning-Costar) were coated with Matrigel (100 μg/cm^2) or Matrigel + HA (50 μg/ml) in Serum-free medium. HT1376 transfectants (3×10^5 cells/well) were plated on the upper chamber in Serum-free medium. The bottom chamber contained growth medium + geneticin. Following 48-h incubation, invasion of cells through Matrigel into the bottom chamber was quantified using the MTT assay (41). Invasion of cells was calculated as (cells in the bottom chamber ÷ cells in upper + bottom chambers) x 100. Invasion by vector transfectants was normalized as 100% (control). Invasive activity of each clone was determined in triplicates in 2 independent experiments.

Pericellular matrix (coat) assay: Pericellular matrices (coats) around transfectants were visualized using a particle exclusion assay involving formaldehyde fixed human erythrocytes as described previously (43,44). Cells were counted in 10 fields (127 – 155 cells/transfectant) per dish and in 2 dishes per transfectant. Cells, which showed a phase bright region around the entire periphery, with an average width greater than or equal to the diameter of one erythrocyte, were counted as having a pericellular matrix. Results were expressed as % cells with pericellular matrix ± S.D.

Tumor xenografts: HT1376 transfectants (2×10^6- or 4×10^6- cells/animal; 10 animals/group) were subcutaneously implanted on the right dorsal flank of 6-week old female athymic mice. After tumors became palpable, tumor size was measured twice weekly and tumor volume was calculated assuming an ellipsoid shape. At day 30, all 10 animals from vector and HYAL1-S tranfectants and 5 animals from HYAL1-AS groups were euthanzied. The remaining 5 mice in HYAL1-AS group were euthanized at day 60. Difference in tumor growth rate (i.e., generation of palpable tumors) and tumor weight at day 30 were statistically evaluated by Tukey-Kramer multiple comparison's test. The experiment was repeated once. Tumor histology was performed at Charles River Laboratories (Wilmington, MA).

Immunohistochemistry: HA and HYAL1 localization: HA and HYAL1 were localized in tumor xenograft specimens by immunohistochemistry using a biotinylated bovine nasal cartilage HA-binding protein and the rabbit anti-HYAL1 IgG, as described previously (17, 18, 27, 34). The HA and HYAL1 stained slides were graded with respect to staining intensity 0 or 1+ (weak), 2+ (moderate) and 3+ (high) staining. All the authors read the slides independently.

Microvessel density (MVD) determination: To visualize microvessels, slides containing tumor specimens were incubated with 3.1-μg/ml of rat anti-mouse CD34 IgG (BD Pharmingen) at 4^0 C

for 18 h. The slides were then sequentially incubated with a biotinylated rabbit anti-rat IgG, an avidin-biotin peroxidase conjugate solution (anti-rat ABC kit, Vector Laboratories), and 3,3'-diaminobenzidine substrate solution (DAKO Laboratories). The slides were counterstained with hematoxylin and the MVD was determined by counting the anti-CD34 stained microvessels (34). MVD was determined by 2 readers independently, by choosing the hot spots and counting the microvessels. MVD was expressed as mean ± SD.

RESULTS

Analysis of HYAL1 expression in HT1376 transfectants: Since HT1376 cells secrete the highest amount of HAase activity among the 11 bladder cancer cell lines (33), we chose HT1376 cell line to generate HYAL1-S (HAase overproducing) and HYAL1-AS (HAase non-producing) stable transfectants. We analyzed 25 - 30 stable clones of each transfectant type for analysis and data on two clones from each category are shown here. As shown in Fig. 1 A, HAase activity (mU/mg) secreted by HYAL1-S (# 1: 83.5 ± 4.5; # 2: 94.5 ± 3.5) transfectants is about 2.5-fold when compared to the vector transfectants (# 1: 33.5 ± 1.5; # 2: 38.5 ± 2.5). There is > 90% reduction in the amount of HAase secreted by HYAL1-AS (# 1: 2.0 ± 0.5; # 2: 4.3 ± 0.4) transfectants when compared to vector transfectants (Fig. 1 A). The amount of HAase activity secreted by HYAL1-AS transfectants is similar to that secreted by non-invasive bladder cancer cell lines such as, RT4 (33). As shown in Fig. 1 B, a ~ 60 kDa HYAL1 protein is detected in the CM of vector (# 1 and # 2) and HYAL1-S (# 1 and # 2) transfectants. However, this protein is not detected HYAL1-AS (# 1 and #2) transfectant CM. The substrate (HA)-gel analysis confirms the presence of a ~ 60 kDa active HAase species in the CM of both vector and HYAL1-S transfectants. As expected the active HAase species is not detected in the CM of HYAL1-AS transfectants (Fig. 1 C).

Effect of HYAL1 expression on cell proliferation, cell cycle and apoptosis: The growth rate of vector and HYAL1-S transfectants is comparable (Fig 2). The doubling time of both vector transfectant clones is about 30-h and that of HYAL1-S #1 and HYAL1-S # 2 transfectants is 26-h and 24-h, respectively. HYAL1-AS transfectants, however, grew about 4 times slower when compared to vector and HYAL1-S transfectants (doubling time: #1: 96-h; # 2: 80-h) (Fig. 2).

As shown in Table 1, HYAL1 expression appears to affect the G2-M phase of the cell cycle. There is a 200% and ≥ 500% increase in the number of HYAL1-AS transfectants in G2-M phase when compared to the vector and HYAL1-S transfectants, respectively (< 0.001; Tukey's multiple comparisons test). Correspondingly, the % of HYAL1-AS cells in S-phase decreases when compared to vector and HYAL1-S cells. HYAL1 expression does not affect the G0-G1 phase (Table 1).

We next analyzed the expression of G2-M regulators, i.e., cdc25c, cyclin B1 and cdc2/p34 proteins, in HT1376 transfectant clones. There is a 3- to 4-fold decrease in the expression of cdc25c and cyclin B1 in HYAL1-AS transfectant clones when compared to that in vector and HYAL1-S transfectants, respectively (Fig. 3 A). The expression of cdc2/p34 in HYAL1-AS transfectants does not change in HYAL1-AS transfectants when compared to the vector transfectants but decreases ~ 1.5-fold when compared to HYAL1-S transfectants (Fig. 3 A). There is also a ~ 2-fold and ~ 4-fold decrease in the cdc2/p34-associated H1 histone kinase activity in HYAL1-AS transfectant clones, when compared to the vector and HYAL1-S transfectants, respectively (Fig 3 B). These results show that HYAL1-AS transfectants are arrested in the G2-M phase of the cell cycle.

We also determined whether HYAL1 expression affects apoptosis. As shown in Table 2, there are no significant differences in apoptosis among vector, HYAL1-S and HYAL1-AS clones. This was further confirmed by using Annexin-V binding to study outward translocation of plasma membrane phosphatidyl serine among HYAL1 transfectants. No differences in phosphatidyl serine translocation were observed among vector (# 1 and # 2), HYAL1-S (#1 and # 2) and HYAL1-AS (#1 and # 2) transfectants. These results show that inhibition of HYAL1 expression affects cell cycle progression but not apoptosis.

Effect of HYAL1 expression on invasion:

The invasive activity of vector transfectant clones (28.8% ± 2.3%) was normalized as 100%. As shown in Fig. 4 A, HYAL1-AS transfectants # 1 and # 2 are 40% and 45% less invasive than the vector transfectant clones. Contrarily, HYAL1-S transfectants are 140% (# 1) and 159% (# 2) more invasive than vector transfectants. Incorporation of HA in Matrigel, does not influence the invasive properties of various HT1376 transfectants (Fig 4 B). These results show that blocking of HYAL1 expression significantly reduces the invasive activity of bladder cancer cells.

Effect of HYAL1 expression on HA-dependent pericellular matrix formation: As shown in Figure 5, the vector and HYAL1-S clones do not exhibit pericellular matrices as the erythrocytes closely abut the surface of each cell and in some cases cover the cells. However, HYAL1-AS cells exhibit a pericellular matrix, as the erthrocytes do not penetrate the matrix and a clear coat surrounds the cells. The percent of cells with pericellular matrix was elevated in HYAL1-AS transfectants (# 1: 85.6 ± 15.9; # 2: 86.7 ± 14.3) when compared to the vector (# 1: 56.3 ± 16.7; # 2: 47.8 ± 15.3) and HYAL1-S (# 1: 21.7 ± 16.25; # 2: 19.61 ± 14.83) transfectants. The differences among HYAL1-AS and vector, HYAL1-AS and HYAL1-S, HYAL1-S and vector were statistically significant ($P < 0.001$). Thus, HA is an important component of the pericellular matrix that surrounds bladder cancer cells.

Effect of HYAL1 expression on tumor xenografts: As shown in Fig 5 A, when injected at 2 x 10^6 cells/site density, there was a 4- to 5-fold delay in the generation of palpable tumors in animals injected with HYAL1-AS transfectant (40 ± 3 days) when compared to animals injected with HYAL1-S (7 days) and vector (10 ± 2 days) transfectants, respectively. ($P < 0.001$). The weight of HYAL1-AS transfectant tumors is 9.1-fold less than that of vector tumors and 17.3-fold less than that of HYAL1-S tumors, respectively (Fig. 5 B and $P < 0.001$). The 1.9-fold increase in the weight of HYAL1-S tumors compared to vector tumors is also statistically significant ($P < 0.05$). The picture of 2 representative tumors from each transfectant group shows that HYAL1-AS tumors are indeed much smaller than the vector and HYAL1-S tumors (Fig 5 C).

We also injected various transfectants at 4 x 10^6 cells/site. As shown in Fig. 5 D, the weight of HYAL1-AS tumors is still 10-fold and 17.7-fold less when compared with the weights of vector and HYAL1-S tumors, respectively ($P < 0.001$). Therefore, blocking HYAL1 expression decreases tumor growth, regardless of the initial tumor inoculum.

Tumor histology report provided by Charles River Laboratories stated that vector and HYAL1-S tumors grew by infiltrating surrounding tissues, including skeletal muscle. The tumors also contained numerous blood vessels. On the contrary, HYAL1-AS tumor growth was described as resembling benign neoplasm. Fig. 6, shows the photomicrographs of representative tumor histology corresponding to vector, HYAL1-S and HYAL1-AS tumors. As shown in Fig 6 A, clusters of tumor cells have infiltrated the skeletal muscle and two blood vessels are present at the periphery. At higher magnification, tumor cells are adjacent to

skeletal muscle fibers. A blood vessel is also present close to tumor cells at the lower left (Fig 6 D). In case of HYAL1-S tumor specimen, the skeletal muscle fibers are entrapped in tumor cells, as are the blood vessels (Fig. 6 B). At higher magnification, tumor cells are present at the edge of a blood vessel indicating infiltration. The tumor cells are surrounding the skeletal muscle fibers and also show a high number of mitotic figures (Fig. 6 E). As shown in Fig. 6 C, the HYAL1-AS tumor has a discrete margin and there is no evidence of infiltration into skeletal muscle. In addition, no large vessels are present in the specimen. At higher magnification, the specimen does not contain any skeletal muscle fibers and only a single capillary is present in the center (Fig. 6 F). These results show that HYAL1 expression influences the invasive phenotype of bladder tumor cells *in vivo*.

Expression of HA, HYAL1 and microvessel density: To determine whether tumor cells in vector, HYAL1-S and HYAL1-AS tumor specimens retain their phenotype, we localized HYAL1 and HA in tumor xenografts. Tumor cells in the vector specimen show moderate expression of HYAL1 (2+ staining intensity), whereas, tumor cells in HYAL1-S specimen show high-level of HYAL1 expression (3+ staining intensity) (Fig 7 panel a, b, c). None to very little HYAL1 staining is observed in HYAL1-AS tumor specimen (0 to 1+ staining intensity). In the vector tumor specimen, there is moderate (2+ staining intensity) HA expression in the tumor-associated stroma, but tumor cells are negative for HA expression (Fig. 7 A, panel d). There is high level of HA expression in tumor-associated stroma in HYAL1-S tumor specimen (Fig. 7 A, panel e). Interestingly, very low HA expression is observed in the stromal compartment in HYAL1-AS tumor specimens (Fig. 7 A panel f).

As shown in Fig 7 B, MVD in HYAL1-S tumor specimens (127.2 ± 29.23; range: 97 – 196) is 3.8-fold higher than that in vector tumor specimens (33.86 ± 5.55; range: 27 – 45), and 9.5-fold higher than that in HYAL1-AS specimens (13.43 ± 5.09; range: 6 – 22) ($P < 0.001$; Tukey's multiple comparison test).

DISCUSSION

Our results show that blocking HYAL1 expression in a bladder cancer line, results in a 4-fold decrease in cell growth rate, suggesting that HYAL1 expression by tumor cells is required for cell proliferation. The proliferation rate of HYAL1-S transfectants, however, is not significantly higher than that of the vector transfectants. Since HYAL1-S transfectants secrete only about 2.5-fold more HYAL1 than vector transfectants, moderate over-expression of HYAL1, in a bladder cancer cell line that already produces significantly higher amounts of HYAL1 (30 mU/mg) may not appreciably alter the cell proliferation rate. Our results, which show that blocking of HYAL1 expression induces cell cycle arrest, are consistent with a report that, HYAL1 expression in an oral squamous cell carcinoma line induces S-phase entry (45). Based on the analysis of cell cycle and G2-M regulators, HYAL1 expression very likely affects cell proliferation by regulating cell cycle.

Our finding that HYAL1-AS transfectants are about 50% less invasive than vector transfectants, and conversely, HYAL1-S transfectants are more invasive than vector transfectants are consistent with our previous observations that HYAL1 levels are elevated in high grade bladder tumor tissues and in patients' urine (8, 17). Most high grade tumors given sufficient time will invade bladder muscle and metastasize, and therefore, present with poor prognosis (1-4).

In addition to the effect of HYAL1 on tumor growth, its effects on tumor infiltration into skeletal muscle are interesting. HYAL1-S and vector tumors infiltrated skeletal muscle HYAL1-AS tumors were benign and did not invade the muscle. Muscle invasion by bladder tumor, is

independent of tumor volume and is ominous, as 60% of patients have distant metastasis within 2 years and 50% die within 5 years (1-6). The observations of this study suggest that HYAL1 plays a role in promoting the invasive potential of bladder tumor cells. It may also explain why urinary HAase levels serve as an accurate marker for detecting high grade bladder cancer, but are not elevated in patients with low grade tumors (1-4). HYAL1 is also an independent prognostic indicator for predicting biochemical recurrence in prostate cancer and increases metastatic potential of a prostate cancer line (29,34,40). Taken together HYAL1 appears to function in bladder tumor growth and invasion.

In tumor xenografts, HA was exclusively localized in tumor-associated stroma, whereas, HYAL1 was expressed by tumor cells. We have previously shown such dichotomy of HA and HYAL1 expression in prostate cancer (18). There is also a synergy between HA and HYAL1 expression. For example, there was considerably less HA in the stroma in HYAL1-AS tumors than there was in vector and HYAL1-S tumors. These observations are consistent with the expression of HA and HYAL1 in human bladder tumors. For example, there is low expression of HA and HYAL1 in G1 tumors when compared to G2 and G3 tumors, respectively (17). The synergy between stromal HA and tumor cell-HYAL1 expression suggests that one or both of these molecules may influence each other's synthesis in the tumor microenvironment.

One of the well studied functions of the HA and HAase system is the generation of angiogenic HA fragments (24,25). These angiogenic HA fragments have been shown to induce endothelial cell proliferation, migration and adhesion (46-48). The secretion of HAase by tumor cells has been shown to induce angiogenesis (32), whereas, HA causes avascularity (49). Angiogenic HA fragments are present in the urine of G2 and G3 bladder cancer patients, suggesting that the HA and HYAL1 system is active in bladder cancer (19). Our observations that HYAL1-S tumors have a significantly higher MVD than vector tumors and HYAL1-AS tumors have the lowest MVD among the 3 tumor groups are consistent with the function of the tumor associated HA-HAase system. Jacobson et al also observed increased MVD in HYAL1 over-expressing rat colon carcinoma xenografts (38).

At the present time the role of HAase as a tumor promoter or a repressor has been controversial. The results presented in this study show that blocking HYAL1 expression reduces tumor growth and invasion. HYAL1 levels in various cancers are associated with high-grade invasive tumors (7,8, 34, 26, 27). However, chromosome region 3p21.3 that contains HYAL1, HYAL2 and HYAL3 genes is deleted in some cancer lines (50-53). Although the tumor suppressor gene in 3p21.3 is not HYAL1, HYAL2 or HYAL3, it originally gave rise to the idea that HAase is a tumor suppressor (54-58). Jacobson et al found that the over-expression of HYAL1 by cDNA transfection in a rat colon carcinoma line decreases tumor growth, although the tumors are angiogenic (38). It is noteworthy that HYAL1-overexpressing transfectants in that study secreted 4 to 5-fold more HAase activity than the HYAL1-S transfectants in our study. Shuster et al injected a large dose (300 U/injection or 75 U/injection X 4 injections) of bovine testicular HAase in MDA435 breast cancer xenografts and observed a reduction in tumor volume over a period of 4 days; however, the effect was not studied beyond 4 days (59). Thus, it is possible that the effect of HYAL1 (and possibly other HAases) on tumor growth and invasion is concentration dependent. While, moderate HYAL1 expression in tumor cells increases their proliferative and invasive potentials, the lack of HYAL1 expression, as well as, very high HYAL1 expression decreases tumor growth and invasion, perhaps by completely degrading the tumor-associated HA matrix. It is also noteworthy that other proteins related to HA synthesis (HA-synthase (HAS) 2 and 3) and HA-receptor RHAMM are also involved in tumor growth and metastasis. For example, blocking HAS-3 expression in prostate cancer cells decreases cell growth *in vitro* and tumor growth *in vivo* (60). HAS-2 expression induces

mesenchymal and transformed properties in normal epithelial cells (44). Interestingly, HAS-2 expression in the absence of HAase decreases tumor growth in glioma cells (61). Interaction between RHAMM and HA fragments is known to induce the MAP-kinase pathway and overexpression of RHAMM is a useful prognostic indicator for breast cancer (62, 63). These results show that the HA-HAase system is involved in the regulation of tumor growth and invasion.

Taken together our study shows that HYAL1 is one of the molecular determinants of bladder tumor growth and invasion, and therefore, it is a sensitive and specific marker for detecting high-grade bladder cancer.

Acknowledgments: We are grateful to Dr. Awtar Krishan Ganju, Department of Radiology and Microbiology and Immunology University of Miami, for his advice on flow-cytometry. We thank Drs. Bryan Toole, Department of Cell Biology and Anatomy, Medical University of South Carolina and Dr. William E Buck Department of surgery, University of Miami, for their advice on pericellular matrix detection experiments. We thank Dr. Charles Clifford, Director of Pathology, and Charles River Laboratories for his help in reviewing and interpreting the histology slides. We also thank Dr. Carlos Perez-Stable, University of Miami for helpful discussions. We thank Mr. Douglas Roach for his assistance with illustrations.

REFERENCES

1. Lee R, Droller MJ. The natural history of bladder cancer. Implications for therapy. *Urol Clin North Am.* 2000; 27:1-13, vii.
2. Heney NM. Natural history of superficial bladder cancer. Prognostic features and long-term disease course. *Urol. Clin. North Am.* 1992; 19(2): 429-33.
3. Droller MJ. Cancer heterogeneity and its biologic implications in the grading of urothelial carcinoma. J Urol. 2001; 165(2):696-7.
4. Hassen W, Droller MJ. Current concepts in assessment and treatment of bladder cancer. *Curr Opin Urol.* 2000; 10(4): 291-9.
5. Soloway MS, Sofer M, Vaidya A. Contemporary management of stage T1 transitional cell carcinoma of the bladder. *J Urol.* 2002; 167(4): 1573-83.
6. Vaidya A, Soloway MS, Hawke C, Tiguert R, Civantos F. De novo muscle invasive bladder cancer: is there a change in trend? *J Urol.* 2001; 165(1): 47-50; discussion 50.
7. Pham HT, Block NL, Lokeshwar VB. Tumor-derived hyaluronidase: a diagnostic urine marker for high-grade bladder cancer. Cancer Res. 1997 Feb 15;57(4):778-83. Erratum in: Cancer Res 1997 57(8):1622.
8. Lokeshwar VB, Obek C, Pham HT, et al. Urinary hyaluronic acid and hyaluronidase: markers for bladder cancer detection and evaluation of grade. *J Urol.* 2000; 163(1): 348-56.
9. Tammi MI, Day AJ, Turley EA. Hyaluronan and homeostasis: a balancing act. *J Biol Chem* 2002; 277(7): 4581-4.
10. Delpech B, Girard N, Bertrand P, Courel MN, Chauzy C, Delpech A. Hyaluronan: fundamental principles and applications in cancer. *J Intern Med.* 1997; 242(1): 41-8.
11. Turley EA, Noble PW, Bourguignon LY. Signaling properties of hyaluronan receptors. *J Biol Chem* 2002; 277(7): 4589-92.
12. Setälä LP, Tammi MI, Tammi RH, et al. Hyaluronan expression in gastric cancer cells is associated with local and nodal spread and reduced survival rate. *Br J Cancer* 1999; 79(7-8): 1133-8.
13. Auvinen P, Tammi R, Parkkinen J. et al. Hyaluronan in peritumoral stroma and malignant cells associates with breast cancer spreading and predicts survival. *Am J Pathol* 2000; 156(2): 529-36.

14. Knudson W. Tumor-associated hyaluronan. Providing an extracellular matrix that facilitates invasion. *Am J Pathol* 1996; 148(6): 1721-6.
15. Ropponen K, Tammi M, Parkkinen J, et al. Tumor cell-associated hyaluronan as an unfavorable prognostic factor in colorectal cancer. *Cancer Res.* 1998; 58(2): 342-7.
16. Lipponen P, Aaltomaa S, Tammi R, Tammi M, Ågren U, Kosma V-M. High stromal hyaluronan level is associated with poor differentiation and metastasis in prostate cancer. *Eur J Cancer* 2001; 37(7): 849-56.
17. Hautmann SH, Lokeshwar VB, Schroeder GL et al. Elevated tissue expression of hyaluronic acid and hyaluronidase validates the HA-HAase urine test for bladder cancer. *J Urol* 2001; 165(6 Pt 1): 2068-74.
18. Lokeshwar VB, Rubinowicz D, Schroeder GL, et al. Stromal and epithelial expression of tumor markers hyaluronic acid and HYAL1 hyaluronidase in prostate cancer. *J Biol Chem* 2001; 276(15):11922-32.
19. Lokeshwar VB, Obek C, Soloway MS, Block NL. Tumor-associated hyaluronic acid: a new sensitive and specific urine marker for bladder cancer. *Cancer Res.* 1997; 57(4): 773-7. Erratum in: Cancer Res 1998; 58(14):3191.
20. Liu N, Lapcevich RK, Underhill CB. Metastatin: a hyaluronan-binding complex from cartilage that inhibits tumor growth. *Cancer Res.* 2001; 61(3): 1022-28
21. Hayen W, Goebeler M, Kumar S, Riessen R, Nehls V. Hyaluronan stimulates tumor cell migration by modulating the fibrin fiber architecture. *J Cell Sci.* 1999; 112(Pt 13): 2241-51.
22. Hobarth K, Maier U, Marberger M, et al. Topical chemoprophylaxis of superficial bladder cancer by mitomycin C and adjuvant hyaluronidase. *Eur. Urol.* 1992; 21(3): 206-210.
23. Itano N, Atsumi F, Sawai T, et al. Abnormal accumulation of hyaluronan matrix diminishes contact inhibition of cell growth and promotes cell migration. Proc. Natl. Acad. Sci. 2002; 99(6): 3609-3614.
24. Lees VC, Fan TP, West DC. Angiogenesis in a delayed revascularization model is accelerated by angiogenic oligosaccharides of hyaluronan. *Lab Invest.* 1995; 73(2): 259-66.
25. West DC, Hampson IN, Arnold F, Kumar S. Angiogenesis induced by degradation products of hyaluronic acid. *Science* 1985; 228(4705): 1324-6.
26. Franzmann EJ, Schroeder GL, Goodwin WJ, Weed DT, Fisher P, Lokeshwar VB. Expression of tumor markers hyaluronic acid and hyaluronidase (HYAL1) in head and neck tumors. *Int J Cancer* 2003; 106(3): 438-45.
27. Posey JT, Soloway MS, Ekici S, et al. Evaluation of the prognostic potential of hyaluronic acid and hyaluronidase (HYAL1) for prostate cancer. Cancer Res. 2003 63(10): 2638-44.
28. Lokeshwar VB, Lokeshwar BL, Pham HT, Block NL. Association of elevated levels of hyaluronidase, a matrix-degrading enzyme, with prostate cancer progression. *Cancer Res* 1996; 56(3): 651-7.
29. Madan AK, Yu K, Dhurandhar N, Cullinane C, Pang Y, Beech DJ. Association of hyaluronidase and breast adenocarcinoma invasiveness. *Oncol Rep.* 1999; 6(3): 607-9.
30. Bertrand P, Girard N, Duval C, et al. Increased hyaluronidase levels in breast tumor metastases. *Int J Cancer* 1997; 73(3):327-31.
31. Delpech B, Laquerriere A, Maingonnat C, Bertrand P, Freger P. Hyaluronidase is more elevated in human brain metastases than in primary brain tumours. *Anticancer Res.* 2002; 22(4): 2423-7.
32. Liu D, Pearlman E, Diaconu E, et al. Expression of hyaluronidase by tumor cells induces angiogenesis in vivo. *Proc Natl Acad Sci U S A.* 1996; 93(15): 7832-7.
33. Lokeshwar VB, Young MJ, Goudarzi G, et al. Identification of bladder tumor-derived hyaluronidase: its similarity to HYAL1. *Cancer Res.* 1999; 59(17): 4464-70.
34. Ekici, S., Cerwinka, W., Ducan, RC, Gomez, P., Civantos, F., Soloway, MS, Lokeshwar, VB. Comparison of the prognostic potential of hyaluronic acid, hyaluronidase (HYAL-1),

CD44v6 and microvessel density for prostate cancer. *Int. J Cancer*, 2004 (In press).
35. Lokeshwar VB, Schroeder GL, Carey RI, Soloway MS, Iida N. Regulation of hyaluronidase activity by alternative mRNA splicing. *J Biol Chem.* 2002; 277(37): 33654-63.
36. Junker N, Latini S, Petersen LN, Kristjansen PE. Expression and regulation patterns of hyaluronidases in small cell lung cancer and glioma lines. *Oncol Rep.* 2003; 10(3): 609-16.
37. Frost GI, Mohapatra G, Wong TM, Csoka AB, Gray JW, Stern R. HYAL1LUCA-1, a candidate tumor suppressor gene on chromosome 3p21.3, is inactivated in head and neck squamous cell carcinomas by aberrant splicing of pre-mRNA. Oncogene. 2000; 19(7): 870-7.
38. Jacobson A, Rahmanian M, Rubin K, Heldin P. Expression of hyaluronan synthase 2 or hyaluronidase 1 differentially affect the growth rate of transplantable colon carcinoma cell tumors. *Int J Cancer.* 2002; 102(3): 212-9.
39. Victor R, Chauzy C, Girard N, Gioanni J, d'Anjou J, Stora De Novion H, Delpech B. Human breast-cancer metastasis formation in a nude-mouse model: studies of hyaluronidase, hyaluronan and hyaluronan-binding sites in metastatic cells. *Int J Cancer* 1999; 82(1): 77-83.
40. Patel S, Turner PR, Stubberfield C, et al. Hyaluronidase gene profiling and role of hyal-1 overexpression in an orthotopic model of prostate cancer. *Int J Cancer* 2002; 97(4): 416-24. Erratum in: Int J Cancer 2002; 98(6): 957.
41. Lokeshwar BL, Selzer MG, Zhu BQ, Block NL, Golub LM. Inhibition of cell proliferation. invasion, tumor growth and metastasis by an oral non-antimicrobial tetracycline analog (COL-3) in a metastatic prostate cancer model. *Int J Cancer* 2002; 98(2): 297-309.
42. Agarwal C, Singh RP, Dhanalakshmi S, Tyagi AK, Tecklenburg M, Sclafani RA, Agarwal R. Silibinin upregulates the expression of cyclin-dependent kinase inhibitors and causes cell cycle arrest and apoptosis in human colon carcinoma HT-29 cells. Oncogene. 2003; 22: 8271-82.
43. Deyst KA, Toole BP. Production of hyaluronan-dependent pericellular matrix by embryonic rat glial cells. Brain Res Dev Brain Res. 1995; 88: 122 - 125.
44. Zoltan-Jones A, Huang L, Ghatak S, Toole BP. Elevated hyaluronan production induces mesenchymal and transformed properties in epithelial cells. J Biol Chem. 2003; 278: 45801 - 45810.
45. Lin G, Stern R. Plasma hyaluronidase (Hyal-1) promotes tumor cell cycling. Cancer Lett. 2001;163(1): 95-101.
46. Slevin M, Kumar S, Gaffney J. Angiogenic oligosaccharides of hyaluronan induce multiple signaling pathways affecting vascular endothelial cell mitogenic and wound healing responses. *J Biol Chem.* 2002; 277(43):41046-59.
47. Lokeshwar VB, Selzer MG. Differences in hyaluronic acid-mediated functions and signaling in arterial, microvessel, and vein-derived human endothelial cells. *J Biol Chem.* 2000; 275(36): 27641-9.
48. Feinberg RN, Beebe DC. Hyaluronate in vasculogenesis. *Science* 1983; 220(4602):1177-9.
49. Senchenko V, Liu J, Braga E, et al. Deletion mapping using quantitative real-time PCR identifies two distinct 3p21.3 regions affected in most cervical carcinomas. *Oncogene* 2003; 22(19):2984-92.
50. Senchenko VN, Liu J, Loginov W, et al. Discovery of frequent homozygous deletions in chromosome 3p21.3 LUCA and AP20 regions in renal, lung and breast carcinomas. *Oncogene*. 2004 [Epub ahead of print]
51. Csoka AB, Frost GI, Stern R. The six hyaluronidase-like genes in the human and

mouse genomes. *Matrix Biol.* 2001; 20(8): 499-508.

52. Kashuba VI, Li J, Wang F, et al. RBSP3 (HYA22) is a tumor suppressor gene implicated in major epithelial malignancies. *Proc Natl Acad Sci U S A.* 2004; 101(14): 4906-11.

53. Ji L, Nishizaki M, Gao B, et al. Expression of several genes in the human chromosome 3p21.3 homozygous deletion region by an adenovirus vector results in tumor suppressor activities in vitro and in vivo. *Cancer Res.* 2002; 62(9):2715-20.

54. Csoka TB, Frost GI, Heng HH, Scherer SW, Mohapatra G, Stern R. The hyaluronidase gene HYAL1 maps to chromosome 3p21.2-p21.3 in human and 9F1-F2 in mouse, a conserved candidate tumor suppressor locus. *Genomics* 1998; 48(1):63-70.

55. Shuster S, Frost GI, Csoka AB, Formby B, Stern R. Hyaluronidase reduces human breast cancer xenografts in SCID mice. *Int J Cancer* 2002; 102(2):192-7.

56. Simpson MA, Wilson CM, McCarthy JB. Inhibition of prostate tumor cell hyaluronan synthesis impairs subcutaneous growth and vascularization in immunocompromised mice. Am J Pathol. 2002; 161: 849 - 857.

57. Enegd B, King JA, Stylli S, Paradiso L, Kaye AH, Novak U. Overexpression of hyaluronan synthase-2 reduces the tumorigenic potential of glioma cells lacking hyaluronidase activity. Neurosurgery. 2002; 50: 1311 - 1318.

58. Wang C, Thor AD, Moore DH 2nd, Zhao Y, Kerschmann R, Stern R, Watson PH, Turley EA. The overexpression of RHAMM, a hyaluronan-binding protein that regulates ras signaling, correlates with overexpression of mitogen-activated protein kinase and is a significant parameter in breast cancer progression. Clin Cancer Res. 1998; 4: 567 - 576.

Table 1: Cell cycle analysis of HT1376 transfectants: HYAL1-S, HYAL1-AS and vector transfectant clones were subjected to flow-cytometry for cell-cycle analysis. The percentages of cells in G0-G1, S and G2-M phases of the cell cycle are shown. The data shown are the average of duplicates from 2 independent experiments. The SD was $\leq 5\%$.

Phase	Vector # 1	Vector # 2	HYAL1-S # 1	HYAL1-S # 2	HYAL1-AS # 1	HYAL1-AS # 2
G0-G1	56.7%	55.8%	55.2%	54.2%	55.9%	57.1%
S	37.7%	38.4%	42.4%	44.3%	31.4%	32.7%
G2-M	5.6%	5.8%	2.4%	1.5%	12.7%	10.2%

Table 2: Analysis of apoptosis in HT1376 transfectants. Apoptotic activity in vector, HYAL1-S and HYAL1-AS transfectant clones was determined and the apoptotic activity in vector # 1 clone was considered as 100% (Control). Data shown are $O.D._{405} \pm$ SE from duplicate measurements in 2 independent experiments.

Transfectant	Free nucleosome $O.D._{405}$	% of control
Vector # 1 (control)	1.8 ± 0.05	100%
Vector # 2	1.5 ± 0.25	83.3%
HYAL1-S # 1	1.79 ± 0.21	99.4%
HYAL1-S # 2	1.91 ± 0.37	106%
HYAL1-AS # 1	1.46 ± 0.16	81.1%
HYAL1-AS # 2	1.83 ± 0.2	102%

FIGURE LEGENDS

Figure 1: Analysis of HYAL1 expression in HT1376 transfectants. A: Measurement of HAase activity. HAase activity (mU/mg) data are presented as mean ± SE from 3 separate experiments. **B. Immunoblot analysis using anti-HYAL1 IgG**. CM (10 μg protein; CM of $5x10^4$ cells) from each transfectant clone were subjected to anti-HYAL1 IgG immunoblotting as described in "Materials and Methods". **C: Substrate (HA)-gel assay.** CM (10 μg protein; CM of $5x10^4$ cells) from each transfectant clone were analyzed by substrate (HA)-gel. In the absence of a specific and well-accepted protein loading control for secreted protein, we used cell number and total protein for normalizing the total amount of CM for each transfectant, for HYAL1 immunoblot analysis and substrate (HA)-gel assay.

Figure 2: Determination of the proliferation rate of HT1376 transfectants. The cell counting data are presented as mean ± SD from triplicate measurements in 2 independent measurements.

Figure 3: Analysis of G2-M cell cycle regulators in HT1376 transfectants. A: Cell lysates of HT1376 transfectants were analyzed by immunoblotting using anti- cdc25c (a), anti-cyclin B1 (b) and anti-cdc2/p34 (c) and β-actin (d) antibodies. Lanes 1 & 2: vector clones # 1 & 2; lanes 3 & 4: HYAL1-S clones 1 & 2; lanes 3 & 4: HYAL1-AS clones # 1 & 2. **B:** H1 histone kinase-associated activity of cdc2/p34 was measured as described in "Materials and Methods". Lanes 1 & 2: vector clones # 1 & 2; lanes 3 & 4: HYAL1-S clones 1 & 2; lanes 3 & 4: HYAL1-AS clones # 1 & 2; lane 7, negative control.

Figure 4: Determination of the invasive activity of HT1376 transfectants *in vitro.* Invasive activity was tested in Matrigel alone (**A**) or in Matrigel + HA (**B**). Invasive activity of vector transfectant clone # 1 (control) was considered as 100%. The data (mean ± SD) presented are from triplicate determinations in 2 independent experiments.

Figure 5: Examination of pericellular matrix in HT1376 transfectants: Pericellular matrices surrounding various HT1376 transfectants were visualized using the particle exclusion assay. The pictures show human erythrocytes surrounding tumor cells. A: Vector # 2; B: HYAL1-S # 2; C: HYAL1-AS # 2.

Figure 6: Examination of the growth of HT1376 transfectant tumors in xenografts. Vector # 2, HYAL1-S # 2 and HYAL1-AS # 2 transfectant clones were injected subcutaneously in athymic mice (10 animals/group) 2 x 10^6 cells/site density. **A:** Measurement of tumor volume. The data are presented as mean ± SD **B:** Tumor weight (g) data are presented as mean ± SD. **C:** Photographs of two representative tumors from each group (i.e., vector, HYAL1-S and HYAL1-AS) taken at necropsy. **D.** Vector # 2, HYAL1-S # 2 and HYAL1-AS # 2 transfectant clones were injected subcutaneously in athymic mice at 4 x 10^6 cells/site density. Tumor weight (g) data are presented as mean ± SD.

Figure 7: Examination of histology of transfectant tumors. Charles River Laboratories provided the tumor histology pictures presented in panels A to F. **Panels A, B, C:** 100X magnification. **Panels D, E, F:** 400X magnification. SM: skeletal muscle fiber; T: tumor or tumor cells; V: blood vessel. The arrow indicates entrapment of skeletal muscle fibers by tumor; WBC: leukocytes.

Figure 8: Localization of HYAL1, HA and microvessels in tumor tissues. A: Localization of HYAL1 and HA. Panels a, b, c: HYAL1 localization. Panels d, e, f: HA localization. Panels a & d: vector transfectant; Panels b & e: HYAL1-S transfectant; Panels c & f: HYAL1-AS transfectant. **B: Localization of microvessels.** The areas of the highest MVD from each type of tumor specimen are presented here, magnification, 400X. Panel a: vector tumor; Panel b: HYAL1-S tumor; Panel c: HYAL1-AS tumor.

Figure 1

Lokeshwar Fig 1 A

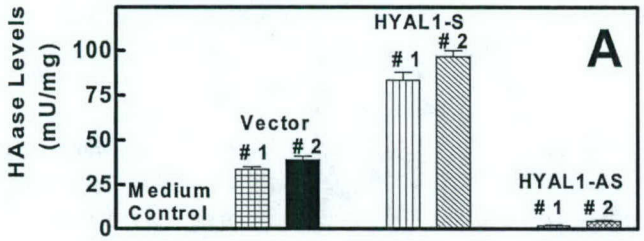

Lokeshwar Fig 1 B

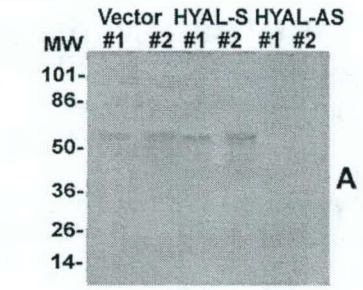

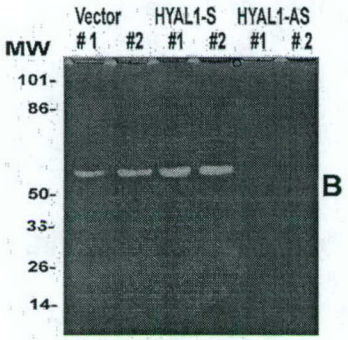

Figure 2

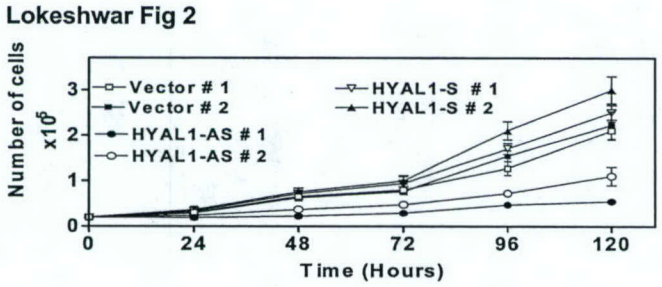

Figure 3

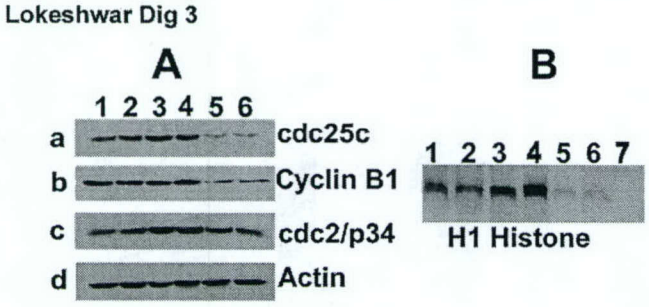

Figure 4

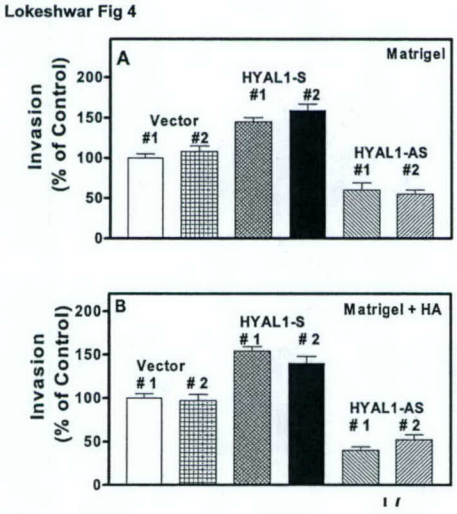

Figure 5:

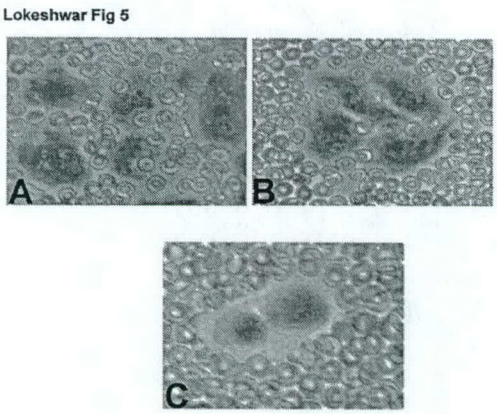

Figure 6

Lokeshwar Fig 6 A,B D

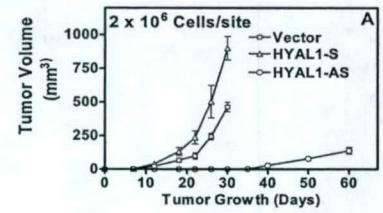

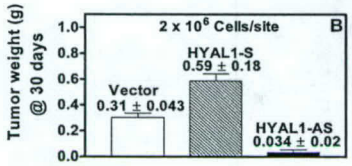

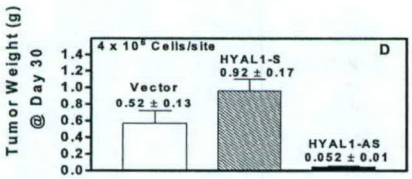

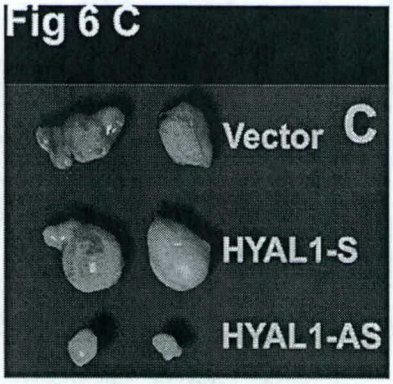

Figure 7

Lokeshwar Fig 7

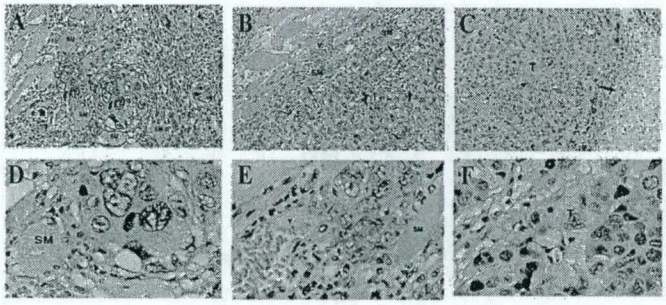

Figure 8

Lokeshwar Fig 8